THIS DOCUMENT CONTAINS
POOR QUALITY PAGES

TITLE: SEISMIC EVALUATION OF BUILDING 102 OF THE GENERAL ELECTRIC VALLECITOS NUCLEAR CENTER

AUTHOR(S): Elton G. Endebrock

SUBMITTED TO: Winston Burkhardt, US Nuclear Regulatory Commission

University of California

LOS ALAMOS SCIENTIFIC LABORATORY
Post Office Box 1663 Los Alamos, New Mexico 87545
An Affirmative Action/Equal Opportunity Employer

Form No. 836 R3
St. No. 2629
12/78

8101290527

UNITED STATES
DEPARTMENT OF ENERGY
CONTRACT W-7405-ENG. 36

SEISMIC EVALUATION OF BUILDING 102 OF THE GENERAL ELECTRIC VALLECITOS NUCLEAR CENTER

Page

SEISMIC EVALUATION OF BUILDING 102 OF THE GENERAL ELECTRIC VALLECITOS NUCLEAR CENTER

SUMMARY

The Engineering Decision Analysis Company (EDAC) and the Los Alamos Scientific Laboratory (LASL) were engaged to determine the structural consequences of vibratory ground motion and fault displacements on Building 102 of the General Electric Vallecitos Nuclear Center (GEVNC). This study is an increment of an assessment made by the Nuclear Regulatory Commission (NRC) to determine the risk associated with the operation of this facility. About 95% of the task of evaluating the structural consequences from vibratory ground motions and from faults intersecting the Radioactive Materials Laboratory (RML) cells was performed by EDAC. LASL completed EDAC's structural evaluation study and determined the consequences of faulting on the Advanced Fuel Laboratory (AFL) and the basement area.

The structural evaluation studies focused on the areas of concern (those parts of Building 102 that may contain a significant inventory of radioactive materials); however, noncritical parts that could influence the response of the areas of concern were included in the analysis. The areas of concern are

1. the critical glove boxes,
2. the AFL located within the basement area,
3. the RML cells, and
4. the Plutonium Analytical Laboratory (PAL).

The noncritical areas included in this study are the high- and low-bay areas.

The structural features of Building 102 were examined, and the interrelationships between the different areas were established. Each area was then analyzed for structural consequences of vibratory ground motions, faulting, and concurrent seismic events. Some important results of the structural capacity evaluation for vibratory ground motions follow.

- The start of structural damage to the AFL critical equipment occurs at about 0.7 g's PGA (peak ground acceleration).
- Except for local cracking, the confinement integrity of the AFL will be maintained up to about 0.9 g's PGA.

- Cracking in the RML cell structure starts to occur at about 0.9 g's PGA.
- The PAL could suffer a loss of confinement starting at about 0.6 g's PGA.

Other noncritical structural components or systems could be severely damaged at PGA levels below 0.9 g's; however, their collapse does not influence the confinement integrity of the areas of concern. A summary of the results of the analysis for the major systems and components is given in Table I.

TABLE I

ESTIMATED CAPACITIES OF SYSTEMS IN TERMS OF PEAK GROUND ACCELERATION[a]

System	Element	Mean Capacity Peak Ground Acceleration (g's)
Low-Bay	Roof Connection to Shear Walls	0.6
	Block Walls - Face (Face Loading)	1.0
	Block Walls (Steel Frame) (Face Loading)	1.0
	Precast Concrete Walls (Face Loading)	0.9
High-Bay	Roof	1.0
	South Wall (Face Loading)	1.0
	East Wall (Face Loading)	0.7
	High Block Walls (Face Loading)	0.4
RML cells	Overturning	1.0
	Cells, Ground Floor	0.9
Basement	Slab, Columns, Footings	1.0
	Exterior Walls	0.6
Equipment	Glove Boxes 37, 39, 41, 44	0.6
	Glove Boxes 23, 50, 51, 51A	1.0

[a] Peak ground acceleration (PGA) is that acceleration to which criteria response spectra are anchored at the zero period.

The study on structural consequences from fault displacements and vibratory ground motion originating from the postulated Verona Fault included only the areas of concern. Some results from this study follow.

- Regardless of the direction of the seismic event, the important above-grade RML cell structure would maintain its confinement function, but could be displaced from its original position.
- The RML cells would not overturn.
- Passive soil pressures will damage some below-grade basement and cell walls with the amount of damage depending upon the magnitude of the fault movements.
- The ventilation ducts between the RML cells and the secondary filters in the basement would probably be damaged.
- The hydraulic rams that open and close the heavy shielding doors would be damaged and probably become inoperative.
- The PAL could suffer a loss of confinement either from the fault displacements or from the vibratory motions.

Structural damage scenarios that describe potential damage to the facility at various levels of fault movements are presented in Section V.

I. INTRODUCTION

The US NRC has undertaken a project to examine the capability of commercial plutonium facilities to withstand adverse natural phenomena (seismic, severe weather, flooding).[1] A review team is used to provide the interdisciplinary expertise necessary for the analysis of each facility. The seismic structural capacity analyses for these facilities are performed by EDAC. During EDAC's review of the GEVNC plutonium laboratory, NRC determined that EDAC corporately was involved in other work for the General Electric Company that gave the perception that a conflict of interest could exist.

NRC subsequently requested that LASL independently assess the General Electric facility for its capability to withstand seismic forces. This included review and use of the EDAC work to the extent applicable and consistent with the guidelines used throughout the natural phenomena study.

For the natural phenomena reviews, the Nathan M. Newmark Consulting Engineering Services (NNCES) provide overview consultation to the NRC staff and their consultants for the site seismic characterization and the structural and equipment capacity evaluations resulting in a second independent review and assessment.

This report contains the results of LASL's and EDAC's assessment and analyses of Building 102 components for the effects of seismic vibratory ground motion from the Calaveras fault and offset from the postulated Verona fault. The methodology, assumptions, and results of the analyses are discussed in detail in subsequent sections of this report.

The examination of the Building 102 capability to withstand seismic phenomena was undertaken in a manner consistent with the natural phenomena review approach, that is, using most likely values of parameters. This approach, for structural and equipment capability, consists of incremental increase in structural loading to establish damage levels. This provides several levels that are related to seismic recurrence interval and attendent failure scenarios for use on subsequent increments of the overall facility risk assessment.

Subsequent to the initiation of this natural phenomena evaluation, the United States Geological Survey (USGS) postulated the existence of a dip/slip fault located on the General Electric property.[2] This postulation was later modified to identify the fault as a possible thrust feature.[3] An initial deterministic analysis was prepared by EDAC to determine the capability of the RML cells to withstand a thrust fault. Subsequently, other components of Building 102 were examined for consequences to incrementally increasing fault displacements. Therefore, this report includes the results of the structural analyses for the shaking, faulting, and combined seismic events.

II. SITE AND FACILITY DESCRIPTION

A. Site Description

The GEVNC is located in the southwest corner of a site that has an area of approximately 1534 acres.[4] This site is situated on the north side of the Vallecitos Valley, which is separated from the larger Livermore Valley to the north by a range of hills. The floor of the Vallecitos Valley is approximately three to four miles in length and a mile wide. The elevations in the portion of the site occupied by the VNC range from 420 to 600 ft above sea level.

The site slopes gently to the south. Sedimentary materials consisting of alluvial deposits of gravel, sand, silt, and clay underlay the study area. These deposits include the Livermore gravels. The total soil thickness (alluvial plus sedimentary deposits) at the site is probably several hundred feet.

B. Facility Description

The layout of the GEVNC in the vicinity of Building 102 is shown in Fig. 1. Building 102 was constructed in 1956 and 1957. Modifications were made during the period from 1969 to 1974. The foundations are spread footings and bell-bottom caissons as shown in Fig. 2. It is of modern construction and was designed to comply with the provisions of the 1952 Uniform Building Code. Building 102 is a one-story structure with a partial basement under the eastern half (Fig. 2). Office and laboratory areas are located on the ground floor, and the AFL is located in the basement (Fig. 3). The RML cells are located in the southeast corner of the ground floor (Fig. 3). The elevation of the roof above the RML cells is greater than the roof elevation of the remainder of Building 102. The region with the highest roof is referred to as the high-bay area whereas the remainder of the ground floor is referred to as the low-bay area.

Precast concrete panels, metal siding, and glass form the exterior walls of Building 102 (Fig. 4). Interior walls are constructed of 8-in. reinforced concrete block, 4-in. reinforced concrete block, and wood studs with gypsum board (Fig. 5). About half of the 8-in. block walls are infills in the structural steel framing. The roof is supported by structural steel framing that includes structural steel tubular columns. In the high-bay area, the RML cells give support to the roof.

Specific areas in Building 102 may contain a significant inventory of radioactive materials at risk. These areas of concern are

1. the PAL,
2. the RML cells, and
3. the AFL.

These areas are therefore the most important in safety considerations and will hereafter be referred to as the critical building areas.

The PAL, shown in Fig. 6, is located on the ground floor of Building 102 and above the basement area. The walls of the PAL are constructed of precast concrete panels on the east side, 8-in. concrete block on the north and west sides, and 4-in. concrete block on the south side.

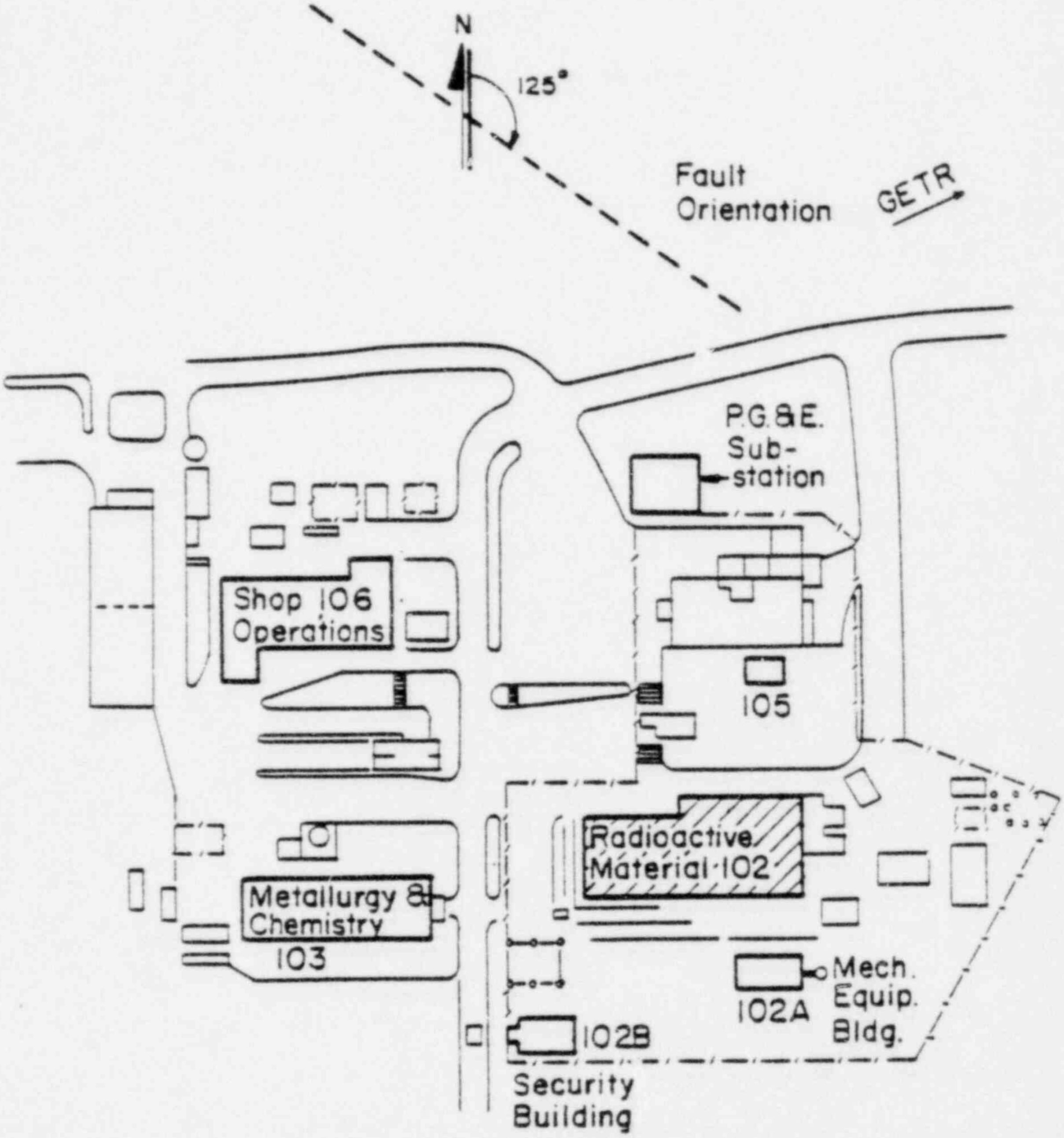

Fig. 1.
Area and surrounding in relation to Building 102.

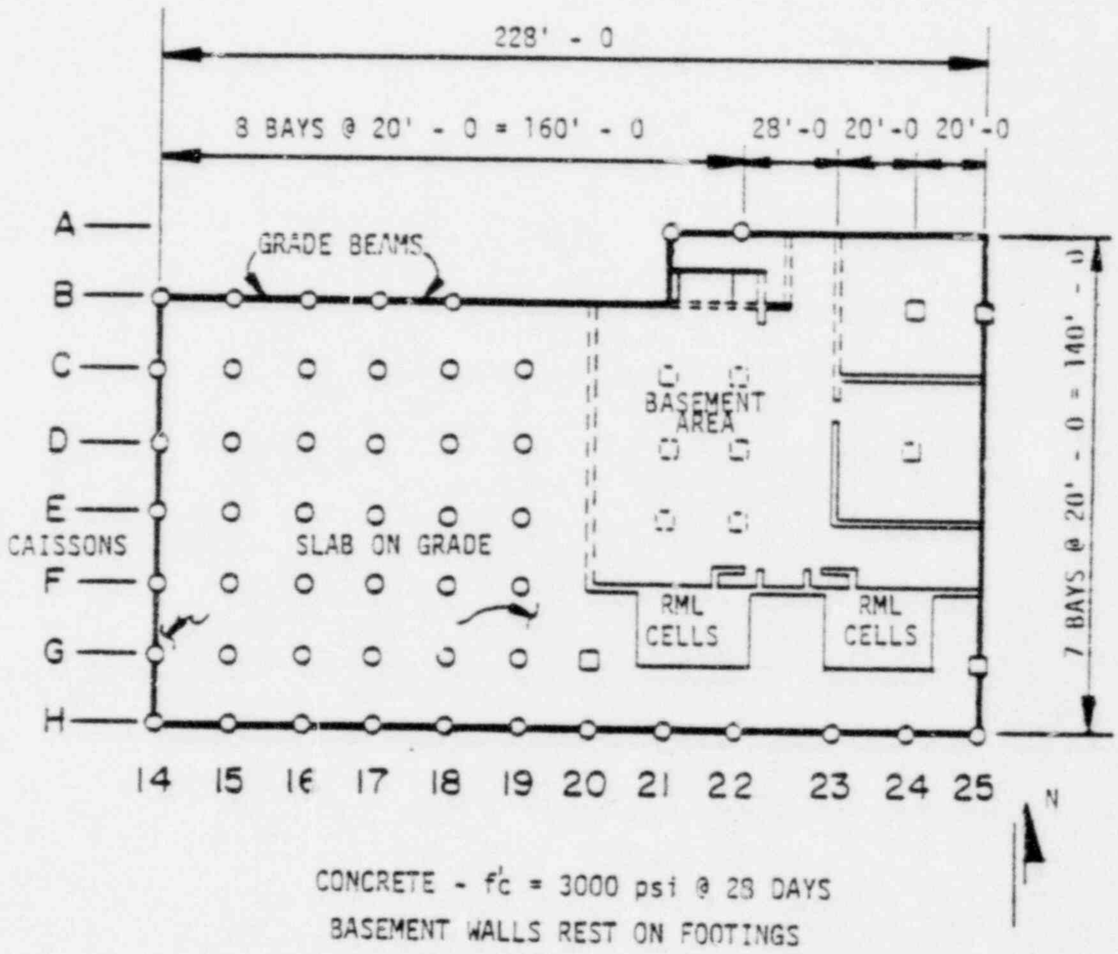

Fig. 2.
Building 102 foundation plan.

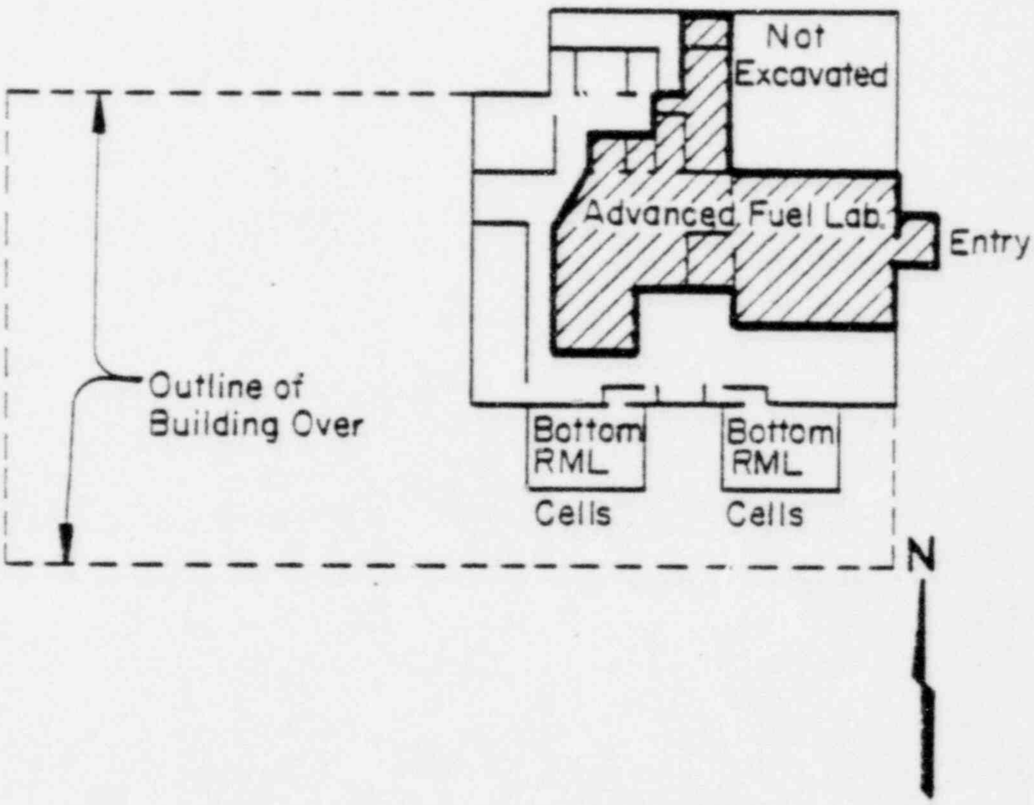

Fig. 3.
Basement plan with critical areas.

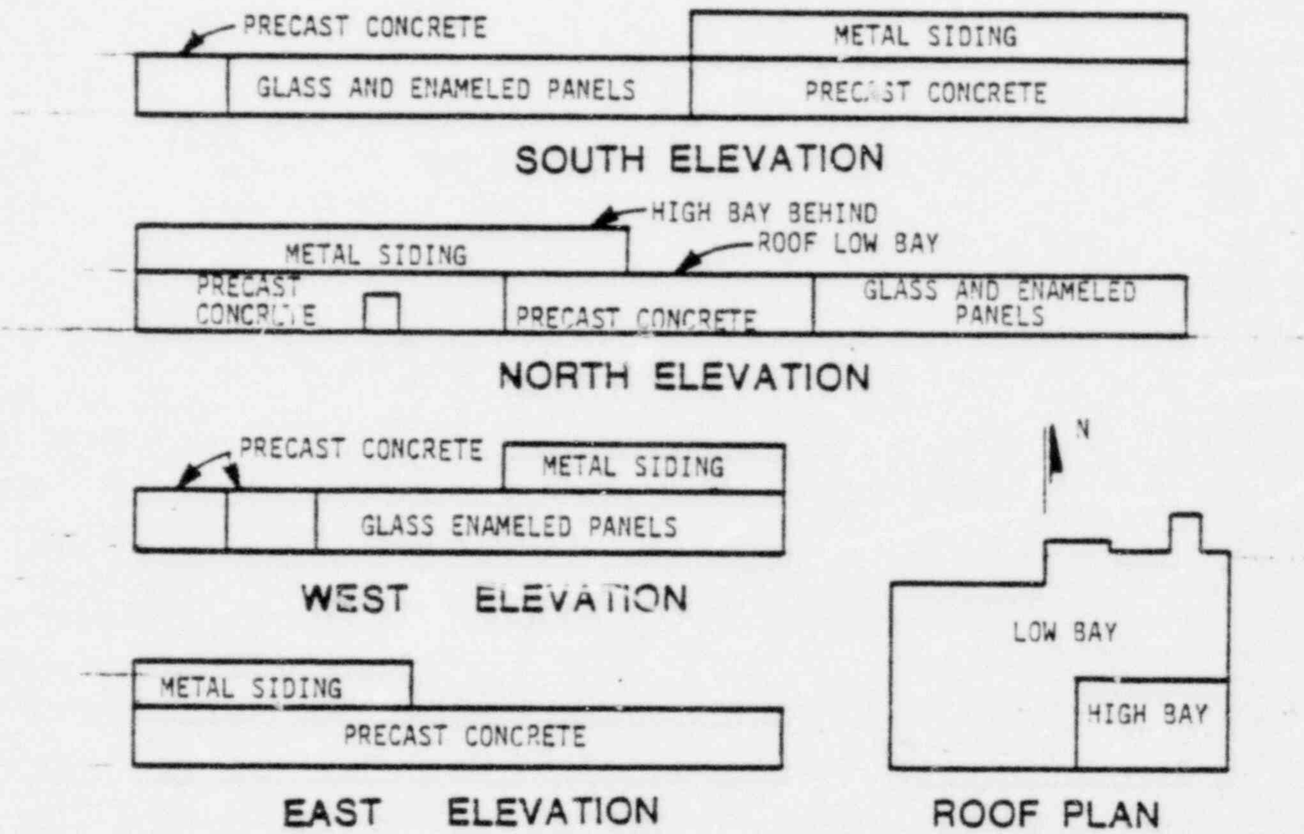

Fig. 4.
Elevations and roof plan.

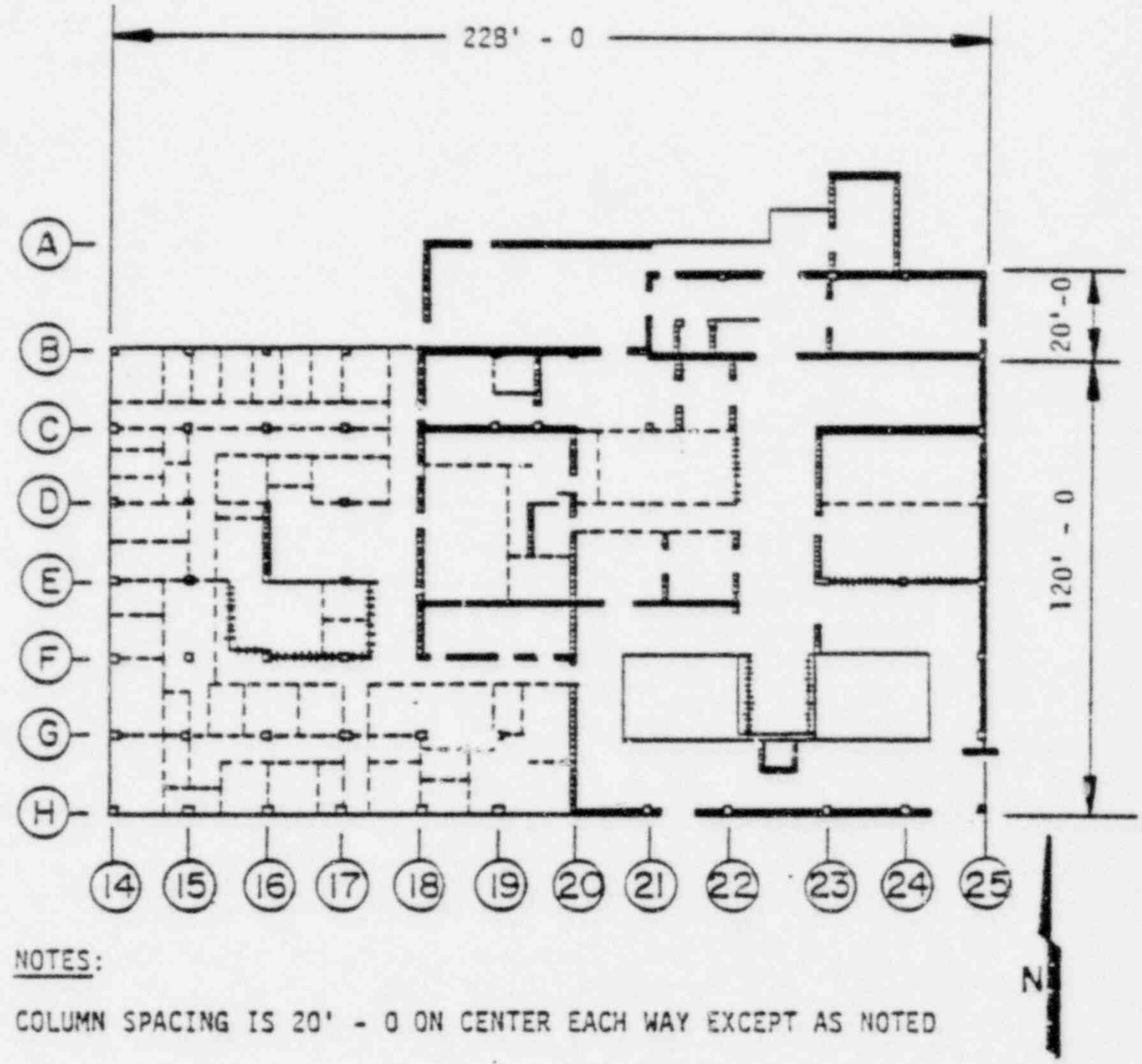

NOTES:

COLUMN SPACING IS 20' - 0 ON CENTER EACH WAY EXCEPT AS NOTED

8" CONCRETE BLOCK

6" PRECAST CONCRETE

4" CONCRETE BLOCK

2 x 4 STUD WALL, 1/2" GYPSUM BOARD DOORS NOT SHOWN

STRUCTURAL STEEL COLUMN

4" CONCRETE BLOCK FLOOR TO ROOF

Fig. 5.
Building 102 ground floor showing wall construction.

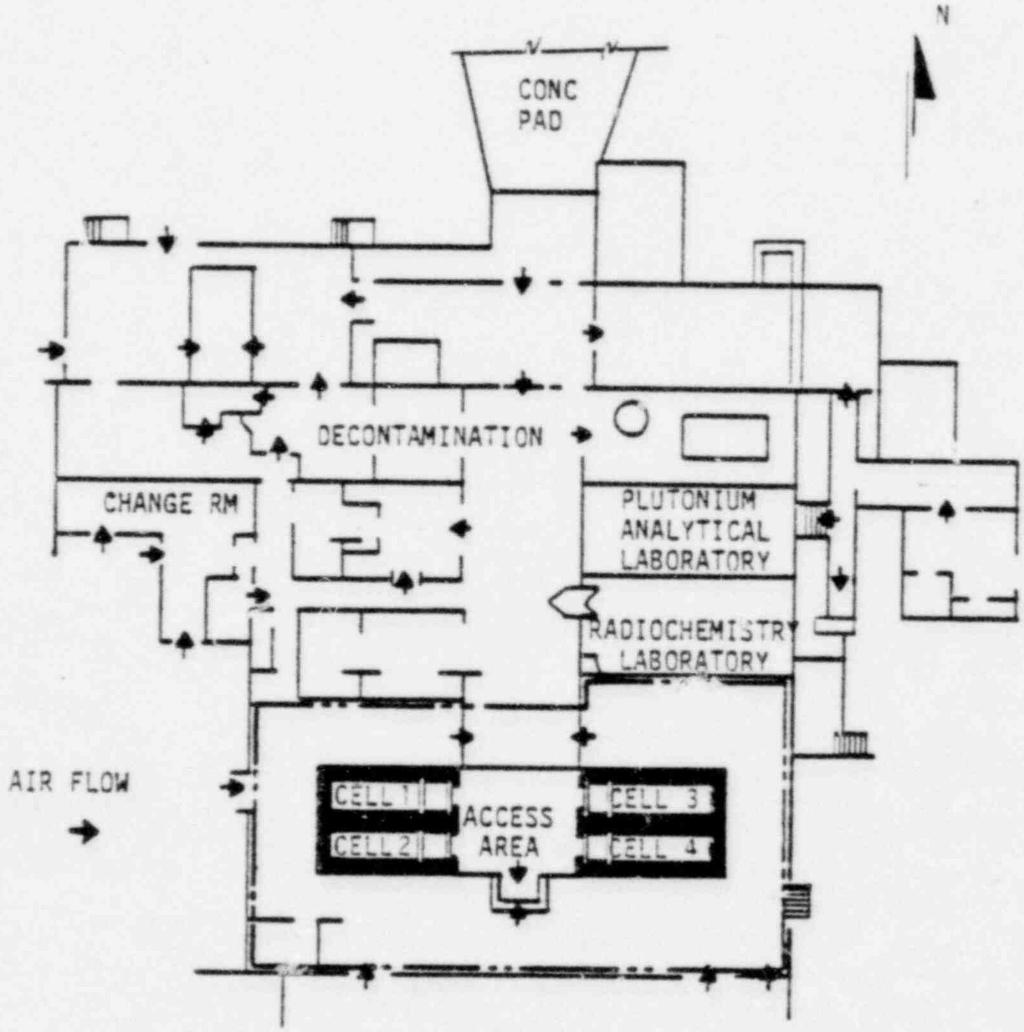

Fig. 6.
Building 102 main floor, radioactive materials areas.

The RML cells are massive reinforced concrete boxes that extend from the basement foundation level to about 17 ft above the ground floor (Figs. 6 and 7).

The AFL is located within the basement area (Fig. 7). The AFL perimeter walls consist of reinforced concrete and concrete masonry walls. The basement area exterior walls are constructed of reinforced concrete. The heavy reinforced concrete basement roof slab is supported by the basement walls, by the reinforced concrete columns, and by the interior walls. The exterior basement walls are supported on concrete footings. The basement floor slab is not connected structurally to the walls, columns, or footings. The critical glove boxes and exhaust equipment in the basement have recently been modified and connected to the basement construction to provide additional seismic support.

C. Seismic Characterization

To proceed with this study, we needed a characterization of the seismic hazard. One source of seismic activity at the VNC site is associated with the Calaveras Fault.[4] The Teknekron Energy Resources Analysts (TERA) Corporation conducted studies that addressed the seismic characterization of events from this source.

The Calaveras Fault is a major structural feature that extends along the entire western side of the Livermore Valley, and its existence, capability, and location are well documented. The site response spectra recommended by the TERA Corporation was the 50th percentile alluvium spectra contained in WASH-1255 (USAEC, 1973) scaled to the desired peak acceleration (Fig. 8). The relationship between return periods and peak ground acceleration was developed by the TERA Corporation, and it is shown in Fig. 9. Newmark recommended that a peak ground acceleration of 0.80 g's be used for anchoring the site response spectra.[5]

Another source of seismic activity, a postulated geological fault referred to as the Verona Fault, is believed to intersect the VNC site.[2] It has been classified as a right lateral thrust fault with an unknown dip angle. The strike of the fault in the vicinity of the VNC is approximately along an azimuth of 125^{o} (north reference). Its capability and exact location is still under study; therefore, to initiate studies on structural consequences, the following capability criteria were employed in these studies.

1. Peak ground acceleration, 0.60 g's.

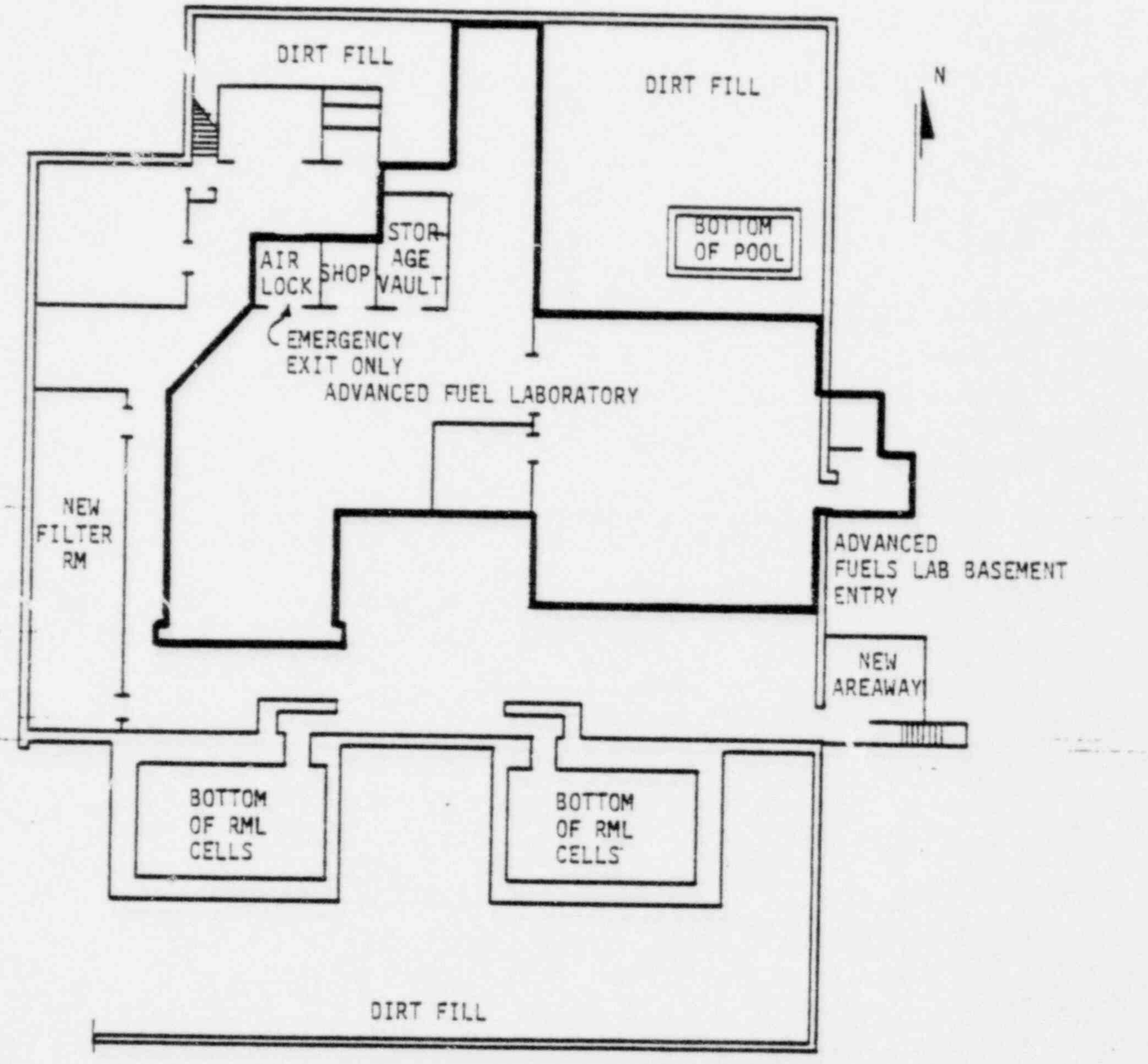

Fig. 7.
Building 102 basement.

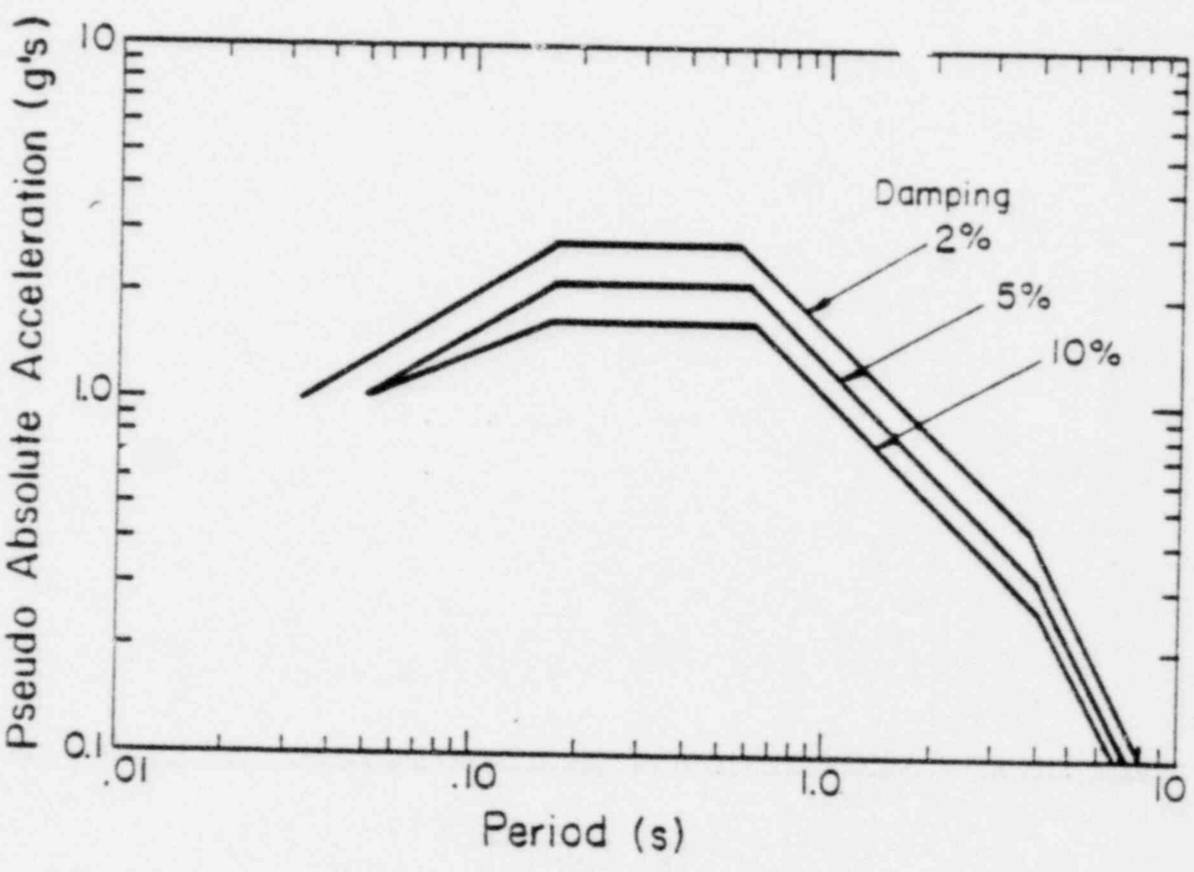

Fig. 8.
Site response spectra

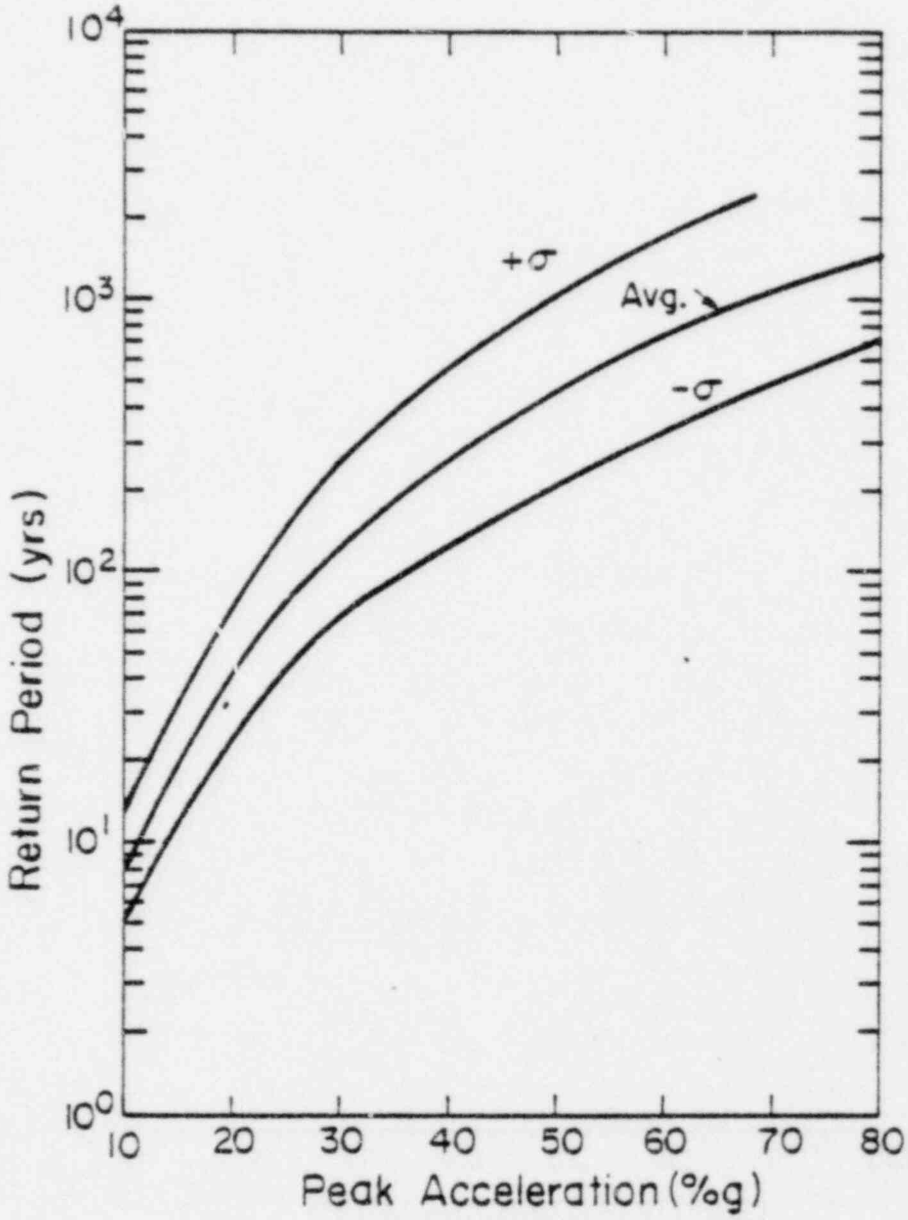

Fig. 9.
Peak acceleration vs return period for the Vallecitos site (TERA Corporation).

2. Maximum fault displacement, up to 8 ft.
3. Dip angle, 15° to 45°.
4. Concurrent events, 0.40 g's horizontal PGA with slip and thrust up to 8 ft.

Because its location has not been established, the Verona Fault is assumed to occur at any site location along the fault strike orientation.

D. Soil Properties

The available soils data for the VNC site are given in Refs. 7 and 8. The site is underlaid by approximately 45 ft of very dense clayey sand and gravel with occasional pockets of clay. The ground water level is at a depth of approximately 20 ft. The upper surface layer is underlaid by very stiff to hard gravelly clay (Livermore Gravel) to a depth of several hundred feet. The surface materials are characterized by an in-situ density of 135 lbs/ft^3 at a 15% moisture content. The results of consolidated-undrained (consolidated-quick) triaxial soil tests indicate a Mohr-circle envelope defined by the Coulomb equation with a shear friction angle of $\phi_{cu} = 30^{\circ}$ and a cohesion intercept of $c_{cu} = 1400$ psf.[6] This is an extremely large value of cohesion for a clayey sand. No attempt was made to interpret the test values in terms of effective stresses or the general behavior of cohesive sands. The test values as reported were used. The ultimate bearing capacity of the soil is $q_{db} = 20$ ksf.[6]

By including the effects of soil-structure interaction resulting from shaking, the shear modulus of the supporting soil must be estimated. Also, the soil shear modulus must be adjusted to compatibility with expected maximum soil strains. Using Refs. 8-11 for guidance, we estimated the equivalent soil shear modulus at 8330 psi (1.2×10^{-6} psf).

III. BACKGROUND AND BASES FOR STRUCTURAL AND EQUIPMENT ANALYSES

A. Introduction

NRC requested that LASL assess the completeness and adequacy of the EDAC's structural evaluations of Building 102 of General Electric's Vallecitos Nuclear Center and, as necessary, revise and amplify EDAC's reported work to complete the analysis. To fulfill this request, we had to review EDAC's studies.

The description of EDAC's investigations of Building 102 and its strength evaluations are presented in three unpublished reports that are referred to as the Task I,[12] Task II,[13] and Faulting Analysis reports.[14] The Task I report contains information such as structural details, behavior of structural elements, strength capacities of structural element construction materials, and material properties, that is needed in assessing the strength capacity of Building 102 and its substructures. No safety-related structural strength assessments are given in this report.

The factual information in the Task I report was verified in a number of isolated instances. Dimensions, reinforcing steel, construction details, and construction materials were noted in the report and compared with the corresponding items shown in the construction drawings. No discrepancies were found.

EDAC's analysis and evaluation of Building 102 to withstand earthquake vibratory motions are documented in the Task II report. This investigation included the entire building; however, the RML cells and the AFL that is located in the basement area were emphasized in the study. Damage scenarios (level of expected structural damage vs expected earthquake peak ground acceleration return period) are included in this report.

The Faulting Analysis report documents EDAC's analysis and evaluation of the structural consequences of postulated faults intersecting the RML cells. In addition, structural consequences of concurrent faulting and earthquake vibratory motions are assessed.

The review of EDAC's Task II and Faulting Analysis reports included examination of the assumptions, the calculational methods, and the analysis methods. Checks were made to determine if the conclusions matched the documentation and computational information and if the information used in the calculation corresponded to the information documented in the Task I report. Sources of information and assumptions were noted. Evaluations and computation not fully comprehended were noted for further consideration.

After both LASL and NNCES had reviewed the studies, LASL met with NNCES to discuss EDAC's studies. We agreed that the items identified below warranted additional attention.

1. The loadings and resistance of exterior basement walls.
2. The PAL located on the first floor.

3. The structural interaction between the RML cells and the basement structure.
4. The secondary filter bank located in the basement.
5. The expected mode of behavior associated with the combined faulting and shaking criteria.
6. The consequences of faults intersecting the basement and AFL.

EDAC's treatment of items 1, 3, and 5 was reviewed in detail. The wall loadings were revised by LASL to always correspond to a cohesive soil. LASL agreed with EDAC's conclusions relating to items 3 and 5; therefore, no significant changes were made here. LASL included items 2 and 4 in the discussion of the capacities of the structural systems that influence the integrity of the PAL and the secondary filter bank. LASL alone considered item 6.

Descriptions and discussions of the methodology and techniques and results of the structural capacity evaluation of Building 102 and its equipment follow. The evaluations focus on those portions of the structure and critical equipment systems whose failure or loss of function could result in possible hazardous release to the environment. EDAC's descriptions, figures, references, discussions, and strength assessments are directly incorporated into this report whenever they are considered applicable and acceptable. The description of LASL's analyses are also included in this report, and the final strength assessments reflect those of EDAC with modifications and changes by LASL.

B. Methodology and Techniques

1. Separation and Interdependence of Component Parts

To facilitate the structural evaluation of Building 102 and its equipment, we divided the overall analysis into five parts. The study focused on the areas of concern, which are, in the order of descending importance,

1. the critical equipment,
2. the AFL and the basement area, and
3. the RML cells.

Other areas that could influence the areas of concern were also analyzed. They are

4. the high-bay area and
5. the low-bay area.

The structural interactions between the parts and systems were considered in the overall evaluations. The interactions between the building system are indicated in Fig. 10. To include the influence of the noncritical areas upon the areas of concern, we first evaluated the noncritical areas. The behavior of the equipment is dependent upon the behavior of the Building 102 structural systems; therefore, the equipment was evaluated after the structural analysis was completed.

The descriptions of Building 102 structural systems, components, and critical equipment are given in the Appendixes. Discussions of the structural details that most influence the responses of the systems are also presented in Appendix A.

The strength capacities of the subsystems listed above were evaluated separately for vibratory ground motion, fault displacements, and concurrent vibratory ground motion and fault displacements. The exceptions were that the high- and low-bay areas were not specifically evaluated for structural consequences for fault displacements because the consequences of their collapse would be no more severe than for vibratory motions. Also, these areas are not areas of concern. The RML cells are within the high-bay area, but they are evaluated separately. The PAL is located in the low-bay area and above the basement area; therefore, during faulting, its structural capacity is determined by low-bay collapse from vibratory motions or by large deformations of the basement roof slab. The assumptions and methodology associated with each of these evaluations are given in the succeeding sections.

2. Vibratory Ground Motion

The vibratory motions are characterized by the 50th percentile alluvium spectra contained in WASH-1255 (USAEC, 1973) as recommended by the TERA Corporation (Fig. 8). These spectra are scaled to the desired peak acceleration.

The analysis includes the elastic and inelastic plastic regimes. Response spectrum techniques were used in the analyses along with conventional static analysis methods. The ductility method of analysis was selected for assessment of nonlinear response and capacity of structural systems for inelastic behavior. This approximate method is an adaptation of the modal spectral method of dynamic analysis.[15-19] General damping and ductility data that were used in the response spectra analyses are given in Table II.[5] Expected damage levels corresponding to incremental peak ground accelerations were constructed.

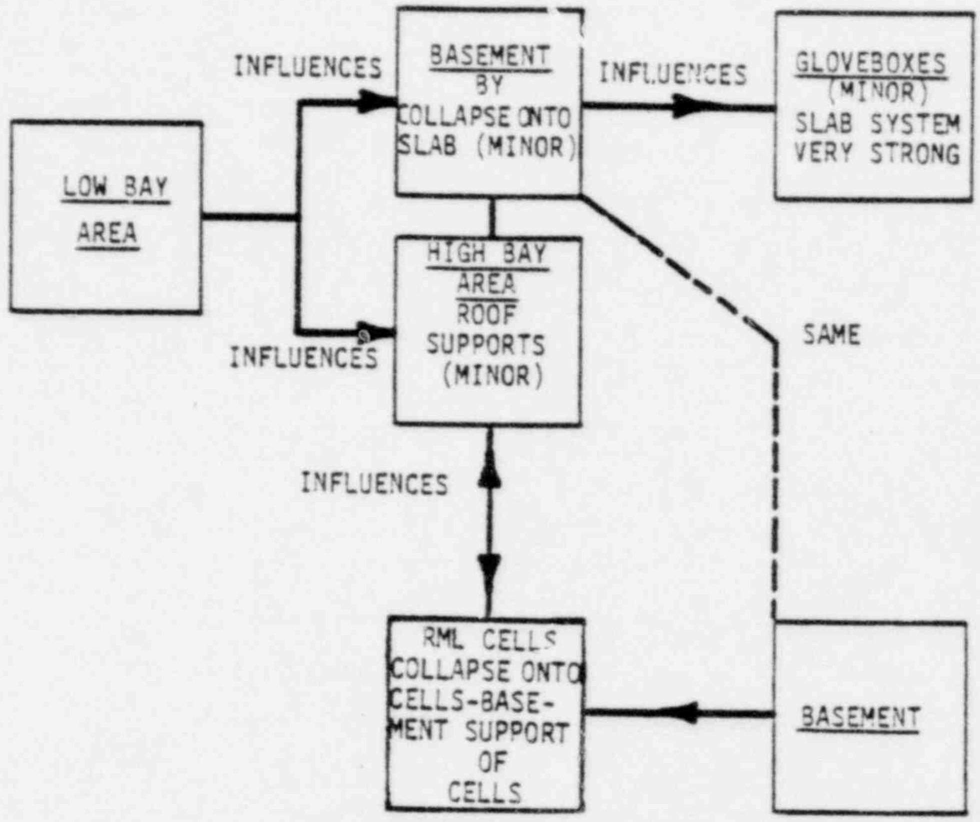

DEPENDENCY

	CRITICAL AREA	
	GLOVEBOXES IN BASEMENT	RML CELLS
BY:		
LOW BAY AREA	MINOR	NONE
HIGH BAY AREA	MINOR TO NONE	MAJOR
RML CELLS	MINOR	-
BASEMENT	MAJOR	SMALL
GLOVEBOXES	-	MINOR

Fig. 10.
Influences and dependency between systems.

TABLE II

DAMPING AND DUCTILITY DATA

(FROM NEWMARK)[5]

Damping

Construction	Percent of Critical
Welded steel	5-7
Reinforced concrete	7-10
Bolted steel	10-15

Ductility

Item	Factor
Light equipment	1.0 to 1.5
Concrete in shear or compression	1.5 to 2.5
Concrete in flexure	2 to 5
Steel in tension and flexure	2.5 to 10
Steel in compression	1.5 to 3

Because Building 102 is of relatively lightweight structure, and because the soil data indicate stiff and dense foundation materials, soil-structure interaction was not generally considered. Soil-structure interaction was, however, considered in the analysis of the heavy RML cells for vibratory ground motions. Soil-liquification was not considered credible because of the high soil density (135 pcf), the level of the water table (at least 19 ft below-grade level), and the large range of soil grain sizes (less than 0.03 in. to 1.6 in.).

Fault Movements

Thrust faulting results in a decrease in distance between reference points located on the surface of the faulting blocks. This general characteristic of free-field thrust faulting is indicated in Fig. 11. For a rigid structure positioned across the fault, the shortening effect cannot occur; therefore, the soil must deform. Assuming the fault kinematics indicated in Fig. 12, the estimated soil deformation is $t\cos\theta/2$. The selected fault displacements are expected to produce soil deformations from 2.9 ft to 4.0 ft.

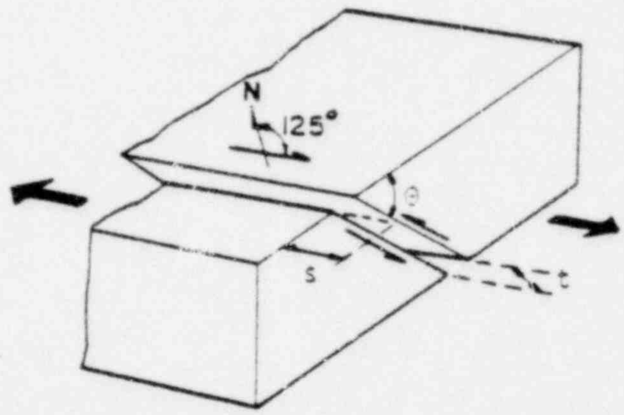

Θ - Dip Angle, $15^{0} \leq \Theta \leq 45^{0}$

t - Thrust ≤8.5 m

s - Slip ≤8.5 ft

0.80 g's ground motion without faulting

Faulting may occur at any location within
site along strike orientation

0.40 g's ground motion concurrent with 1.7-ft fault movement

Fig. 11.
Faulting study criteria.

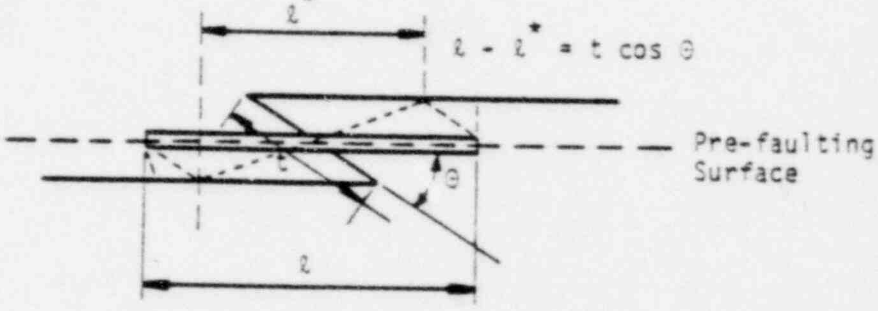

Fig. 12.
Thrust faulting characteristics.

The thrust and slip of a fault will induce earth pressure loads on a buried structure. The fault movements must be accommodated by either the structure, the soil, or both. To determine the failure mode, the passive earth pressures must be estimated. Passive earth pressures depend upon the magnitude of the movement of a wall into a soil mass. The amount of wall movement necessary to activate the maximum passive resistance of a dense sand is within the range of 2-5% of the wall height.[20,21] For a wall height of 12 ft, displacements within the range 0.25-0.60 ft activate the full passive resistance of the soil. The postulated maximum fault movements (currently under study) are expected to be as great as 8.0 ft; therefore, full passive soil pressures are assumed for walls that can withstand the maximum passive pressures. Once the full passive soil pressure has been activated, additional movements do not increase the pressures, which is our approach for the faulting analysis in not looking at more severe movements.

The passive earth pressures are based on a cohesive soil.[22] The soil parameters for determining the passive pressures are the internal angle of friction (ϕ), the adhesion (a), the cohesion (c), and the wall roughness angle (δ). There is no available information on the wall adhesion and the wall roughness angle. These two parameters increase the calculated resistance of the soil. For uncertain conditions, Ref. 20 indicates that the wall friction can be taken as one-half of the internal angle of friction, and the wall adhesion can be taken as one half of the cohesion. The wall adhesion (a) was therefore taken as c/2, and δ was taken as $\phi/2$.

The passive earth pressures distribution for a cohesive soil is

$$p = K_p\ (\gamma z + q) + 2c\sqrt{K_p},$$

where p is the passive soil pressure,

K_p is the passive soil pressure coefficient,

γ is the soil density (135 pcf),

z is the soil depth,

c is the cohesion (1400 pcf), and

q is the surcharge pressure.

Two basic loading conditions caused by combined thrust-slip faulting were considered.

1. Passive soil pressures caused by the shortening characteristics of thrust faulting and the rotational movement induced by slip faulting.

2. Loss of continuous base slab soil support resulting in alternate support configurations for dead weight resistance.

The strength evaluations were determined using equivalent static analysis techniques for the postulated loading distributions and the support conditions. In the following sections, we discuss the analytical cases, the loadings developed from the selected seismic criteria, and the results.

The structural consequences from fault movements were evaluated using deterministic methods. An ultimate capacity analysis only was used; however, expected damage arising from fault displacements of different magnitudes has been evaluated. The procedure for estimating the structural damage was to select a fault movement magnitude and then estimate the structural damage. Because of the complexity of the soil-structure systems, considerable judgment was required in estimating the damage levels.

4. Concurrent Vibratory Motion and Fault Movements

The many soil and structure interactions that occur when a building is subjected to concurrent shaking and faulting are complex. Because documented cases of engineered structures subjected to this seismic event are rare, experience in treating this subject is severely limited, and considerable judgment is required in evaluating structural consequences. A study of the interactions between shaking and faulting was conducted, and preliminary damage estimates were made. As a result of this study, we assumed that faulting was followed by shaking. Because any damage from shaking would be in addition to any structural damage from faulting, we believed that this procedure leads to the maximum estimated damage to the structures.

IV. RESPONSE TO VIBRATORY MOTION

A. Low-Bay Area

1. Interactions and Assumptions

The low-bay area response to earthquake vibratory ground motions is nearly independent of the responses of the RML cells, the basement, and the equipment contained in the basement. Interaction between the high-bay and low-bay areas is limited to a shear wall that they share (line 20 of Fig. 5).

The analysis of the low-bay area was a conventional equivalent static load study based on the following assumptions.

- The roof diaphragm is rigid relative to the shear walls.
- The walls had rigidities and capacities only in the direction of their lengths.
- Each wall section was considered individually because the steel columns can provide only limited force transfer and strain continuity from wall section to wall section.

Except for the inertial loading that they can contribute to the low-bay area, the additions to Building 102 were considered as separate structures. The annex to Building 102 is structurally separate from Building 102 and was not included in the analysis.

2. Description, Discussion, and Results of the Structural Capacity Study

The mass center of gravity of the roof diaphragm is required for both the elastic and ultimate capacity evaluations. The mass associated with the roof consists of the roof itself, the ceiling, the mechanical and electrical equipment supported by the roof, and one-half of the mass of all walls that are not self-supporting. The weight of the roof and equipment is estimated at 18 psf, and one-half of the weight of the non-structural partitions is estimated to average 24 psf for a total of 42 psf. Including the tributary weight of the concrete block and precast concrete shear walls, the effective weight of the entire low-bay roof system is 1160 kips. The center of gravity of the tributary mass to the diaphragm is shown in Fig. 13.

The elastic capacities of the individual walls are given in Table III. Openings, such as doors and windows, were considered in the analysis of capacity and rigidity of the shear walls. Rigidities were calculated considering only shear deformations. Under elastic conditions, the capacity and rigidity of the steel columns are small; hence, their effect was neglected. The capacity estimates given in Table III are associated with the dowels between the top of the walls and the steel roof beams or the Robertson steel deck. The center of rigidity or shear center (located as shown in Fig. 13) was calculated using conventional procedures.

Using 2% damping, the nominal elastic capacity of the low-bay area is about 0.05 g's PGA applied in either the N-S or E-W direction. The dominant deformation is torsion about the shear center. Because the interior partitions and 4-in. concrete masonry walls were not considered as structural walls, this elastic capacity estimate is conservative.

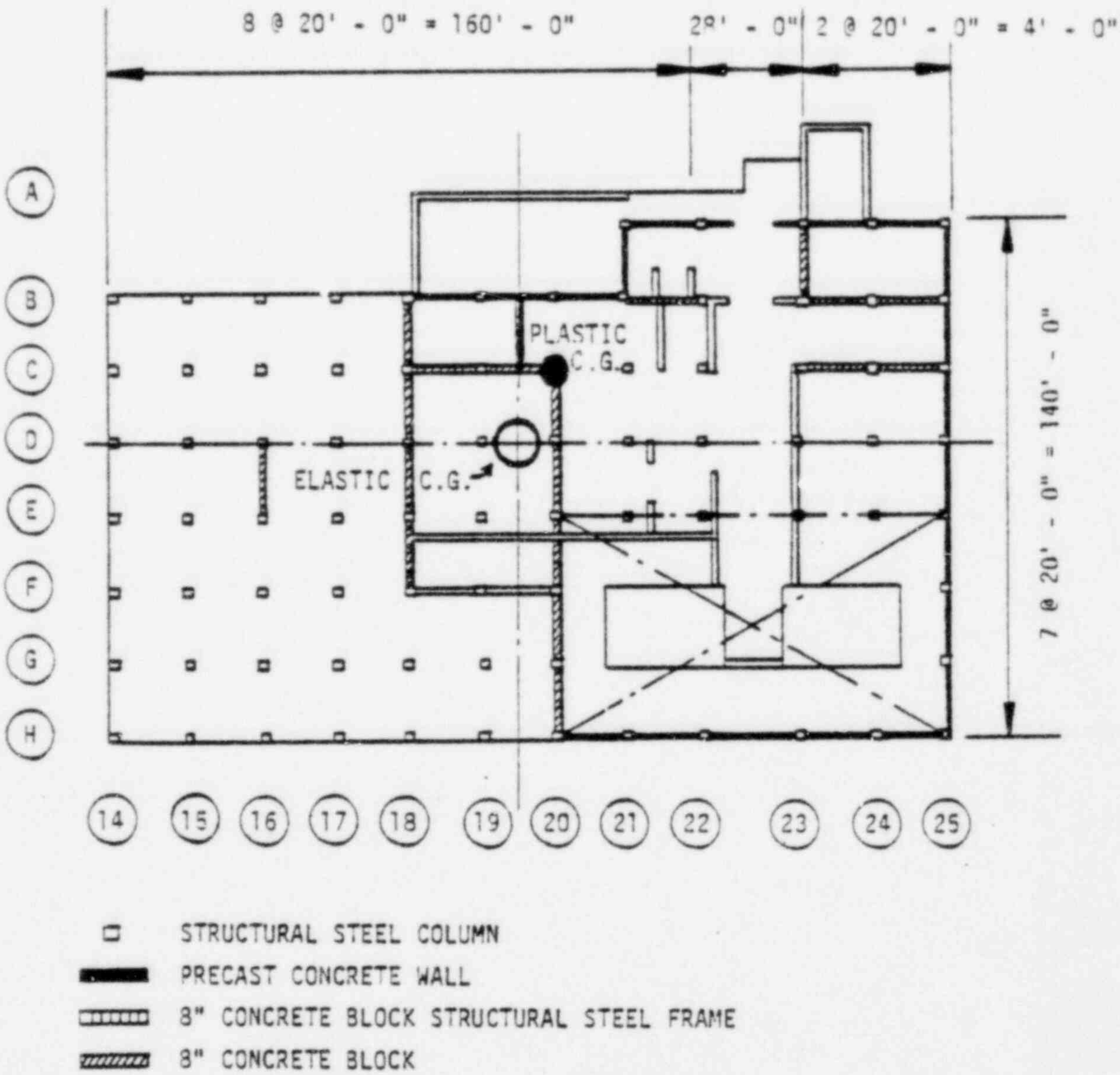

Fig. 13.
Low-bay roof diaphragm elastic and plastic centers of gravity.

TABLE III
LOW-BAY SHEAR WALL CAPACITIES

Wall No.	Elastic Capacity (kips)	Plastic Capacity (kips)
16-D-E	7.5	62.2
18-B-F	30.0	242.2
18-A-B	9.0	9.0
20-C-E	7.5	
20-E-F	7.5	
20-F-G	7.5	
20-G-H	7.5	302.2
21-A-B	5.0	14.0
21.3-B-C	10.0	20.0
21.2-D-E	7.5	15.0
22-B-C	10.0	20.0
22-D-E	7.5	15.0
23-ADD	10.0	20.0
23-A-E	22.5	45.0
23.9-ADD	10.0	20.0
25-A-E	20.0	60.0
F-18-20	15.0	122.2
F-18-19	15.0	
E-20-21	7.5	
E-21-22	7.5	60.0
C-23-25	15.0	122.2
B-18-20	10.0	
B-20-21	5.0	46.0
B-21-22	7.5	
B-21-23	4.0	
B-23-25	15.0	242.2
A-18-21	15.0	30.0
A-21-24	15.0	
A-24-25	5.0	60.0
ADD-23-24	7.0	14

The ultimate capacities of the individual shear walls are given in Table III. These shear wall capacities are determined by the capacities of the dowel connections between the top of the block walls and the steel roof system, the clip inserts that connect the precast wall panels to the steel roof frame, and the structural steel columns that project above the shear walls. The dowels and clip inserts are brittle and inelastic, whereas the steel columns are ductile. Also, as the columns yield, friction forces develop between the top beam of a bounding frame and the shear wall; hence, the loss of dowel capacity will be partially compensated by the development of additional capacity from the shear walls until the walls collapse or the structural steel joints fracture. The steel columns provide slightly more than one-half of the total lateral capacity, and the brittle connections provide the balance of the capacity. If strong ground motions continue for several building periods, the concrete block walls without a bounding frame are likely to collapse once the roof connection is broken.

The low-bay area mean N-S capacity is 845 kips. For all walls at their mean capacities, the center of gravity of resistance is shown in Fig. 13. The distance between the mass and resistance centers of gravity decreases as the low-bay moves from the elastic to the plastic regimes; hence, torsion effects are not as great at ultimate capacity.

The damping, ductility, and building period values are needed to estimate the overall strength capacity of the low-bay area. Considering the connection details and the nonlinear behavior of the low-bay structural elements, the damping was taken as 10%. Because the building period is unknown, the maximum amplification on the 10% response spectrum (Fig. 8) was used. Using a ductility of 1.65 and the maximum amplification of 1.65, the overall amplification factor is unity. Some of the low-bay shear walls are more severely strained than others; however, because the shear wall tests exhibited significant ductility, the ductility factor of 1.65 can be justified.

The low-bay strength capacities were determined by dividing the estimated ultimate low-bay capacities by the product of the low-bay roof weight and the overall amplification factor. The estimated static capacities of the low-bay area are therefore 0.7 g's in the N-S direction and 0.6 g's in the E-W direction.

Because the PAL is located in the low-bay area, its strength capacity is closely related to the capacity of the low-bay area.

B. High-Bay Area

1. Interactions and Assumptions

The high-bay area shares a shear wall with the low-bay area (Line 20 of Fig. 5). This wall was included in the analysis of the low-bay area; therefore, its resistance was not included in this analysis. The high-bay area interacts with the RML cells because the high-bay roof derives lateral support from the top of the cells and, if the south wall or the concrete masonry walls located adjacent to the cells collapse, the RML cells might receive additional loading. Because the RML cells are massive in comparison to the high-bay structure, we assumed that, in this capacity study only, the RML cells are rigid. The analysis is a conventional equivalent static load study based on the same assumptions used in the analysis of the low-bay area.

2. Description, Discussion, and Results of the Structural Capacity Study

The ultimate capacities of the various structural elements that are included in the high-bay structural system are found in Appendix B. The dead load of the high-bay roof system without the south wall is 24.5 kips.

For N-S motions, the south wall frames at plastic capacity can transfer a maximum horizontal force of 57 kips (1.0 g's static equivalent) to the roof system. With the roof dead load, the maximum possible disturbing force at 1.0 g's acceleration is 81 kips. The eight steel columns (lines 20 and 25 of Fig. 13) and the steel bracing between the tops of the cells and the roof system have a total mean resistant capacity of 133 kips; thus, the strength in the N-S direction is limited by the knee-braced frames to an equivalent mean static capacity of 1.0 g's. Collapse occurs to the north toward the RML cells. If this wall impacts the RML cells, they will not be damaged.

The two N-S high block walls (lines 22 and 23 of Fig. A-6) would contribute to the resistance of the roof system provided that they do not fail. The dynamic capacity of these walls is about 0.5 g's normal to their surfaces (in the E-W direction); therefore, it is unlikely that they can survive to an acceleration of 1.0 g's. Their effect on the resistance of the roof system was neglected.

For E-W earthquake motions, the resistance to inertial forces is provided by the perimeter columns, the roof-to-cell steel bracing, and the E-W concrete block wall that is located between the cells and that connects to the Robertson steel deck. The total mean resisting capacity in the E-W direction is 153 kips. Earthquake-induced horizontal forces in the E-W direction are less than those induced by N-S earthquake motions (81 kips); therefore, the roof system is capable of surviving earthquake accelerations in excess of 1.0 g's.

The first structural element in the high-bay area to damage would be the two interior high block walls. Their capacity is about 0.5 g's, and they would collapse around the RML cells. The next structural element to fail would be the east wall. Its capacity is about 0.7 g's, and it would fall to the east with possible damage to the east side columns. The capacity of the high-bay roof is in excess of 1.0 g's, but, because it is connected to the RML cells, its capacity is determined by the overturning capacity of the RML cells.

C. RML Cells

1. Interactions and Assumptions

The two RML cells are two-story reinforced concrete boxes. The ground floor reinforced concrete floor slab over the basement, the basement wall, and the wall footing are continuous with the cell construction. The structural features of the RML cells are shown in Appendix B. Figure 14 shows the section through the window and equipment openings that determine the strength of the cells. The lower 17 ft 4 in. of the cells are in contact with the soil on three sides. On the north or basement side, the cells have a common party wall with the basement. The basement floor slab is not connected to the basement walls. The heavy ground floor slab over the basement is continuous with the cells on the north side only. The slab on grade on the other three sides of the cells does not connect to the cells.

The analysis of the RML cells was performed using simplified engineering procedures to determine the structural consequences of vibratory ground motions. The cells are both stronger and more resistant to rocking in the E-W than in the N-S direction; hence, a detailed analysis of the cells in the E-W direction was not considered necessary. Because of the relatively heavy weight of the cells, soil structure interaction was considered in the dynamic analysis of the cells. The weight of the heavy shielding doors was included in the analysis, but they were not considered to resist motions.

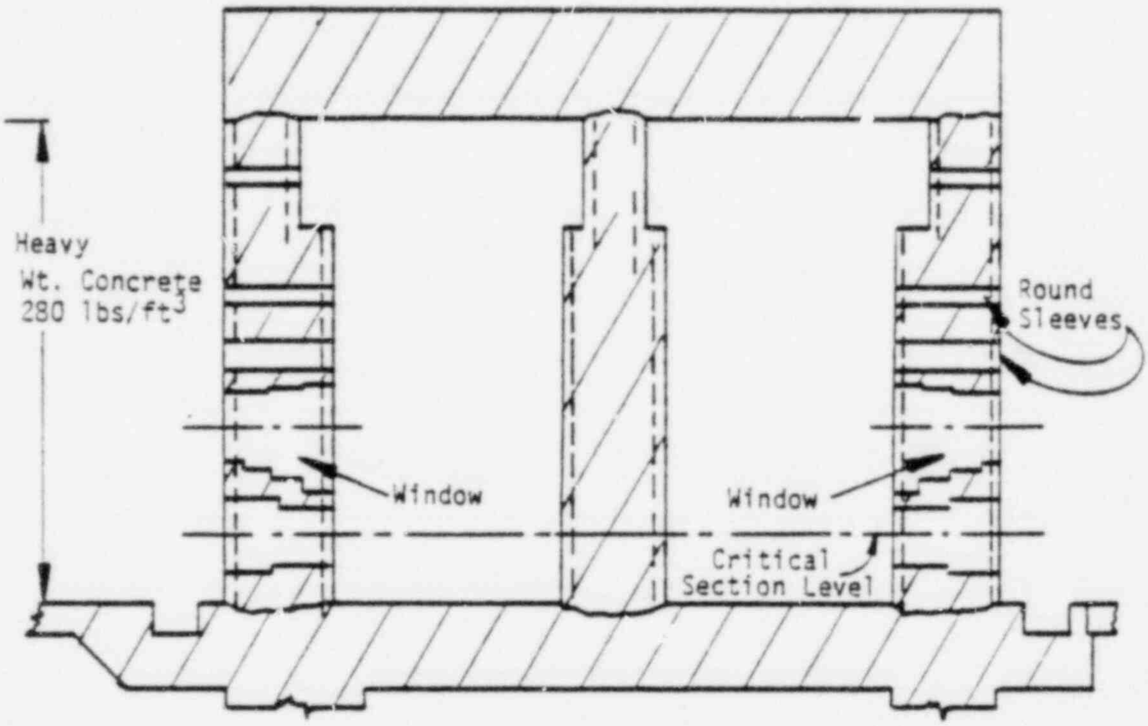

a. Partial section through cell showing windows.

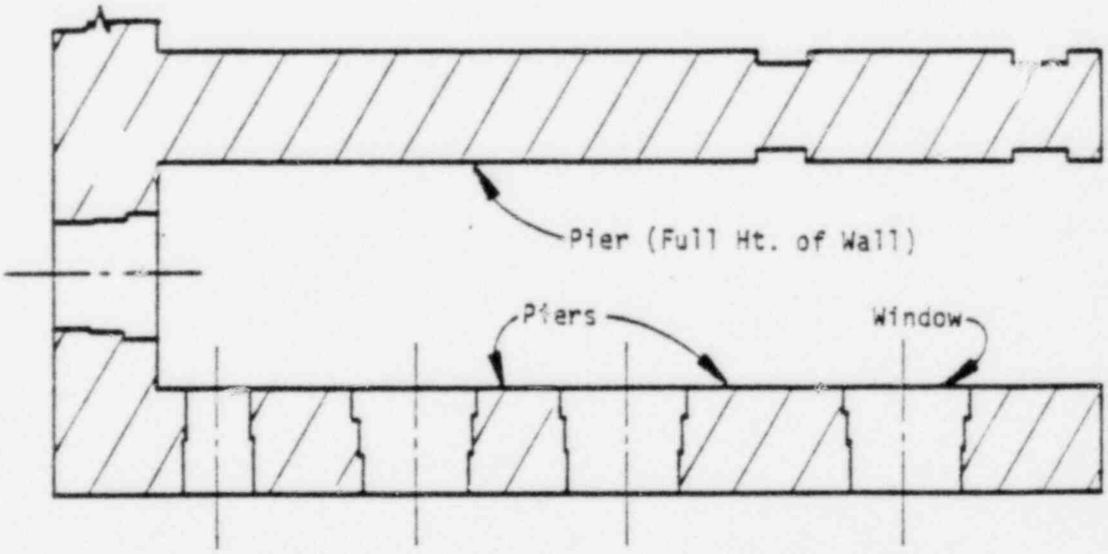

b. Partial horizontal section through windows showing piers.

Note: All doors and openings lined with steel plate welded joints.

Fig. 14.
Sections through RML cells showing windows and openings in cell walls.

2. Description, Discussion, and Results of the Structural Capacity Study

The total weight of each cell unit is 2930 kips, and its center of gravity is 18 ft above the mat footing level. or about 2 ft above the ground floor level. The weight includes the weight of the high-bay roof that is tributary to the cells, but neglects the weight of the small access wall that extends into and is continuous with the basement system. The resulting mean soil pressure under the cells is 3.6 kips/ft^2.

The ground floor slab will resist rocking motion. Reinforcing steel (25.79 in.^{2}) connects the floor slab over the basement to the cells at the ground floor level. The mean axial tensile capacity is 1210 kips at yield of the reinforcing steel. Considering the ground floor capacity to be that of the steel alone, overturning is incipient at a load equivalent to a static horizontal acceleration of 1.0 g's. The basement wall has only a minor influence on the response to motion in the N-S direction.

A dynamic analysis of the RML cell unit was made to determine the fundamental period of vibration in the N-S direction. A simple single mass and fixed-base model of the above-grade part of a cell unit yielded a period of vibration of 0.02 s; hence, the cell structure was considered to act as a rigid body. Another dynamic model was developed to obtain the vibration modes associated with soil-structure interaction. The ground floor reinforced concrete slab acts as a spring, and its stiffness was calculated assuming that the floor slab acts as a deep beam supported by the N-S basement walls. The soil-structure constants were calculated using formulas from Novak.[25] The dynamic model is shown in Fig. 15 along with the values of the parameters. The first mode of vibration is foundation rocking with a period of 0.14 s. The second mode (horizontal translation) has a period of 0.076 s. Using 10% damping and a ductility of 2.0, the dynamic capacity is limited by the vertical reinforcing in the walls of the cells in the piers. The capacity level of 0.90 g's is associated with the start of limited cracking in the piers between the observation openings. The failure mode is shown in Fig. 15. The cells response elastically up to their capacity.

Overturning of the RML cells is not probable. The cell displacements at the ground level are limited by floor slabs. In addition, soil pressures acting on the below-grade part of the cells add resistance to overturning.

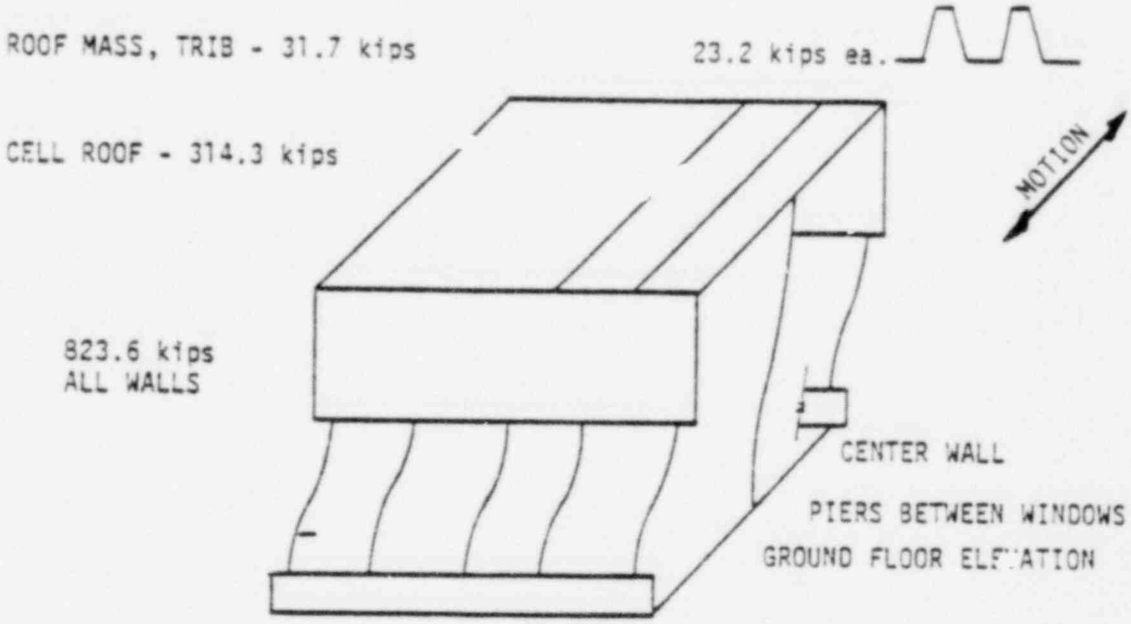

a. Deformation in piers

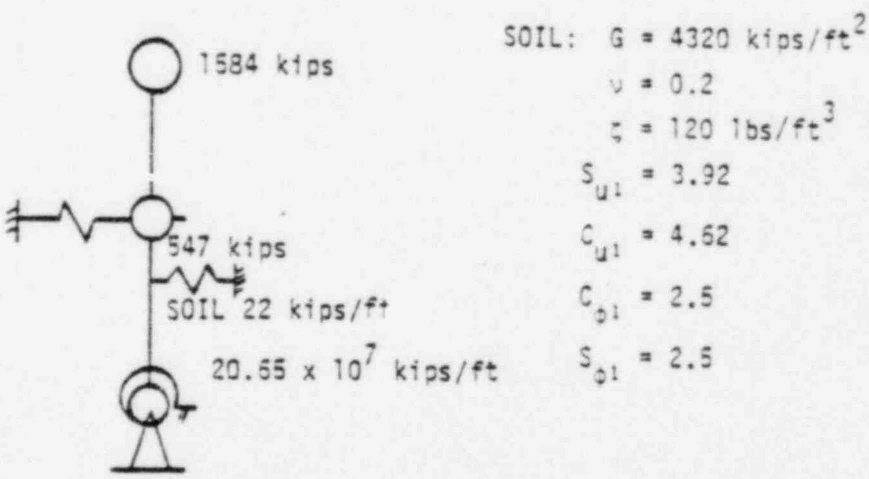

b. Dynamic model

Fig. 15.
Structural models.

Material from adjacent construction may collapse onto the cells; however, damage to the cells would be negligible.

D. Basement and AFL

1. Interactions and Assumptions.

The RML cells are monolithically connected to the basement roof slab and to sections of the south basement exterior walls. Also, the RML cells form a part of the south basement enclosure (Fig. 6). The basement roof slab serves as a floor slab for part of the low-bay area. The PAL is located on the ground floor and above the basement area. Any collapse of structural elements in the low-bay area and above the basement area would produce additional loads on the basement roof slab.

The basement capacity analysis was based on an equivalent static load study and the capacities of the structural elements forming the basement structural system.

2. Description, Discussion, and Results

A standard working stress analysis similar to that used in the original design was performed by EDAC. This analysis was used to identify possible weaknesses in the design and to obtain an estimate of the level of conservatism in the original design. The working stress design was satisfactory, and consistent normal levels of conservatism were used.

An ultimate strength static load type analysis using yield line concepts for assessment of the capacity of the basement roof slab, columns, and column footings was also performed. The live load capacity at ultimate is about 700 lbs/ft^2. This compares with an actual average live load plus the weight of the walls and roof that does not exceed about 200 lbs/ft^2. The capacity of the columns, walls, and footings is consistent with the capacity of the slab. Collapse of the ground floor construction onto the slab may produce minor vibrations and cracking, but the basement roof slab will not collapse under this loading.

Because the relative deformations between the roof and floor slabs will be small, little or no load will be applied to the block partition walls around the AFL and in a direction parallel to their length; hence, they do not act as shear walls. The shear forces will be carried by the exterior concrete basement walls. The interior concrete block walls are restrained against rotation at top and bottom for deformations perpendicular to the wall face. As fixed-end beams, their period of vibration is about 0.01 s; therefore, they respond as rigid bodies to earthquake vibratory ground motion.

Another evaluation was a pseudo-dynamic analysis of the outside reinforced concrete basement walls for out-of-plane loads that are produced by soil pressures. The earthquake surcharge is associated with a 0.6 g's horizontal acceleration and, assuming that the wall acts as a simple beam, the basement walls attain their ultimate strength at this loading. The seismic surcharge was computed in accordance with Seed and Whitman with a 0.6 g's maximum acceleration.[26] An equivalent fluid pressure for one-half the soil unit weight distributed uniformly from top to bottom of the walls was used for the earthquake surcharge. The analysis used a trapezoidal loading on the wall of 330 psf at the top of the wall and 990 psf at the bottom of the wall. The wall height is 11 ft.

LASL and EDAC concluded that the reinforced concrete ceiling slab, column, bearing wall, and footing system have sufficient strength to survive the vertical loads produced by the roof and ground floor walls collapsing onto the slab and by vibratory ground motion. The concrete partition walls are adequate for similar vertical load levels. The capacity of the block walls for loads normal to their face is 1.9 g's based on the yield strength of the vertical reinforcing steel and assuming that they are connected to the basement roof and floor slabs.

E. Critical Equipment

1. Interactions and Assumptions

The structural condition of the glove boxes is dependent upon the structural condition of the basement floor and roof slabs and the AFL block walls. The glove boxes are connected to these structural elements. The ventilation ducts are connected to the roof slab and the glove boxes.

The capacities of the glove boxes were determined using response spectrum techniques and an equivalent static load study.

2. Description, Discussion, and Results

Including the stand and the enclosed equipment, glove boxes 37, 39, 41, and 44 each weigh approximately 1300 lbs. Without equipment, they each weigh about 1000 lbs. The stand weighs about 200 lbs. Without the bolted connection between the glove box and the stand, incipient overturning would occur at a horizontal static acceleration of 0.5 g's acting perpendicular to the face of the glove box.

Horizontal loads applied perpendicular to the faces of glove boxes 37, 39, ar 41 are resisted by the two end stand frames. For motions in this direction, the first mode period of vibration is 0.09 s. If a load is applied to these same glove boxes and in the direction of their length, resistance to motion is provided primarily by the rear three-legged bent because the center leg in front is removable and no horizontal pipe brace is provided (Fig. 16). Torsional motion is resisted by the two end bents and by the back bent. The period of vibration of the assembly in the longitudinal direction is 0.2 s. Assuming elastic response and 5% damping, the capacity is 0.7 g's PGA with the failure associated with the failure at the foot of the frame connection and of the connection of the tie downs to the frame. Failure of the tie downs would allow the glove boxes to slide on the floor, but they will not overturn; hence, the ultimate capacity is somewhat larger than 0.7 g's PGA. Even minimal yielding will allow the glove box and stand to move and vibrate on the floor; therefore, no allowance for ductility is made in this assessment. Each of the corner legs is connected to the floor slab by a 1/4-in. bolt through the foot on the adjusting screw (Figs. 16 and 17). These light connections were not considered in the capacity evaluation. If these light connections are considered to be fully effective, the capacity of the glove box assembly is increased to about 1.0 g's PGA.

Glove box 23 is rigidly connected to the block wall behind it and to the reinforced concrete floor slab; therefore, its capacity to resist motion depends on the connections and the wall and slab. Glove boxes 51 and 51A are similarly connected to the reinforced concrete wall behind the glove box and the overhead reinforced concrete slab, whereas glove box 50 is connected to the reinforced concrete floor slab and the overhead slab. These connections are rigid in nature and resist relative displacements in both horizontal directions. They have a static load capacity in excess of 1.0 g's PGA.

The steel straps used for connections are stronger than the 1/4-in. and 3/8-in. Phillips Red Head expansion bolt connections to concrete or concrete block. The connections to the glove boxes are also stronger than the connection to the concrete or the concrete block.

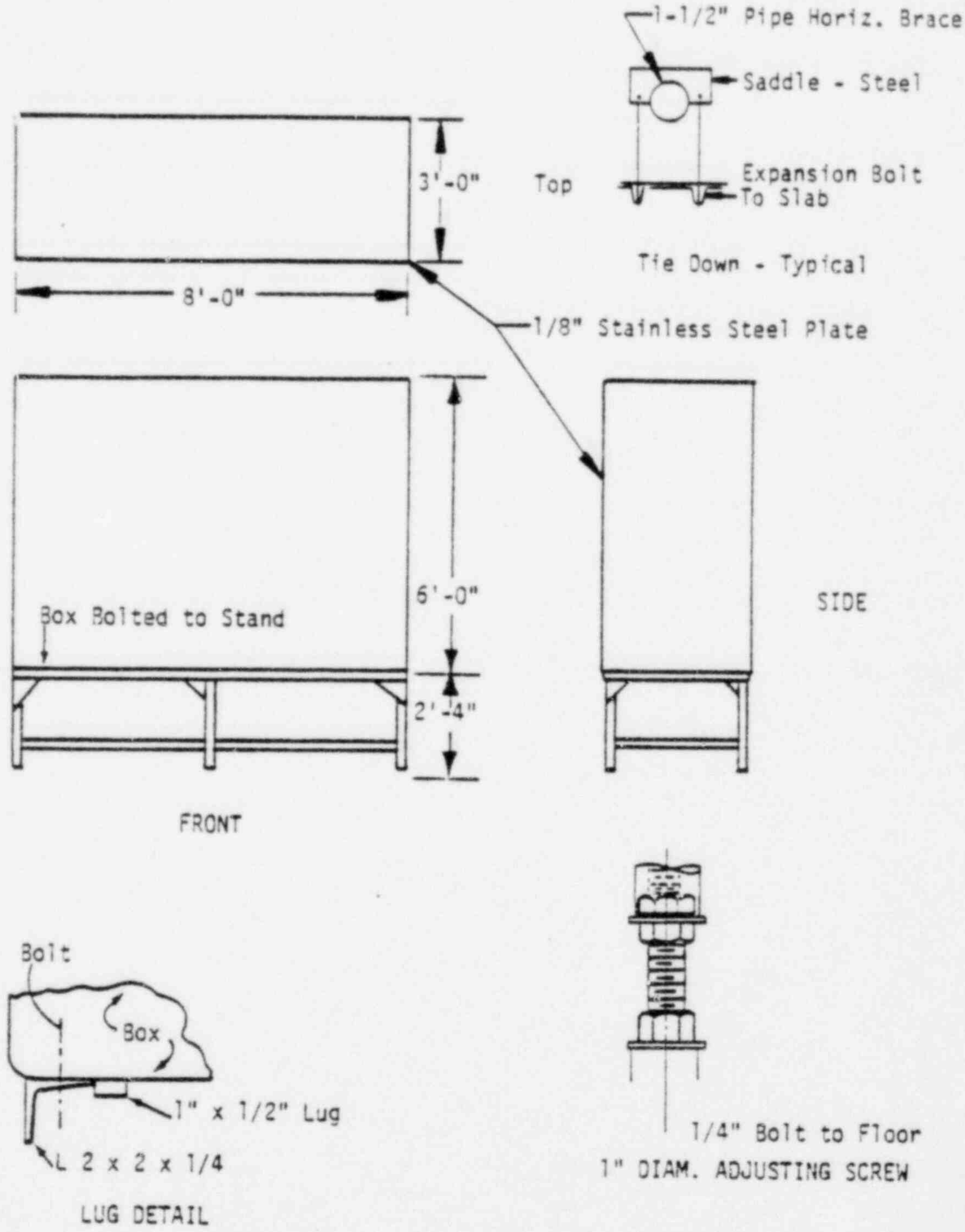

Fig. 16.
Glove box and stand, glove boxes 37, 39, 41, and 44.

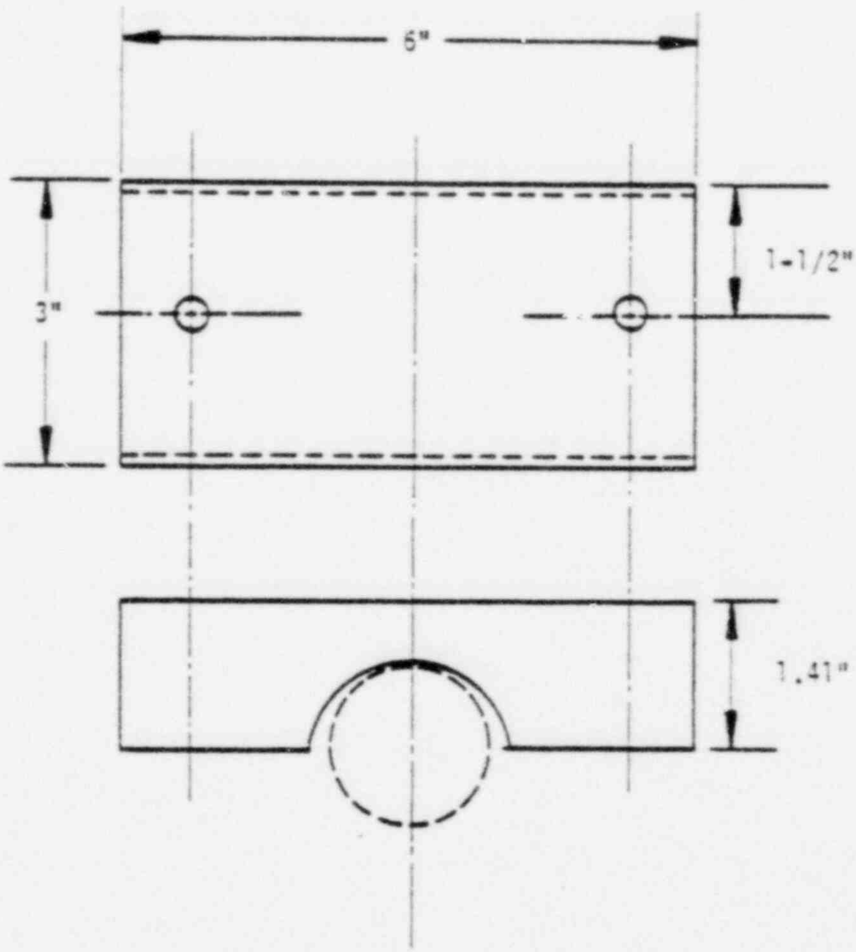

Fig. 17.
Details of saddle.

V. RESPONSE TO FAULTING

A. Introduction

Structural consequences from faulting were not addressed for the low-bay area. Except for the PAL, this part of building 102 does not include critical areas pertinent to safety. The PAL is located above the basement area; therefore, its structural consequences from faulting are directly related to the basement structure.

The high-bay area provides protection for the working area about the RML cells, and therefore it does not include critical areas. Structural consequences from faulting were not considered for this area.

B. RML Cells

Passive earth pressures that develop during faulting can be large and produce structural damage. The precise distribution of passive pressures around the perimeter of the below-grade walls is unknown and difficult to estimate. A possible distribution is suggested in Fig. 18. The suggested distribution is judgmental and is presented only to show the basic disturbing forces imposed by fault movements occurring under the RML cell foundation. This pressure distribution is partially based on a review of Ref. 27.

Because of the fault orientation, the full passive pressures will not act normal to the RML cell or basement walls nor will the full passive pressure be developed along the entire length of these walls; however, in the analyses, the below-grade walls were assumed to be subjected to a full passive pressure distribution along the length of the walls. This assumption leads to overestimates of the applied loads and has the effect of neglecting the directional properties of the fault.

Three wall sections were selected (Fig. 19) for yield-line analyses with full passive pressure distribution. Wall section (1) is a 1- by 12-ft strip of the 12-in. thick basement wall. The length of this wall is greater than twice its height; hence, the 1-ft wide strip is used. Wall section (2) is a 14-ft by 9.5-ft by 12-in. RML cell retaining wall panel. Wall section (3) is a 12-ft by 19-ft by 26-in. RML cell foundation wall. The aspect ratios of walls (2) and (3) are less than two; hence, two-dimensional effects are considered in the yield-line analyses of these walls.

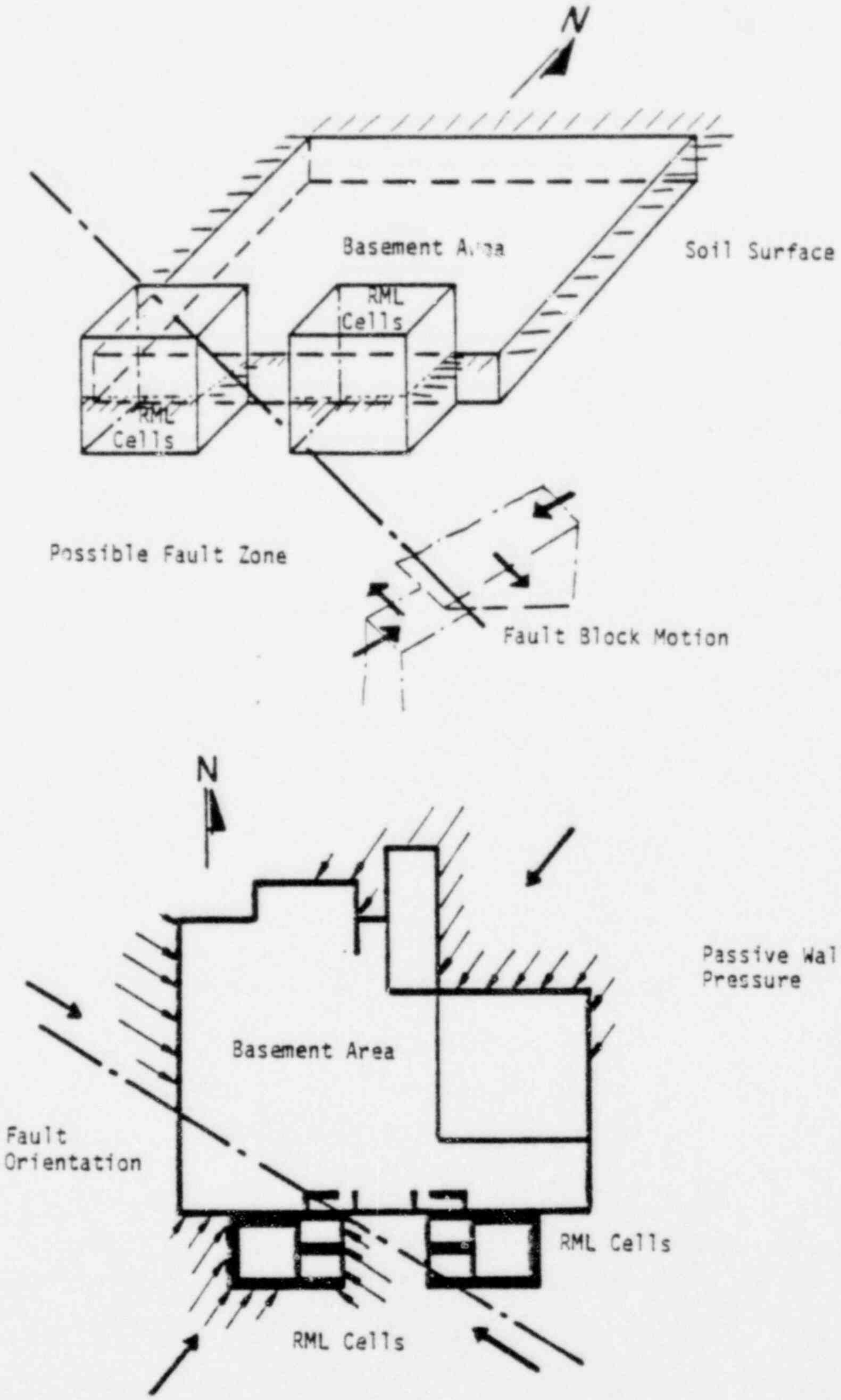

Fig. 18.
Fault location and suggested passive wall pressure distribution.

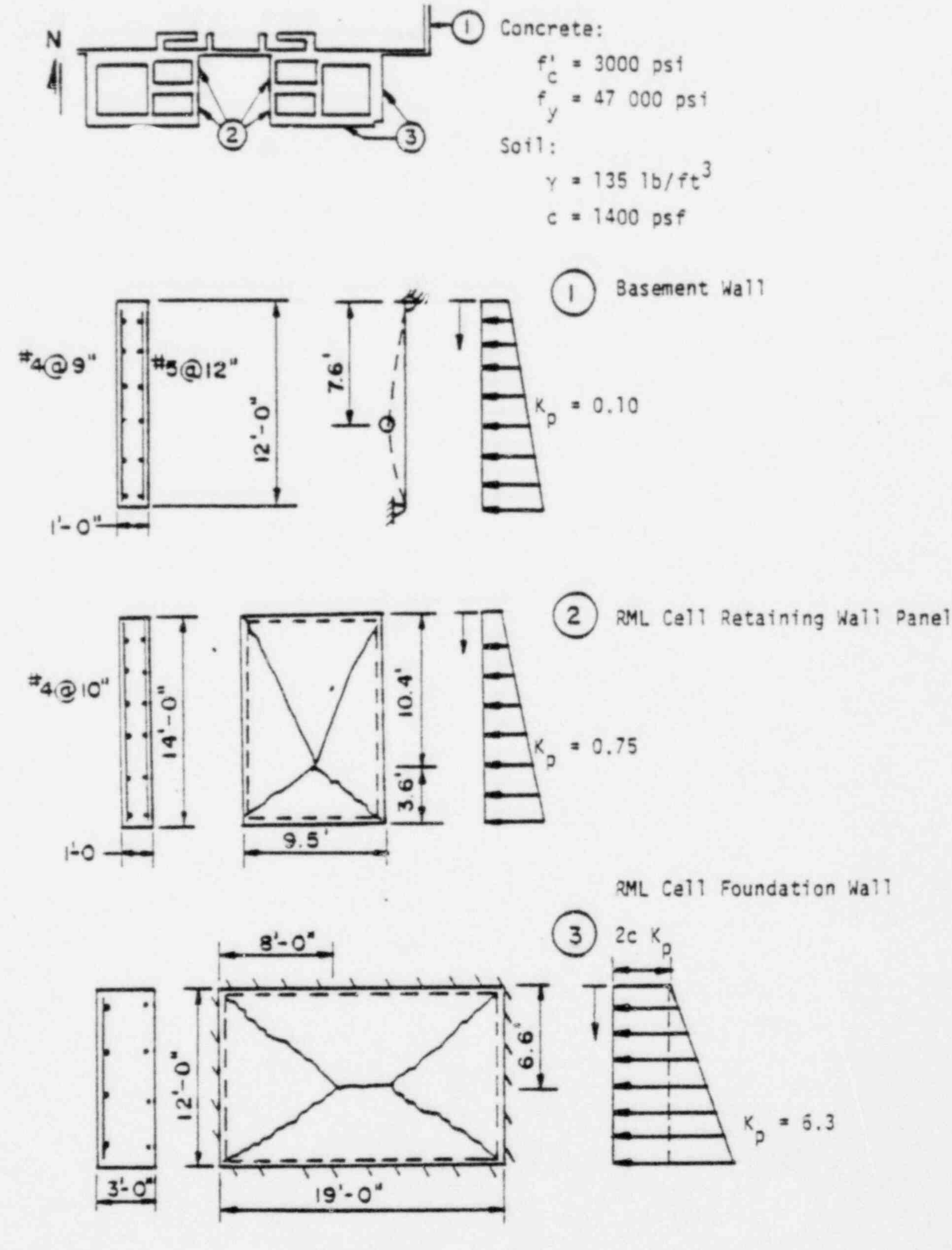

Fig. 19.
Summary of wall yield-line analysis.

We consider Ref. 22 to provide the best available procedure for estimating the static passive resistance of cohesive soil. Using the soil parameter values $\phi = 30^{\circ}$, $\delta = 15^{\circ}$, c = 1400 pcf, and a = 700 pcf, the total horizontal wall thrust per unit width P is given as

$$P = 1/2\ K_p\ H^2 + (qK_p + 2c\ \sqrt{K_p})\ H = 2.32\ H^2 + 4.14\ qcH,$$

where H is the wall height.

The surcharge q is used only if the soil above the walls support a part of Building 102. A conservative q-value of 250 pcf was used in the analysis of wall section (3). Wall section (1) had no surcharge and, because wall (2) would fail before the full passive pressure was activated, the refinement of including the effect of q was meaningless.

For each of the wall sections, the minimum value of the coefficient of passive pressure, K_p, needed to produce a collapse mechanism was determined. The yield-line collapse mechanisms and the coefficients of passive pressures are indicated in Fig. 19.

The total thrust per unit width required to produce the yield-line collapse mechanism and the maximum thrust developed by passive earth pressures for the wall sections are given in Table IV. Failure is expected whenever the passive pressure thrust exceeds the thrust producing the yield-line collapse mechanism. The 12-in. walls would therefore be expected to fail, whereas the 36-in. wall would not be expected to fail in flexure.

The applied pressure magnitudes obtained from a yield-line analysis represent an upper bound; however, consideration of deep beam effects (thickness/span ratio $\leq$ 1/4), in-plane edge restraint,[28] and the development of membrane forces will result in an underestimate of the total wall capacity. Consideration of these effects coupled with the assumptions on the passive pressure distribution, yields wall capacity estimates of total wall resistance that represent a lower bound of the total capacity. In addition to the yield-line capacity evaluation, the shear capacity of the 36 in. wall section was determined. The results indicate that the shear resistance (assuming a punchout failure mode and τ_{ult} = 110 psi) is approximately equal to the yield-line wall thrust. The wall capacity is therefore greater than the applied soil pressure, and failure of the 36-in. cell walls is not probable for the imposed faulting criteria.

TABLE IV

APPLIED AND RESISTING LOADS FOR SEVERAL CONCRETE WALLS

	Yield-Line Collapse $(P/H)_{fail}$ (lbs/ft)	Maximum Passive Pressure $(P/H)_{max}$ (lbs/ft)
12-in. Basement--slab	970	11050
12-in. Cell retaining--wall	3130	12700
36-in. Cell foundation--wall	12130	12080

The failure of the 12-in. retaining wall panel does not have any major structural consequences for the RML cell load-bearing foundation walls. The panels serve only as a soil-retaining wall, and thus the only consequence of failure is entry of soil into the nonfunctional below-grade space of the RML cells. Failure of the basement walls will have only a minor effect on the response of the RML cells. The ground floor slab that is integrally connected to the cells transfers in-plane shear forces to the basement walls provided the slab-cell connection remains effective. If the slab-cell connection is severed, the basement slab and wall system helps to prevent overturning of the RML cells.

If a structure rests on both fault blocks and fault movement occurs, the loss of continuous base support is probable. The final actual support condition cannot be predicted; hence, the support conditions that produce the most severe structural stress conditions are used. The postulated support cases considered (Ref. 29) are indicated in Fig. 20. In one case we assume that the RML cell is supported at two edges and, in the second case, we assume that the RML cell is supported near its middle. These two support cases are referred to as the simple span and cantilever supports. The passive distributions and soil failure zones caused by fault movements are indicated in Fig. 20.

The basement walls and the basement roof slab are monolithically connected to the RML cells. The effects of these structural elements were evaluated. The minimum vertical shear resistance of the basement walls and the basement

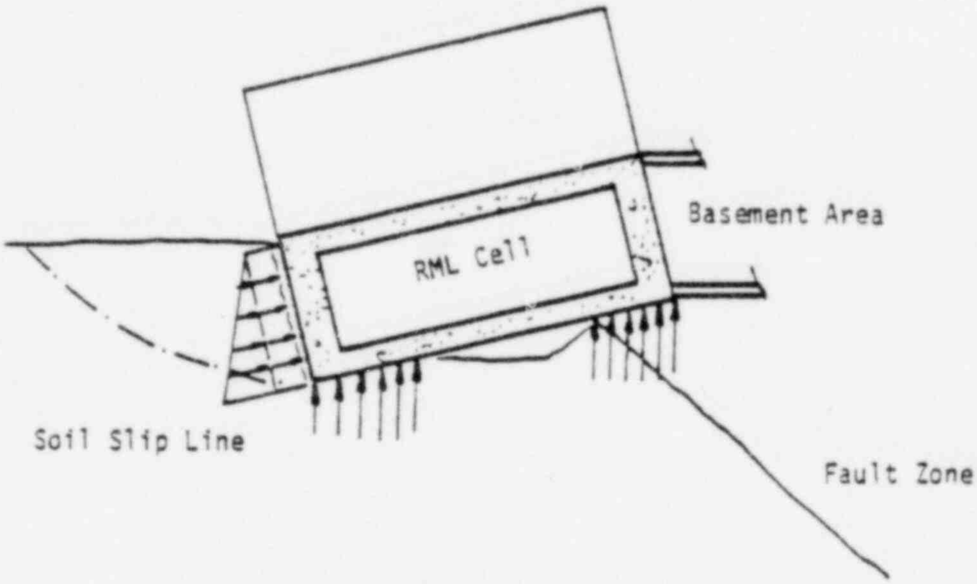

a. Case I: Simple span support.

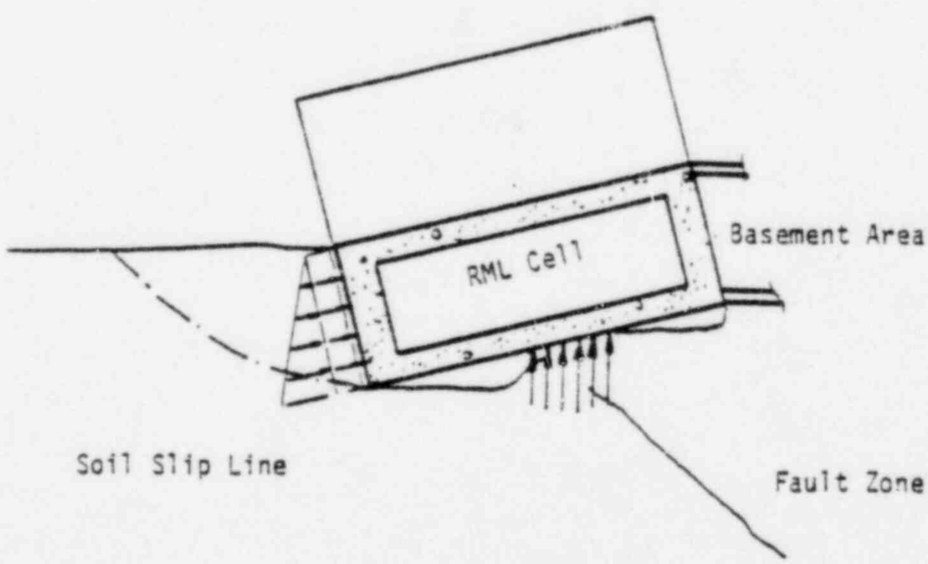

b. Case II: Cantilever support.

Fig. 20.
Surface offset analysis cases.

roof slab was computed. The shear resistance of these structural elements is about 30% of the total weight of a RML cell. This resistance is insufficient to consider the basement walls and roof slab to act as a support in the loss of base support analyses.

The tensile strength of the basement roof slab was computed and compared to the reaction required to prevent movement of the cell away from the roof slab. The maximum tensile strength developed by the basement roof slab is about one-half of the strength required to prevent cell movement away from the slab.

The interaction of the basement floor slab with the cells was also evaluated. The floor slab is not monolithically connected to the cells; therefore, the interaction is directional. For passive earth pressures pushing the cells towards the basement area, the basement floor and the basement roof slab will prevent large rotations of the cells. Because of the postulated Verona Fault orientation and movements, the cells would be pushed toward the basement area. Compressive axial forces would then develop in the floor slab. Computations indicate that the induced compressive axial forces will not buckle the basement floor slab.

Because of the lack of a specifically defined faulting criteria, the most severe loading conditions have been assumed. The interaction of the basement walls and basement roof and floor slabs with the RML cells is uncertain under these conditions; hence, this interaction is neglected. Neglect of this interaction leads to an underestimate of the capacity of the RML cells to resist seismic forces.

The loss of continuous base support results in a redistribution of reactions to the dead load (gravity) forces. These dead load forces were assumed to be resisted by the below-grade box structure that consists of the foundation walls, base slab, and cell floor. Distributed and concentrated dead loads supported by the RML cell foundation were transformed to a line load acting along the cell box diagonal as shown in Fig. 21.

The cell box structure was analyzed as a simply supported beam and as a cantilevered beam. The flexural resistance of the box structure was conservatively estimated from the axial forces in the steel reinforcement in the cell floor and base slabs. The shear resistance was computed considering only the concrete area in the foundation walls and the concrete shear strength.

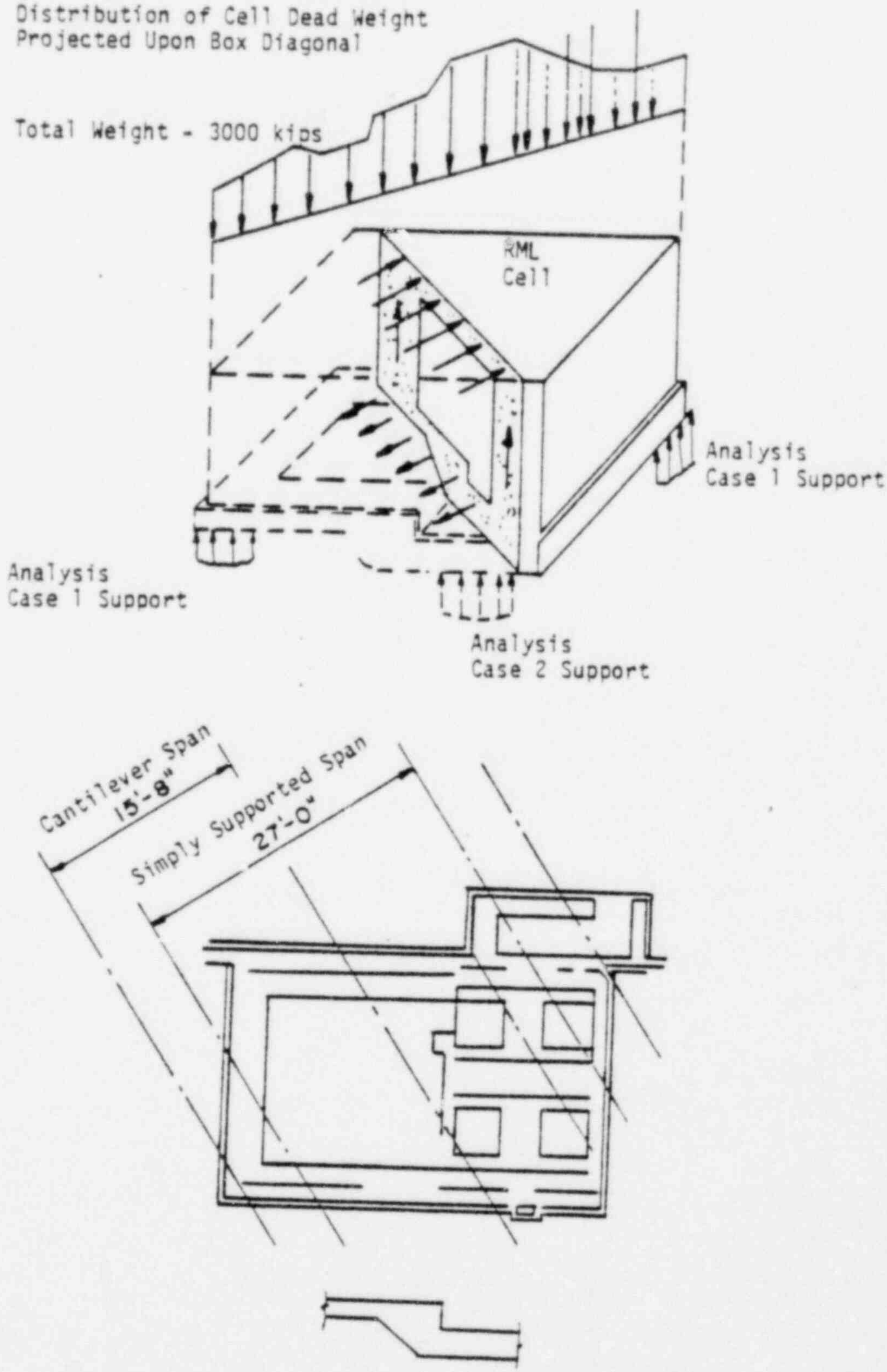

Fig. 21.
Cell dead weight reaction.

The analyses show that the slab steel reinforcement is stressed to about 70% of the yield strength (47 000 psi) from the dead weight loads for both assumed support conditions. The dead loads produce shear forces within the walls that are about 50% of their ultimate shear capacity. The box structure is not independent from the above-grade cell structure; hence, the entire cell has greater resistance than the simple box beam considered in the analyses.

The loss of continuous base support beneath the RML cells leads to increased soil pressures at the remaining reaction regions. The effects of these localized soil pressure increases on the RML cell structure are examined. The soil-bearing pressure is limited to 20 ksf; hence, the contact area between the soil and the cell cannot decrease below a value compatible with the cell weight and the soil bearing pressure. Before determining the minimum contact area, we had to evaluate the strength capacity of the base slab. The computed bearing pressures corresponding to the assumed mechanisms occurred within the range of 4-5 ksf. The bearing pressures in the vicinity of the assumed support points will approach the ultimate soil bearing pressure of 20 ksf; hence, damage to the base slab is probable. Approximately 40% of the base slab area is bearing foundation wall; thus, the loss of slab resistance will simply transfer the bearing loads to the areas directly beneath the foundation walls.

The wall surface shear forces that depend upon the wall roughness and the soil cohesion are an additional consideration. The direction of these wall shear forces depends upon the relative movement between the soil and the cell foundation walls. These surface forces were assumed to act upwards when the passive soil pressures were computed because of increasing the passive soil pressure. An upward surface force would aid in supporting the cell, thereby resulting in a smaller soil-bearing pressure. If the surface forces acted downward, the soil bearing pressures and/or soil bearing contact area would be increased; however, the computed passive soil pressures would be less. The actual surface force magnitudes and directions cannot be determined without a knowledge of the exact fault location and fault dip angle; hence, they were not directly included in the cell support analyses.

We conclude that the above-grade RML cell structure will not suffer major structural damage from loss of base support from the defined fault displacements. The cells have the strength to act as either a simple or cantilevered beam. The foundation base slab could be damaged by the redistribution of soil-bearing pressures; however, its failure only affects the below-grade nonfunctional space of the RML cells. The cell retaining walls could collapse and soil enter the below-grade cell space; however, this does not affect safety.

C. Basement and AFL

1. Introduction

The procedure for evaluating the structural consequences was:

(1) Evaluate the strength characteristics of the structural elements and examine the interaction between the different structural elements; and

(2) Assume specific fault parameters (location and direction) and determine probable damage levels to the basement area, glove boxes, and containments as the fault slip and thrust increase.

The task of evaluating the structural consequences of faults is arduous. Strengths of individual structural elements are simple to evaluate; however, structural systems coupled with fault interactions are difficult to evaluate. The basement structural system includes exterior and interior walls, columns, and roof and floor slabs, all interacting to form a highly indeterminate system. Indeterminate systems provide greater overall strength because the loads carried by individual structural elements that become overloaded are transferred to adjacent structural elements that are not overloaded. Collapse of the system does not occur until a sufficiently large number of structural elements fail; hence, a local failure does not lead to collapse of the entire structure.

The evaluation of the loads that act upon the structure presents the major difficulty in determining the structural consequences. The loads determine the structural behavior, yet they depend upon the structural behavior and fault characteristics. The fault parameters--direction, width, and slip and thrust magnitudes are currently unknown. Information on the soil properties at the site is minimal, and the properties will change because faults disturb the soil. In addition, the presence of structures within the fault zone can locally change the fault characteristics. Little documented information on the effects of structures on faults is available. The available information is very limited.[30] Evaluations of the structural consequences of faults intersecting structures therefore requires considerable judgment.

LASL established that fault movements cannot shear the basement structure. Because the basement walls fail at relatively low passive soil pressures, forces of the magnitude required to shear the basement structure cannot develop. The maximum passive soil pressures considered in this study were taken from Ref. 22. These pressures were based on incomplete soil test data and on undisturbed soil samples. During a fault the soil would be locally disturbed; hence, its properties would change. The strength of disturbed soil is less than the strength of undisturbed soil. The weaker the soil, the less the damage to a structure subjected to fault movements. LASL also assumed that the fault movement rates were slow and that inertial forces could be neglected.

2. Evaluation of Structural Damage From Faults Intersecting the Basement

The primary confinement of the radioactive materials is the glove boxes; therefore their integrity is the primary consideration in this study. We looked at the structural action that can lead to damage or collapse of the glove boxes.

The primary confinement area has walls in contact with the soil on the north and east sides as indicated in Fig. 6. All three of these wall sections are short (about 15 ft), and they could collapse in a fault; however, only the collapse of the wall section on the southeast side could damage glove box 51 and possibly glove box 50. The two confinement walls in the northeast corner of the Fuel Lab East may suffer slight damage, but they are not likely to collapse. They are protected by the basement area that was later backfilled with soil. The heavy RML cells protect most of the south side; however, there are three short basement wall sections that could collapse during a fault. These wall sections are all about 20 ft from the south confinement walls of the fuel labs; hence, they pose no threat to the confinement walls unless the fault movements are severe. On the east side, there is a distance of about 20 ft between the exterior basement wall and the confinement wall of the Fuel Lab West. The basement wall could collapse and allow soil to enter the between-wall space; however, the fault movement would have to be in excess of about 25 ft before failure of the west confinement walls becomes credible. Collapse of the west exterior basement wall could lead to a partial collapse of the roof slab over the space between the basement and confinement walls; however, the collapse hinge in the roof slab would form outside the drop panels. This would not necessarily lead to damage to the confinement wall because the wall and columns would continue supporting the roof slab over the fuel labs. Also, the soil pushing into the between-wall space would prevent the roof slab over this space from collapsing onto the basement floor.

In the previous discussion, we examined the structural consequences resulting from slip movements, but slip and thrust occur simultaneously. Both fault movements produce passive soil pressures. The cause of the pressures on the walls was not considered; hence, the evaluations remain valid. Passive soil pressures have a limiting value that is independent of the direction, provided the soil is considered isotropic.

The vertical movement caused by the thrust movement tends to raise one side of the basement structure relative to its opposite side. This movement is the most severe when potential damage to the glove boxes and confinement area is considered. These vertical fault movements could produce localized differential displacements in the structure as indicated in Figs. 22 and 23. These differential vertical movements can lead to crushing of the walls, both exterior and interior, in the fault zone width. This could cause a breach in the basement confinement and the primary confinement walls; however, because these walls are located below-grade, their failure alone would not result in an open path to the atmosphere. Because several glove boxes are attached to an interior wall, these glove boxes might be damaged.

A vertical differential displacement can also produce the flexural failure mode shown in Fig. 24. Two plastic hinge lines would form, one on each side of the fault zone. Because of the reinforcing steel, the slab section will not collapse, but concrete debris could fall upon the glove boxes below the hinge line and damage the glove boxes.

The vertical fault movement can also cause the floor slab to move upward toward the roof slab. This action can severely damage the glove boxes that extend from the floor to the roof. The floor slab upward movement is limited by the presence of the column footings and the interior concrete masonry walls. As the floor slab tends to move upward, the column footings will pick up the loads; hence, the floor slab upward movement is limited.

Both the roof slab and floor slab failure distortions are made more severe by the thrust movements. Compressive forces develop within the planes of the floor and roof slabs and the walls. These forces would cause the walls and slabs to buckle in the region of the fault zone because of the distortions induced by the fault movements. The effect is to cause more damage to the glove

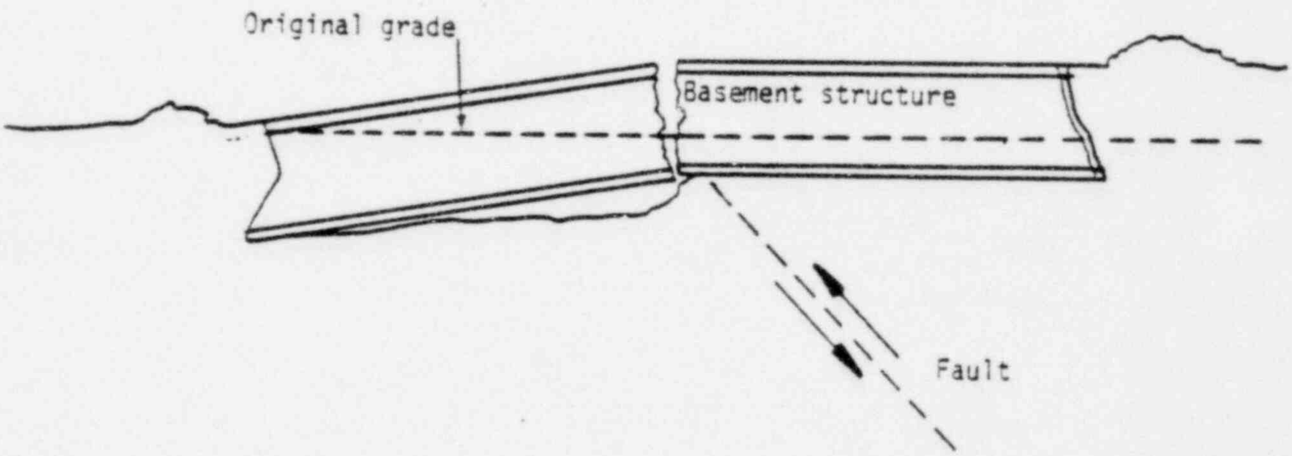

Fig. 22.
Possible faulting failure mode.

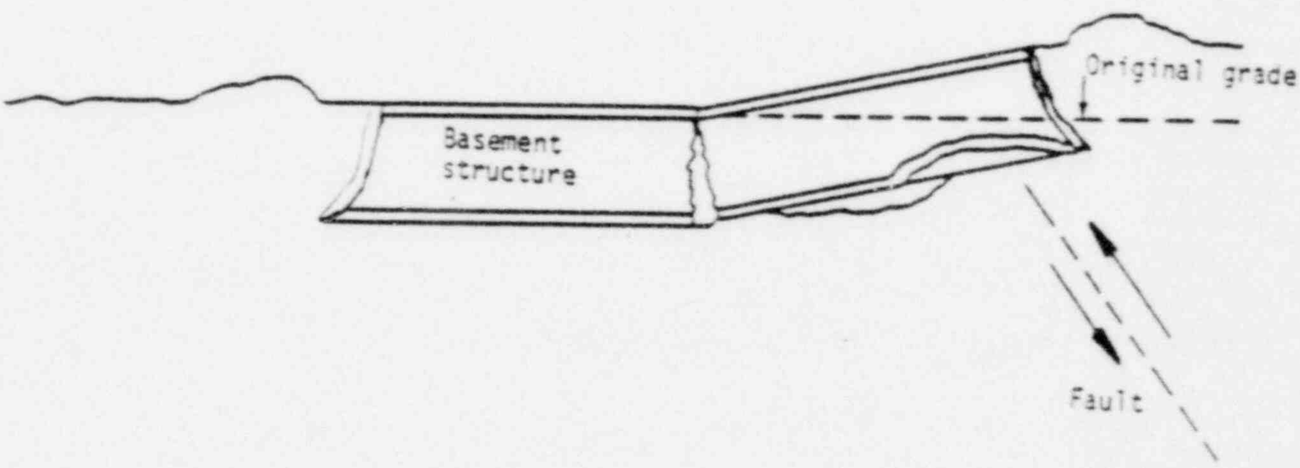

Fig. 23.
Possible faulting failure mode.

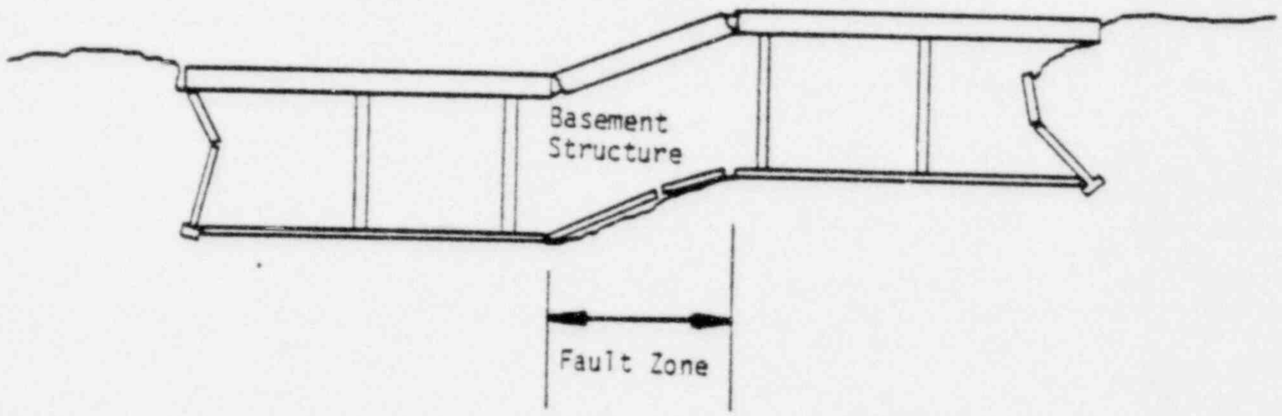

Fig. 24.
Possible faulting failure mode.

boxes through structural distortions and falling debris. For the most probable fault orientation, only two or three of the glove boxes would be damaged.

The amount of damage is dependent upon the magnitude of the slip and thrust. These evaluations have considered incremental slip and thrust magnitudes of up to about 8-9 ft.

For the movement considered, possible penetrating cracks could develop and paths to the atmosphere could exist, even though they would be of limited size. Complete collapse of the roof slab into the basement area is not expected.

D. Critical Equipment

Damage to the glove boxes is dependent upon the damage to the basement structure. Significant damage to some of the glove boxes might occur, particularly if a part of the roof slab collapses into the basement area. The floor to ceiling glove boxes would be damaged if the floor slab was pushed toward the roof slab as a result of the upward movement of the floor slab.

VI. COMBINED RESPONSE TO VIBRATORY MOTION AND FAULTING

A. Introduction

Faulting was not considered for the low-bay area, and the vibratory motion response of the low-bay area is discussed in Section IV.A.

Faulting consequences were not considered for the high-bay area, and vibratory motion response is discussed in Section IV.B.

B. RML Cells

Because the effects of concurrent faulting and vibratory ground motion (shaking) are difficult to quantify, their interaction is closely examined and discussed.

Shaking reduces the soil stiffness; therefore, the soil deformations required to develop the full passive soil pressures would increase. If a wall displacement of 5% of its height is necessary to activate the full passive soil pressures and this displacement is increased by 40%, the required soil displacement is about 12 in. Fault movements of 1.6-3.0 ft would therefore activate the full passive soil pressures; hence, the analyses for consequences resulting from the loss of continuous base support remain valid.

Vibratory ground motion has little influence on the faulting response of the cells; however, faulting can influence the shaking response of the cell structure. Faulting can cause damage to the below-grade cell structure and alter its foundation support conditions, thereby decreasing structural and soil stiffnesses, redistributing the dead load stresses, changing the overturning resistance, decreasing the soil-structure natural frequencies, and increasing damping through larger displacements, disturbed soil, and damaged structural elements. These changes effect the below-grade part of the RML cells only, and their response is dominated by the soil-structure frequencies; hence, concurrent faulting and horizontal shaking should not produce significant additional forces in the important above-grade cell structure above those produced by shaking alone.

The cell response to vertical vibratory motion requires examination. A single mass model with a vertical soil spring and damper was developed using Ref. 15 as a guide. The natural frequency was calculated as 6 Hz with the effective soil damping of 41%. Using 10% viscous damping, a ductility factor of 2, and the vertical response spectra (Ref. 5) for the facility site, amplification of the vertical ground motion is not expected, and the maximum additional vertical loading from concurrent shaking and faulting is 0.27 g's (2/3 of 0.40 g's).

In the faulting analysis, the redistributed dead loads caused by the loss of continuous foundation support developed about 70% of the cell structures' flexural capacity and about 50% of its shear capacity. The cell structure can therefore support the additional loadings associated with the response of 0.27 g's vertical ground motion. The combined dead and seismic vertical loads would develop about 90% of the cell structures' flexural capacity.

Analyses that underestimate the overturning resistance of the cells, based on static application of lateral forces to an isolated cell (ignoring soil and structural restraints), indicate that the cells are stable for the given criteria.

This study indicates that the effects of surface faulting will not significantly affect the above-grade RML cell structure, hence, the combined stresses in the cell structure above the ground floor slab are essentially equal to the vibratory ground motion stresses resulting from the 0.40 g's ground motion assumed concurrent with faulting.

C. Basement Area

From vibratory motion (shaking) alone, the basement walls reach their ultimate strength at a static equivalent PGA of about 0.6 g's. The basement columns, slab, and footings reach their capacities at about 1.0 g's. The PGA for vibratory motion concurrent with faulting is 0.4 g's (Section II.C). Fault movements of 4-6 in. can cause cracking in the basement walls, and larger fault movements will produce more extensive basement structural damage. The evaluation of the damage caused by concurrent vibratory motion and faulting is established by considering the damage levels produced by faulting and evaluating the possible additional damage produced by shaking.

Faulting disturbs the soil within and adjacent to the fault zone, and the properties of disturbed soil are different from undisturbed soil. The strength and shear modulus of disturbed soil is less than for undisturbed soil; however, the damping in disturbed soil is larger. The increased soil damping would probably neutralize any increase in structural response resulting from a lowered shear modulus. The structural response to shaking could, however, be sufficient to cause collapse of walls damaged by the fault movements, particularly the interior concrete masonry walls. Collapse of the masonry walls can lead to a path to the atmosphere and a loss of confinement. Shaking could also cause an increased movement of the basement floor slab into the basement space and therefore cause additional damage to the floor-to-ceiling glove boxes. Shaking could also lead to collapse of part of the basement roof slab that is located above the fault zone. Because of the large reserve strength of the basement columns, collapse of the entire basement roof slab into the basement space is not likely. Damage levels from concurrent shaking and faulting are presented in Section VII.C.

D. Critical Equipment

During concurrent faulting and shaking, any damage to the glove boxes and equipment would be principally caused by the fault displacements. Because some equipment supports may be structurally damaged from faulting, shaking would tend to increase the damage beyond that produced by faulting alone. The safety consequences of this event would be little different from those from faulting alone.

VII. DISCUSSIONS, RESULTS, AND STRUCTURAL DAMAGE SCENARIOS

A. Discussion and Results

The vibratory ground motion response analysis of Building 102 was divided into the analysis of five subparts. These subparts, listed in the order of their importance, are:

1. basement and AFL,
2. glove boxes and exhaust equipment,
3. RML cells,
4. high-bay area, and
5. low-bay area (including PAL).

The analysis of Building 102 has demonstrated that the AFL (located in the basement of Building 102) and its equipment will not be structurally damaged up to a PGA in excess of 0.6 g's. The reinforcing steel in the piers between the windows of the RML cells will start to yield at the ground floor level at 0.[illegible] g's PGA. The low-bay area, and therefore the PAL, will be severely damaged at a PGA of about 0.6 g's. The three high block walls adjacent to the RML cells are estimated to have an ultimate capacity of 0.5 g's.

Because of the dependency of response on the exact character of the postulated loadings and the uncertainties in component capacities, the quantitative estimates of ultimate capacities include considerable judgment. Many of the components have ultimate capacities that are large relative to their limits of elastic behavior, whereas some of the components exhibit brittle characteristics. An infinite number of response paths exists between the total system's elastic behavior limit and its ultimate capacity. We are concerned with forecasting the likely response to all levels and types of earthquake with any source orientation, duration, and time histories. Making detailed calculations for each possible response pattern is not practaical; therefore, this study has focused on the identification of limits of various types, general response characteristics, and the evaluation of interactions between structural systems.

B. Interaction of Building 102 Subparts

The low-bay area, if it collapses, will load the basement roof slab and affect the strength of the high-bay area. The glove boxes and associated exhaust equipment located in the basement area are not influenced by the collapse of the high- and low-bay areas. The response of the basement and high-bay areas influence the response of the RML cells; however, this influence is small and was not directly incorporated in this analysis. These interactions, along with the relative influence of the behavior of each system upon the glove boxes and the RML cells, are given in Fig. 10. Under vibratory ground motion, the interaction between the glove boxes and RML cells is small.

C. Damage Scenarios

The damage scenarios from vibratory motion that are given in Tables V--XII are based on mean capacities of the structural resisting systems. The return periods are those recommended by the TERA Corporation (Fig. 9).

Table V contains the response and damage levels associated with ground motion up to 0.1 g's, and Table VI contains the response and damage levels associated with motions in the range of 0.1 g's to about 0.4 g's. In Table VII, we consider severe ground motion in the range of 0.4 g's to about 0.8 g's,

TABLE V

DAMAGE SCENARIO FOR PEAK GROUND ACCELERATIONS UP TO 0.10g's

(T about 8 years)

Area of Concern	Building Structural and Equipment Events
Basement, AFL and critical equipment	No damage to basement.
	No damage to equipment.
RML cells and high-bay area	No damage to RML cells.
	Possible light cracking in high concrete block walls.
Low-bay area	Light cracking in concrete block walls.
	Damage to dowels between roof diaphragm and tops of concrete block shear walls. Cracking at joint between concrete block walls and structural steel. Limit of elastic response of roof shear-wall system is about 0.05 g PGA. Deflection will be small at this load level.

Discussion:

It is unlikely even minor repairs will be needed after this event.

TABLE VI

DAMAGE SCENARIO PEAK GROUND ACCELERATIONS IN THE RANGE 0.1g's TO 0.4g's

(T up to 270 years)

Area of Concern	Building Structural and Equipment Events
Basement, AFL, and critical Eeuipment	No damage to basement or equipment. Light cracking is possible, particularly at construction joints in basement area, and small differential motion could occur between glove boxes, stands, and supports.
RML cells and high-bay area	Light to moderate cracking damage to high concrete block walls on north side of RML cells on each side of the 28 ft bay. Collapse is unlikely because walls are reinforced and doweled to adjacent construction.
	No direct damage to structural system of RML cells. Light cracking at construction joints is likely.
	Cracking at joints between precast wall panels is likely.
Low-bay area	Light to moderate cracking at joints between precast walls. Damage to dowels connecting shear walls to structural steel. Differential motion between roof system and concrete block shear walls of about 1/4 in. Moderate to severe cracking at joint between structural steel and concrete block.

Discussion:

Repairs to high block walls may be needed after moderate earthquake ground motion. No damage in AFL is likely, and RML cells will be undamaged structurally.

TABLE VII

DAMAGE SCENARIO FOR PEAK GROUND ACCELERATIONS IN THE RANGE 0.4 g's TO 0.8 g's

(T up to about 1030 years)

Area of Concern	Building Structural and Equipment Events
AFL equipment and critical equipment	Glove boxes 37, 39, 41, and 44 will slide and vibrate relative to floor, with motion restricted by loosened saddle tiedowns. Glove boxes and exhaust equipment will likely not be damaged structurally. Glove boxes 23, 50, 51, and 51A will move in accord with basement construction to which they are connected. Glove boxes supported by connections to both floor and ceiling may be slightly displaced partly from differential motion when portions of ground floor (low-bay) wall and roof system fail.
Basement	Reinforced concrete construction will be damaged. There will be differential motion on construction joints and light to moderate cracking of the ceiling slab. The basement reinforced concrete walls reach yield at 0.6 g's PGA. Damage will depend on the duration of the earthquake strong motion. No general collapse will occur, but some local failures are possible. Concrete block partition walls will be cracked because of differential motions.
RML cells and high-bay	High concrete block walls fail with partial collapse. Block wall between cells on south side will fail. Precast concrete walls on east side of high-bay area will fail (0.7 g's PGA) from loss of connection to steel frame and these walls will fall to the east away from the RML cells. Steel columns on east side may fail. Structural system of RML cells will be undamaged in terms of their own response pattern.
Low-bay area	Roof and shear wall system will be severely damaged at about 0.6 g PGA with some collapse onto the ground floor slab over the AFL. The PAL structural containment breached.

Discussion:

Although complete collapse is not likely, extreme intensity and long duration ground motion will produce severe damage on the ground floor with some collapses. The collapse of the roof and wall systems may crack the RML cells. The AFL is protected by the heavy reinforced concrete ceiling slabs from collapse on the ground floor level. The reinforced concrete structural system of the basement will be damaged at about 0.6 g, and the ceiling slab will be subject to loads from ground floor damage at about the same load level. No general collapse will occur in the basement structural system although local failures are likely.

TABLE VIII

DAMAGE SCENARIO FOR PEAK GROUND ACCELERATIONS IN EXCESS OF 0.8 g

(T up to about 1030 years)

Area of Concern	Building Structural and Equipment Events
AFL, critical equipment	General failure and collapse is unlikely although there may be severe differential motions.
Basement	No collapse of the overall structural system is likely at these levels of earthquake vibratory ground motion, depending upon the duration. The general collapse is unlikely as the structural components are well reinforced and constructed. Local failures of the walls and floor could damage the glove boxes or the exhaust system with the possible attendant loss of containment.
RML cells, high- and low bay areas	Severe damage with some collapse in the high- and low-bay areas and moderate cracking in piers of RML cells.

TABLE IX

DAMAGE SCENARIO FOR FAULT DISPLACMENTS UP TO 0.5 FT

Area of Concern Building Structural and Equipment Events	
Basement, AFL, and critical equipment	Local light cracking in the basement walls. Possible small visible crack across roof slab. Slight heaving of floor slab. No damage to glove boxes.
RML cells	No damage to RML cells

TABLE X

DAMAGE SCENARIO FOR FAULT DISPLACEMENTS IN THE RANGE OF 0.5 TO 1.0 FEET

Area of Concern	Building Structural and Equipment Events
Basement, AFL, and critical	Moderate to severe cracking in the basement walls adjacent to fault zone. Moderate cracking roof slab about columns that are located near edges of fault zone. Moderate heaving of floor slab. Light damage to floor-to-ceiling glove boxes.
RML cells	Light to moderate cracking in RML cell soil retaining walls. Light cracking in base slab possible.

TABLE XI

DAMAGE SCENARIO FOR FAULT DISPLACEMENTS IN THE RANGE 1.0- TO 5.0-FT

Area of Concern	Building Structural and Equipment Events
Basement, AFL, and critical equipment	Severe cracking in basement walls adjacent to fault zone. Separation of basement wall and roof slab joint possible in the fault zone. Soil enters space between the basement walls and the AFL. Possible light damage to the AFL walls on the north side. Penetrating cracks possible in the roof slab (path to atmosphere possible). Significant heaving of floor slab. Floor-to-ceiling glove boxes could be partially crushed.
RML cells	Moderate to severe cracking in the soil retaining walls. Moderate to severe cracking in the base slab.

TABLE XII

DAMAGE SCENARIO FOR FAULT DISPLACEMENTS IN THE RANGE 5.0- TO 9.0-FT

Area of Concern	Building Structural and Equipment Events
Basement, AFL, and critical equipment	Collapse of basement walls within and adjacent to the fault zone. Soil is pushed into the space between the basement walls and the AFL walls. Depending upon fault zone location, insignificant to moderate damage to the AFL walls on the north side and to a wall section on the west side. Heavy localized cracking in roof slab with possible severe heaving of floor slab. Severe damage possible to floor-to-ceiling glove boxes. Damage to other glove boxes from falling concrete chunks is possible.
RML cells	Severe damage to soil 12-in. below-grade retaining walls. Soil could enter the nonfunctional below-grade space of the cells. Severe cracking in the base slab possible. Above-grade functional part of cells not damaged. Ventilation ducts could be severed from secondary filter bank.

whereas in Table VIII, we examine the responses for acceleration levels larger than 0.8 g's PGA.

Damage scenarios for various fault displacement ranges are given in Tables IX--XII. Considerable judgment was excerised in the development of these damage scenarios. The damage levels are dependent upon the magnitudes and interactions of the slip and thrust displacements, but the fault displacement criteria only specify a total displacement. Because the structural damage is concentrated within and adjacent to the fault zone, the location, direction, and width of the fault zone is important. Vibratory ground motion concurrent with faulting also contributes to the damage levels.

The damage levels given in Tables IX--XII are therefore based on the maximum total displacement occurring independently as a slip and as a thrust and on the fault zone occurring anywhere under the basement area in a direction

125^0 measured from the north reference in a clockwise rotation. Combined faulting and vibratory ground motion damage was included in the fault displacement damage scenarios.

APPENDIX A
DESCRIPTION OF STRUCTURAL SYSTEMS AND EQUIPMENT

I. INTRODUCTION

The detailed descriptions of the Building 102 systems and their important structural components and equipment are presented in this appendix. The systems described are the

1. low-bay area,
2. high-bay area,
3. RML cells,
4. basement and AFL, and
5. critical equipment.

II. LOW-BAY AREA

The low-bay area was constructed using structural steel framing, concrete masonry, and precast concrete walls. Vertical loads are resisted by the steel framing, and horizontal loads are resisted by shear walls.

The roof system employs simple beam framing (no continuity) supported by steel columns that rest on bell-bottom caissons. The roof construction includes Robertson steel roof deck welded to the structural steel roof framing (Fig. A-1). This combination forms a diaphragm for the transmission of horizontal forces from one element to another. The roof diaphragm is supported by the structural steel tubular columns. Typical column details are shown in Figs. A-2 and A-3.

The low-bay walls include 4-in. and 8-in. concrete masonry walls, precast concrete wall panels that form the exterior walls, metal siding panels, and

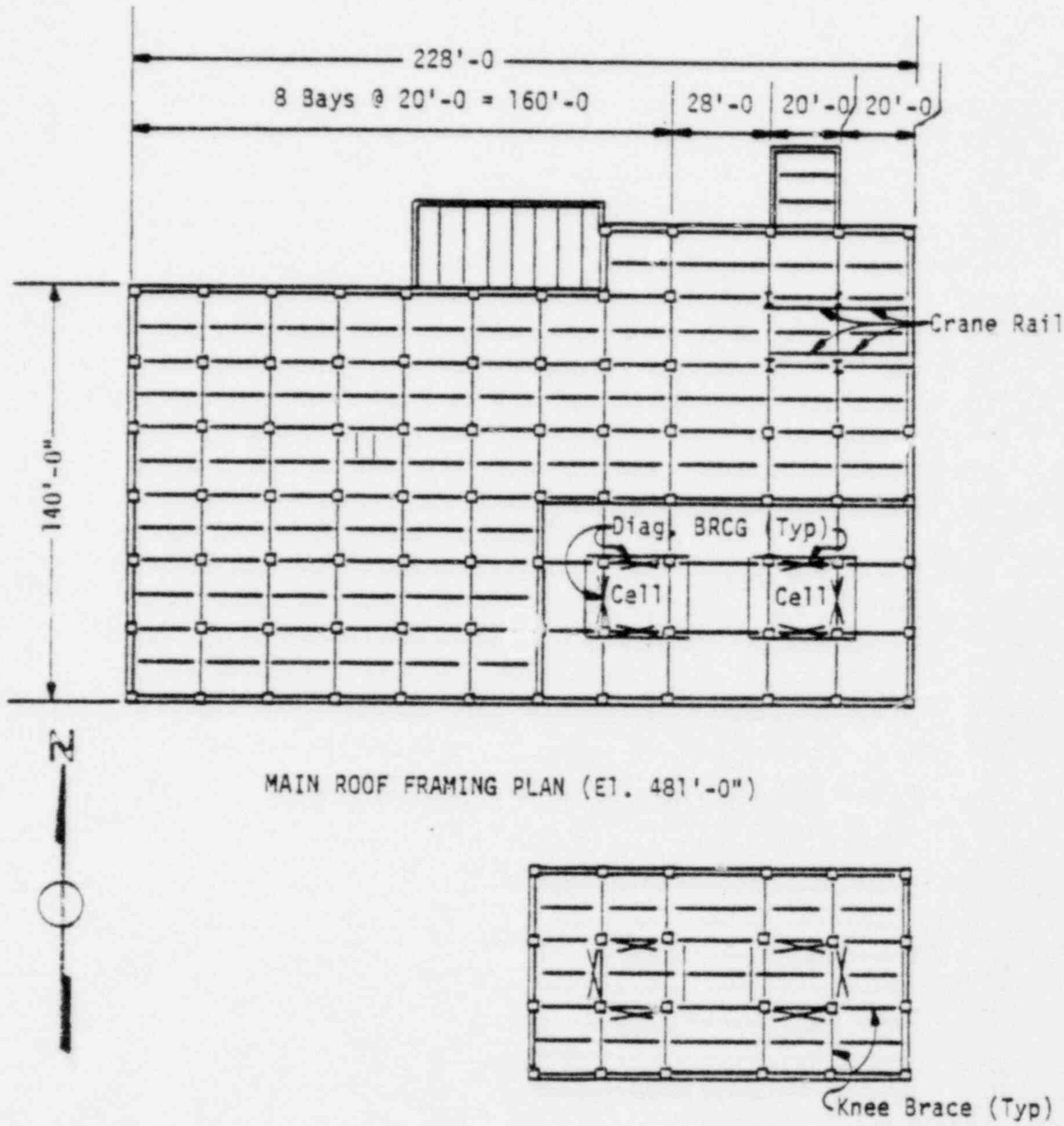

Fig. A-1.
Primary steel roof framing plan.

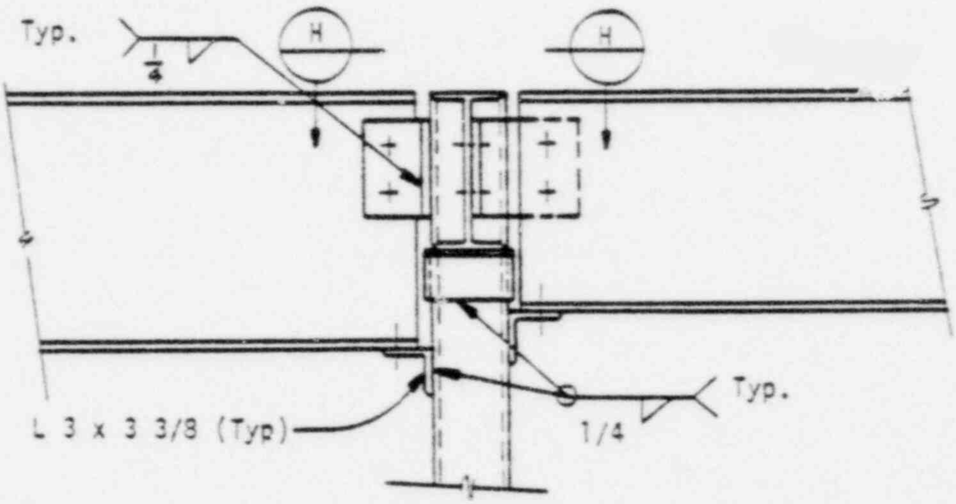

TYPICAL COLUMN -TO-

BEAM CONNECTION

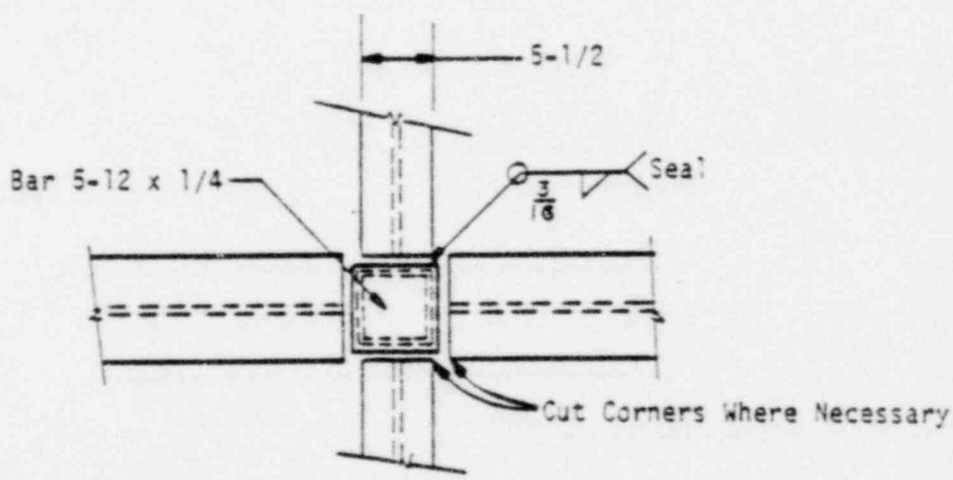

SECTION H

Fig. A-2.
Typical structural steel connections.

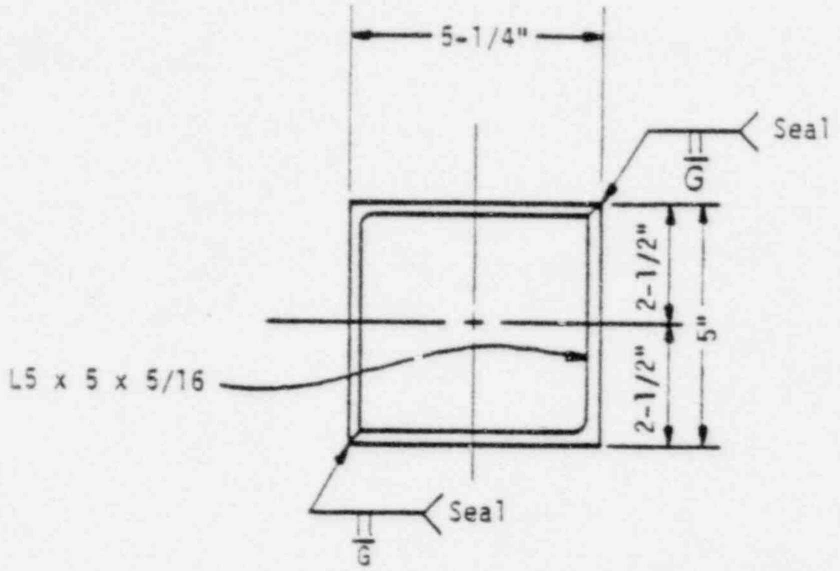

TYPICAL COLUMN SECTION

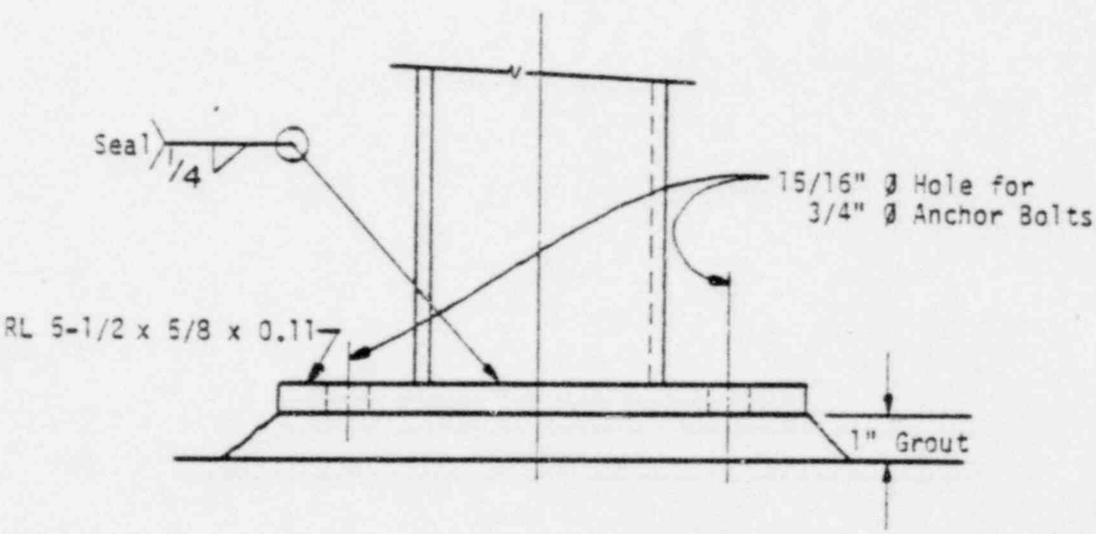

TYPICAL BASE PLATE

Fig. A-3.
Typical column details.

wood and gypsum board partitions (Fig. 5). Only the 8-in. reinforced concrete masonry walls and the precast concrete wall panels were considered as structural load resisting members in the analysis.

The strength capacity of the low-bay area is strongly dependent upon two connection details. They are: (1) the dowels between the top of the concrete block shear walls and the structural steel roof framing, and (2) the light-angle inserts at the top of the exterior precast concrete walls that are used to connect these walls to the structural steel. The behavior of these connections is highly dependent upon the number of load cycles at load levels at or near their ultimate strengths. These connections will not carry a load in subsequent cycles until the distortion of the structure overcomes the permanent inelastic member deformation that resulted from previous load cycles.

III. HIGH-BAY AREA

The high-bay area is located in the S-E corner of Building 102. Its dimensions are 60 ft N-S by 108 ft E-W (Fig. 6). The roof is 9 ft 8 in. higher than the low-bay roof. The walls on the south and east sides of the area are the same type of precast concrete panels as used in the low-bay. These precast panels connect to light structural steel girts that span between the steel columns. Nonstructural metal wall is used between the top of the precast panels and the high-bay roof. On the west side, the structural steel roof frame contains a block wall that extends to the height of the low-bay roof. Nonstructural metal wall is used above the low-bay roof level. On the north side, there are no structural walls below the low-bay roof level. Four feet inside the north wall of the high-bay area, a concrete block shear wall extends from the ground floor slab to the low-bay roof level as shown in Fig. A-4 between lines F and E. This wall extends to the metal deck of the low-bay roof and is connected to it; therefore, it does not influence the high-bay area.

The high-bay structural frame system is shown in Fig. A-5. The two RML cells that are centrally located in the high-bay areas give lateral and vertical support to the high-bay system (Figs. A-5 and A-6). Steel truss bracing from the cells to the roof are shown in Figs. A-6 and A-7. Knee braces are provided as shown in Fig. A-7 between the columns that connect to the precast concrete exterior wall panels and to the roof beams.

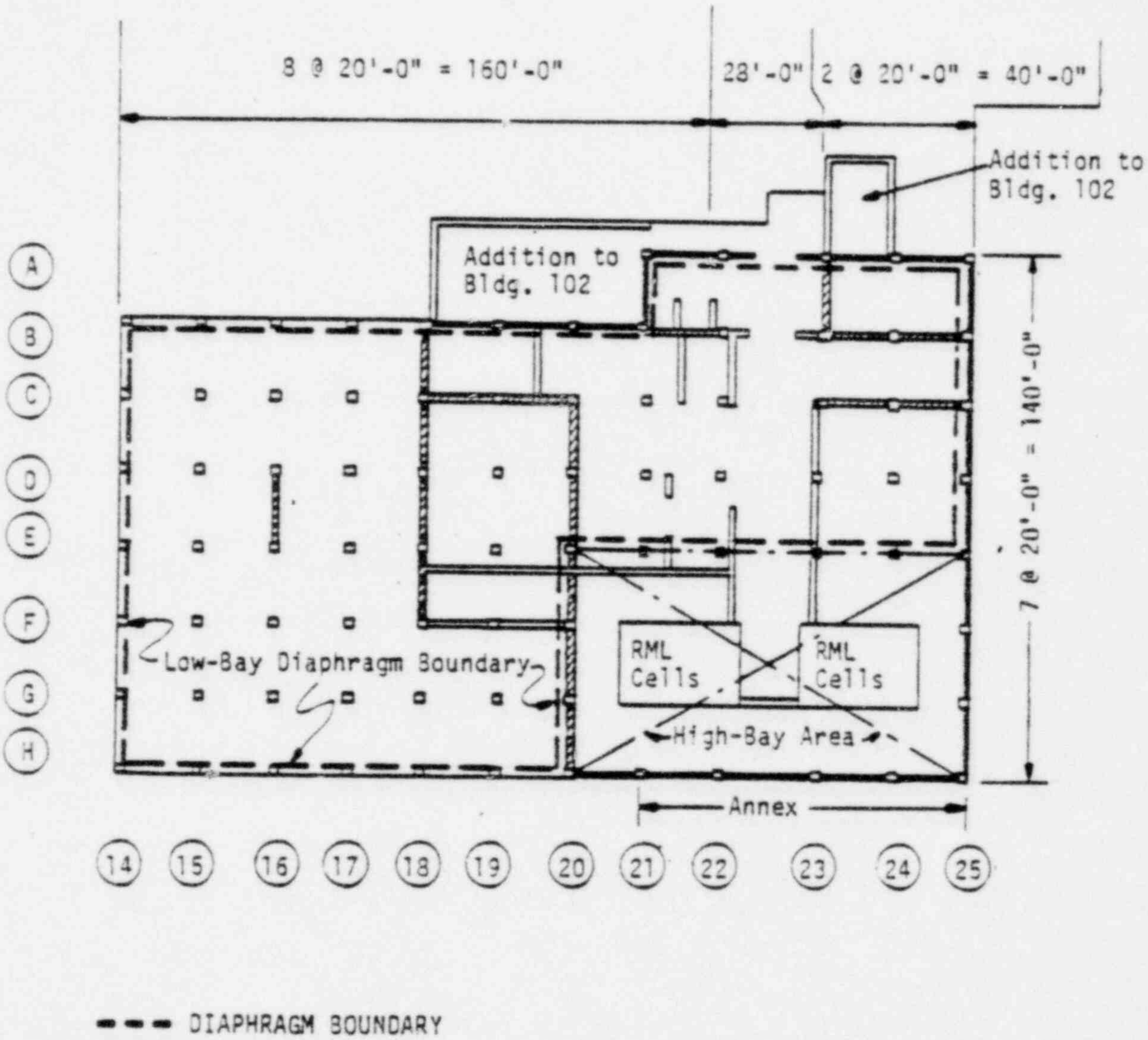

Fig. A-4.
Low-bay roof diaphragm.

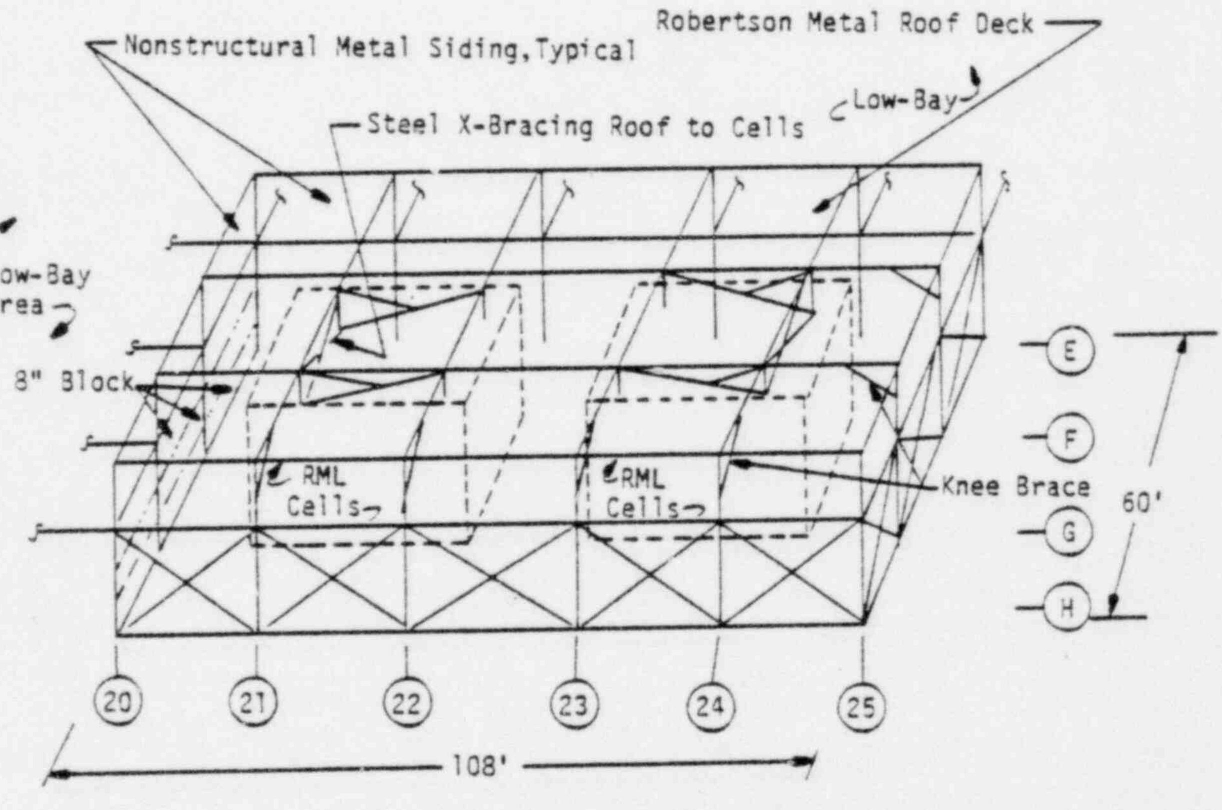

Fig. A-5.
High-bay structural system.

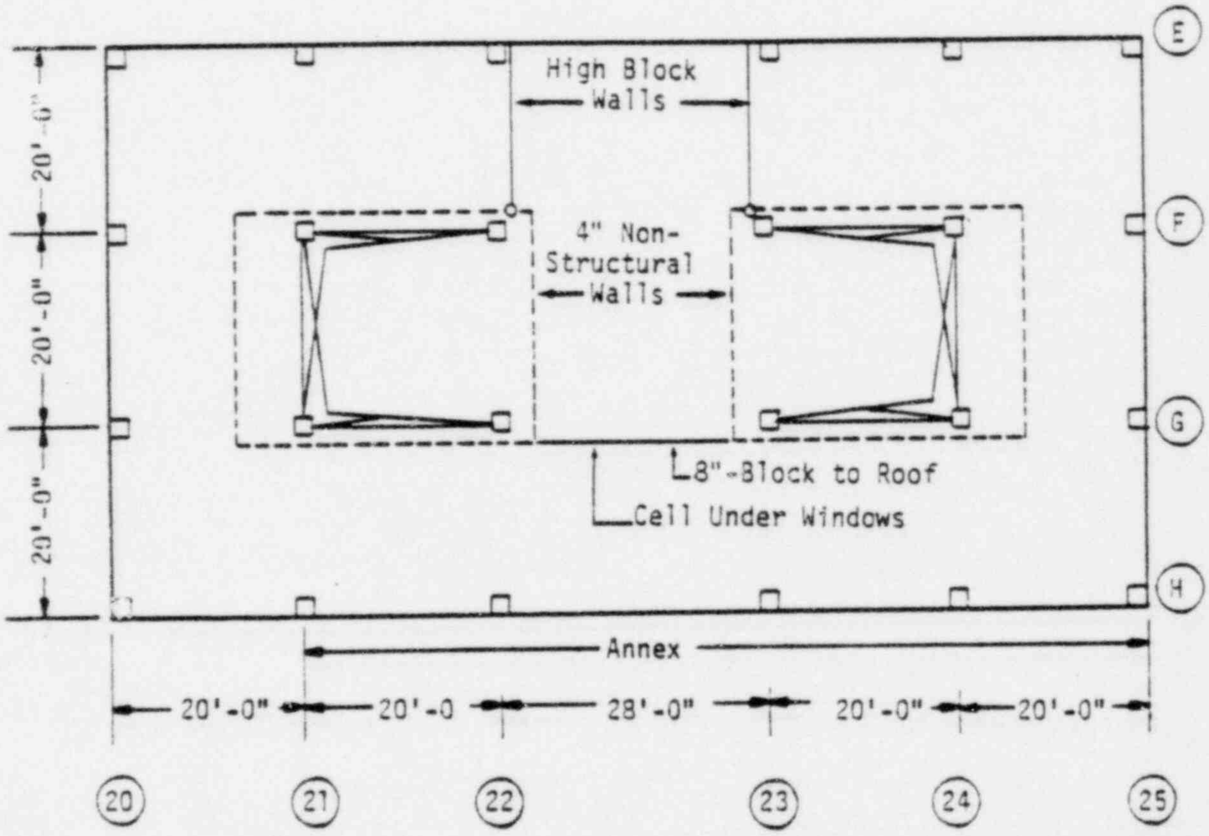

Fig. A-6.
Lateral force resisting system at high bay.

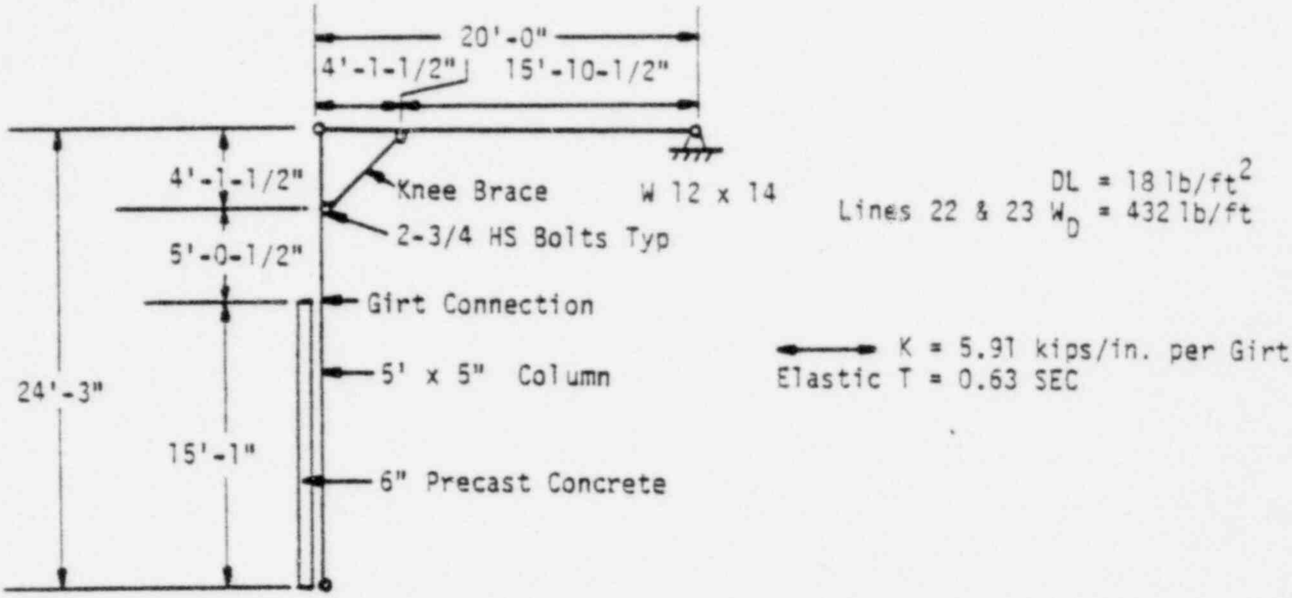

a. Exterior Wall Details.

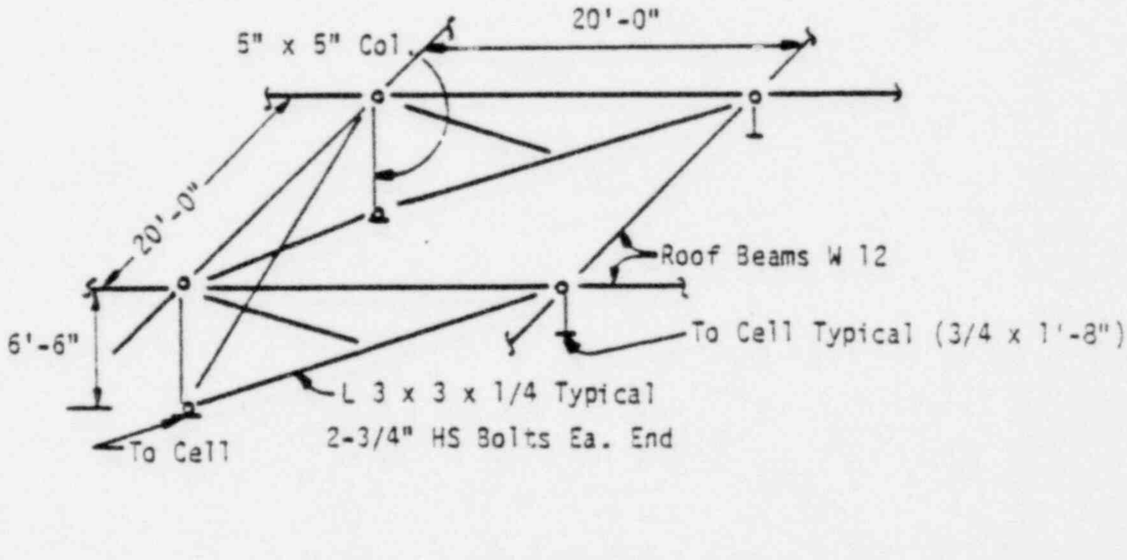

b. X-bracing roof framing to RML cells.

Fig. A-7.
High-bay structural steel framing.

Two concrete block walls (near Lines 22 and 23 in Fig. A-6) extend from the floor slab to the high-bay roof metal deck. These walls are connected by dowels to the RML cells. Two 4-in. block nonstructural walls extend from the top of the cells to the roof (Fig. A-6). An 8-in. block wall that is located at the south sides of the RML cells and between the cells extends from the top of a small cell to the roof. This wall is also dowel-connected to the RML cells.

The annex to Building 102 (Fig. A-6) is structurally separate from the structural system of Building 102 and was not considered in this analysis. The structural steel columns of the annex are located 2 in. from the exterior steel columns of Building 102 (Lines 20--25, Fig. A-6). The south wall of the high-bay area will therefore receive support from the annex frames if it fails toward the south; consequently, the south exterior wall of the high-bay area is constrained to collapse toward the north.

IV. RML CELLS

The RML cells are located within Building 102 as shown in the text in Fig. 2. Figure A-8 shows an exploded view of the RML cell construction. The cell is shown in more detail in the plan views in Fig. A-9 and in the sections given in Figs. A-10--A-12.

The cel. construction is massive reinforced concrete. Approximately 70% of the volume of the below-grade box structure (base mat, foundation walls, and cell floor) is concrete. The volume of the above-grade structure (cell walls and roof slab) is approximately 50% concrete and steel. The volume fraction of the concrete and steel of the RML cells is much greater than for the usual concrete structure. The above-grade cell walls are high-density (ferrophosphorous aggregate) whereas the remainder of the structure is normal weight structural concrete.

The amount of reinforcing steel is essentially the minimum required for temperature and shrinkage effects. The ratios of reinforcement area to gross concrete area are tabulated below:

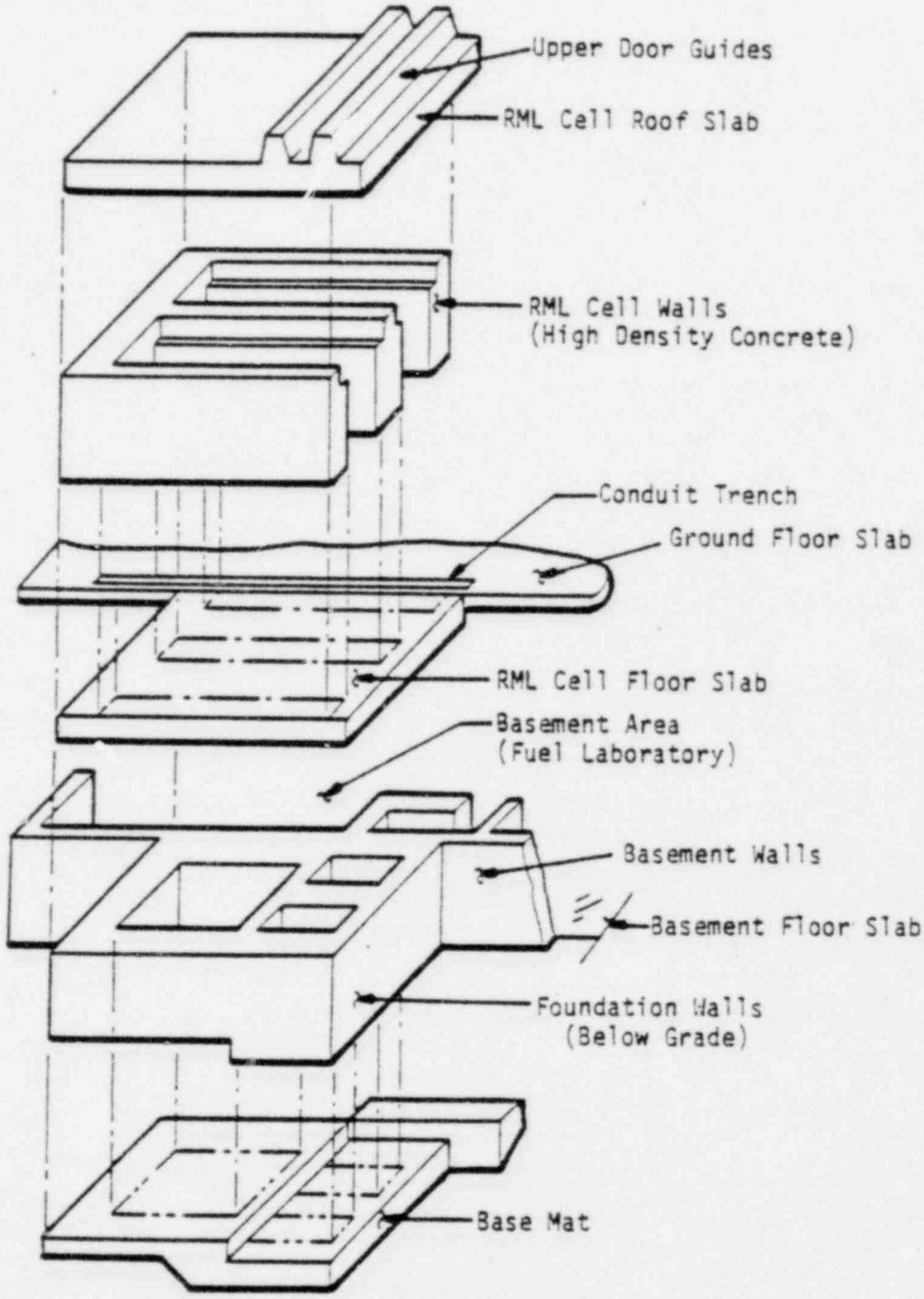

Fig. A-8.
Exploded view of RML cell construction.

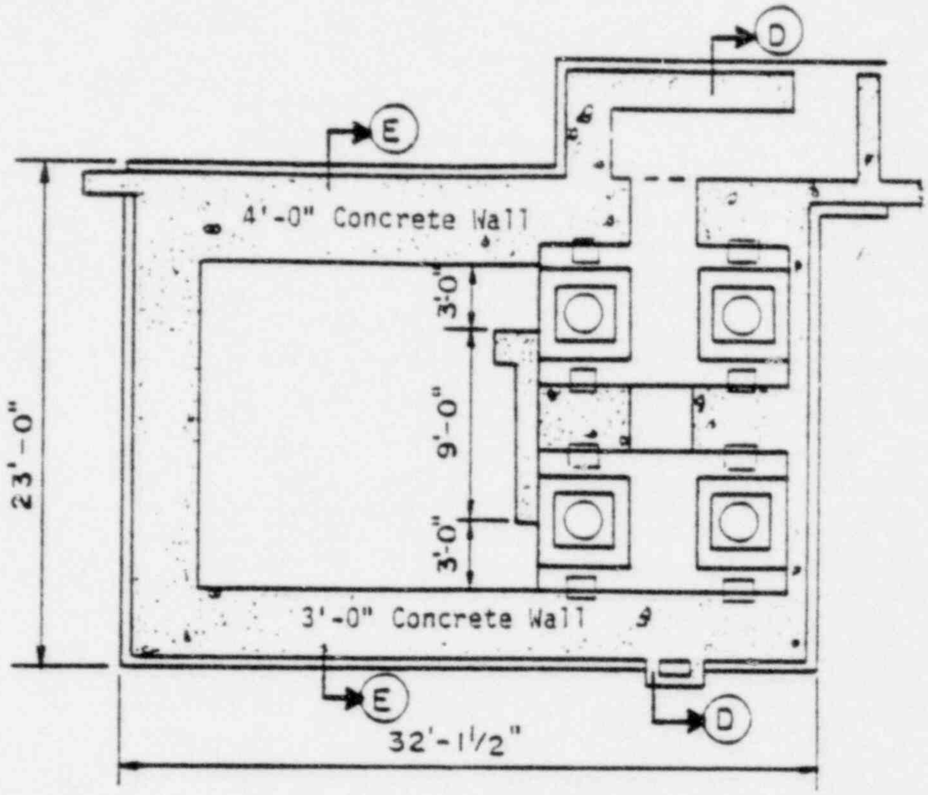

a. Foundation Plan A.

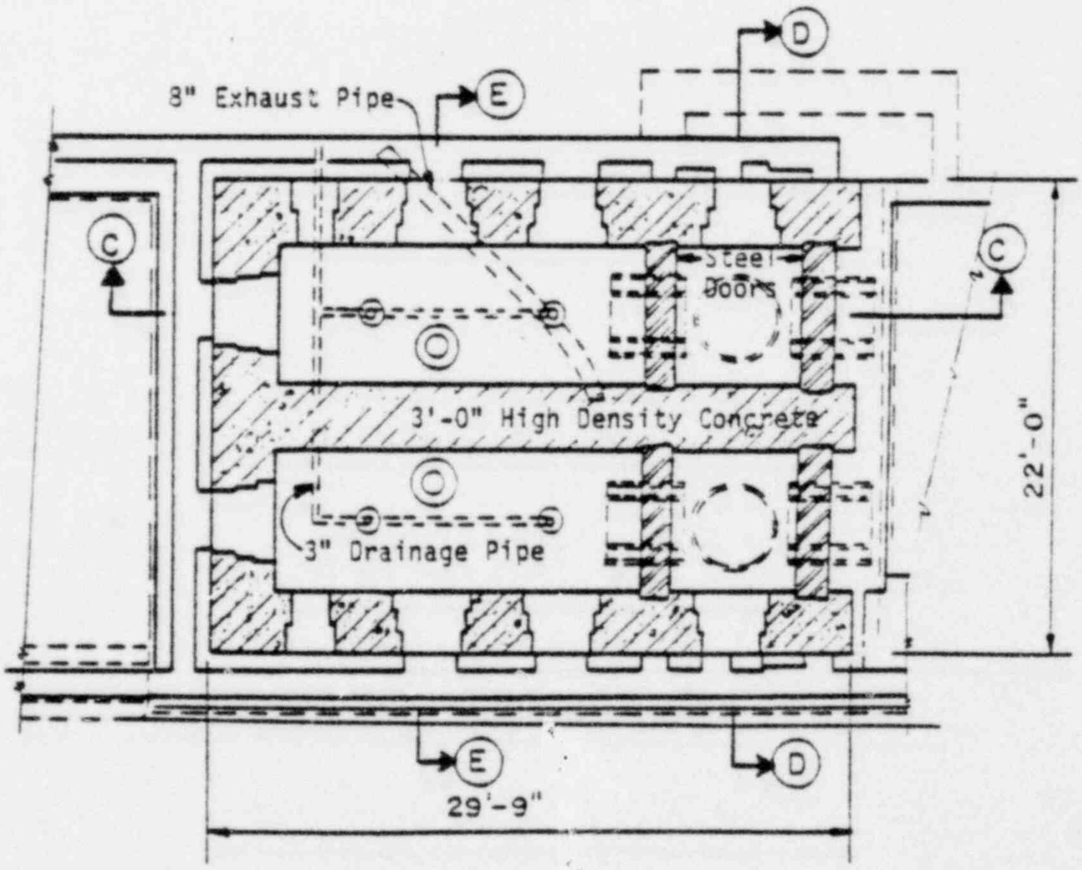

b. First Floor Plan B.

Fig. A-9.
RML cell plan views.

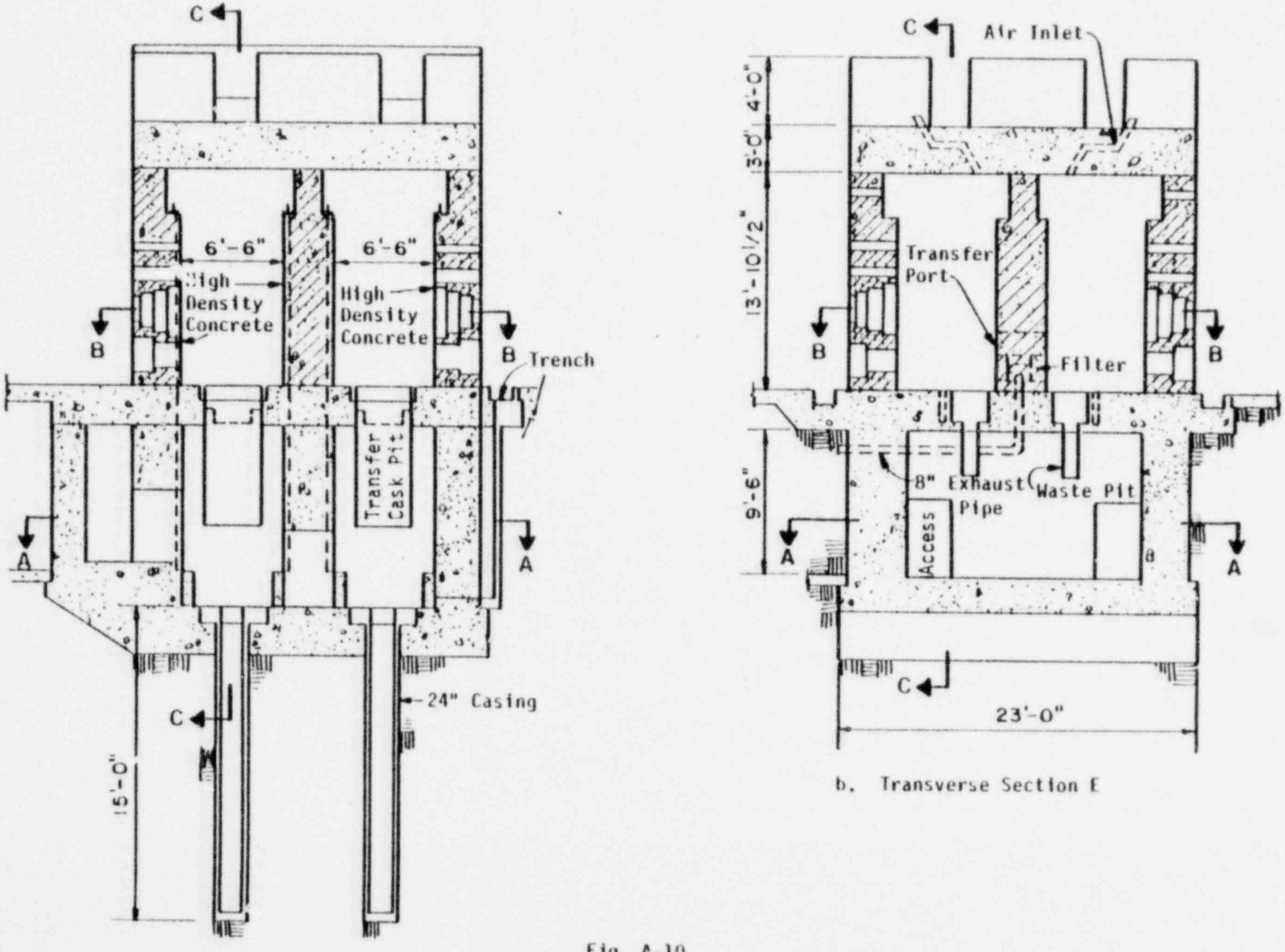

a. Transverse Section D

b. Transverse Section E

Fig. A-10.
RML cell transverse sections.

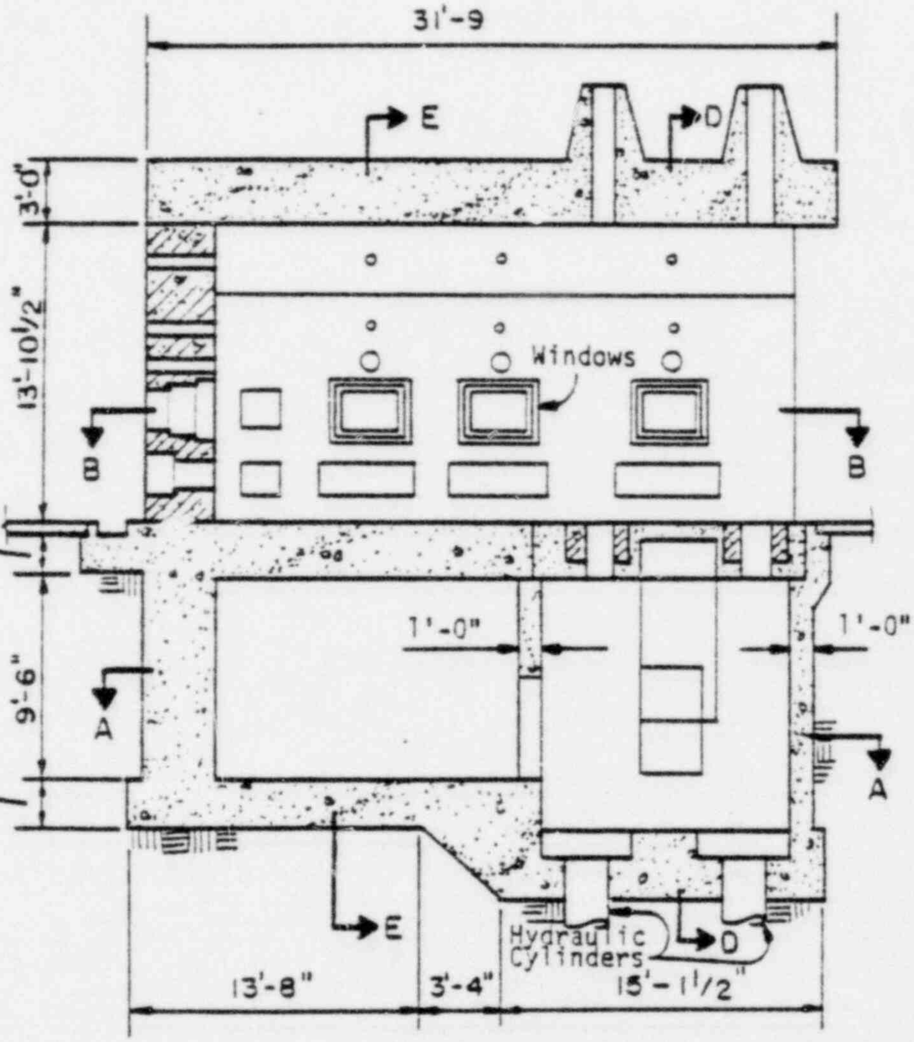

Fig. A-11.
RML cell longitudinal Sec. C.

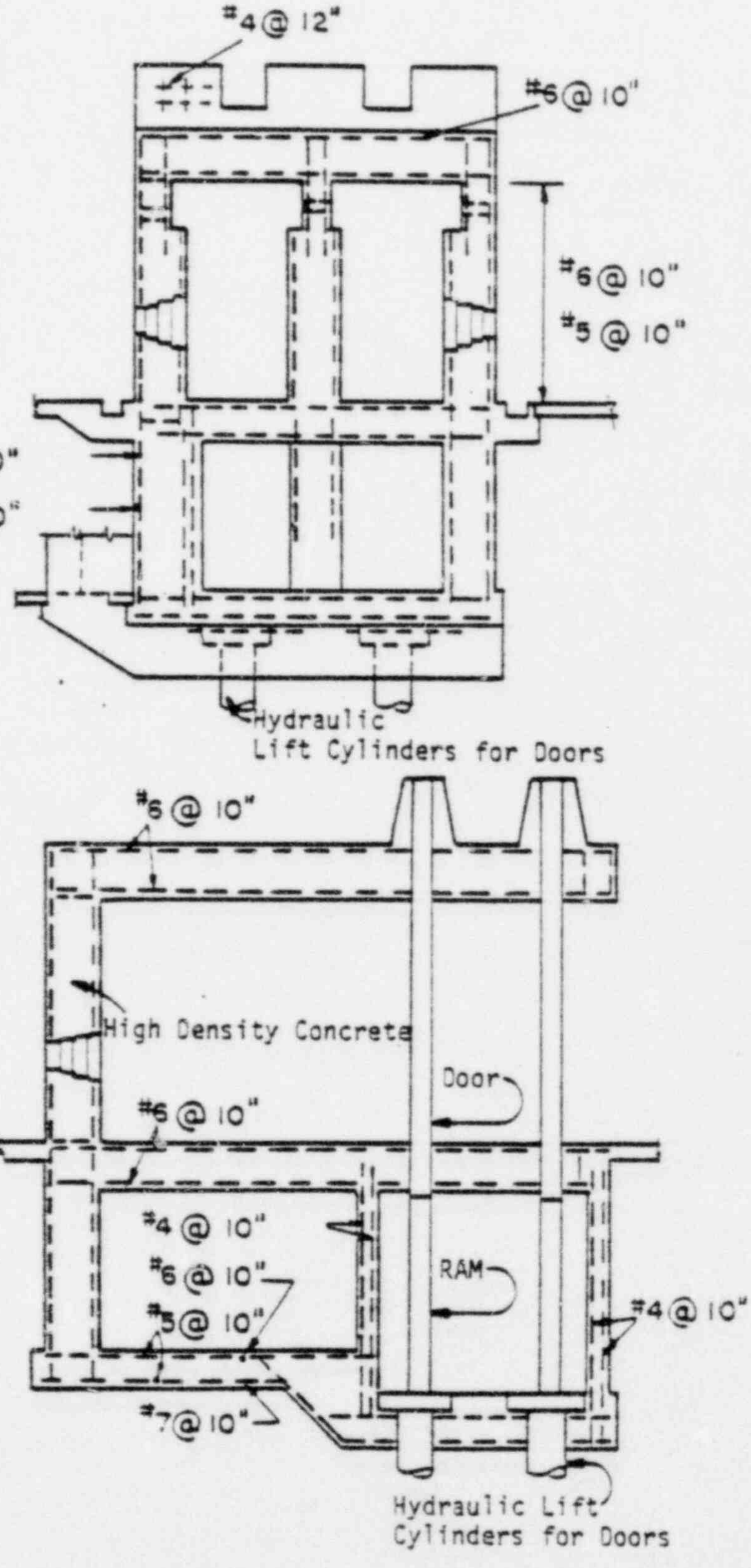

Fig. A-12.
RML cell reinforcement.

Component	Steel Reinforcement Ratio A_s/bh	ACI (1971) Temperature and Shrinkage Requirement
Base Slab	0.0026	$\geq$ 0.0020
Walls		
Vertical	0.0013-0.0017	$\geq$ 0.0015
Horizontal	0.0018-0.0024	$\geq$ 0.0025
Roof Slab	0.0024	$\geq$ 0.0020

The RML cells are not independent from the structural system of Building 102. The ground floor slab over the basement area is connected to each cell as shown in Fig. A-13. This floor is supported (in terms of in-plane shear transfer) by the below-grade basement walls. The basement floor slab is not connected to the cells nor to the basement walls; it is essentially a floating slab.

The basic function of the RML cells is radiation shielding; however, they also serve as confinement barriers. The functional space of the cell is located entirely above-grade. The spaces enclosed within the below-grade box structure are nonfunctional, providing only dead space for door operation and transfer cask placement. Exhaust and cell drain piping are located within the below-grade space as shown in Figs. A-9 and A-10. Two 8-in. and one 10-in. ventilation exhaust ducts serve cells 3 and 4. The primary exhaust filters are located within the cell. There are four ventilation input openings (5- by 5-in.) in the roofs of each cell. These openings are not protected by HEPA filters. The drains are 3-in. pipes. Two sets of massive steel doors (15- and 18-in. thick) form a radiation lock for the transfer cask pit as indicated in Fig. A-9. The doors have two sections: (1) a smaller section that is lifted up by an actuator reacted by the roof slab, and (2) a larger section that is lowered by hydraulic rams contained within the below mat casings as shown in Fig. A-10. When the doors are in a closed position, shear pins are inserted through the walls and into the doors to prevent accidental opening. During operations, one set of doors remains closed; hence, confinement integrity of the operational space of the cells is maintained.

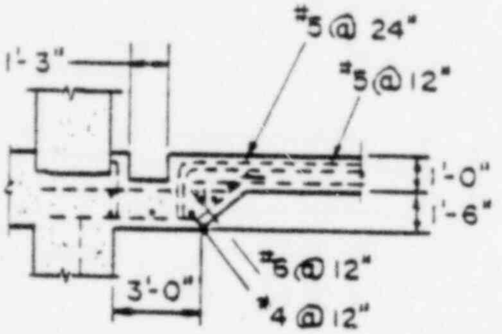

Detail A

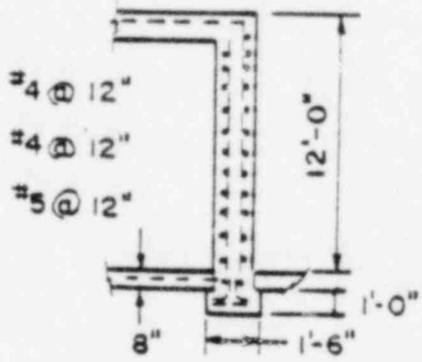

Detail B

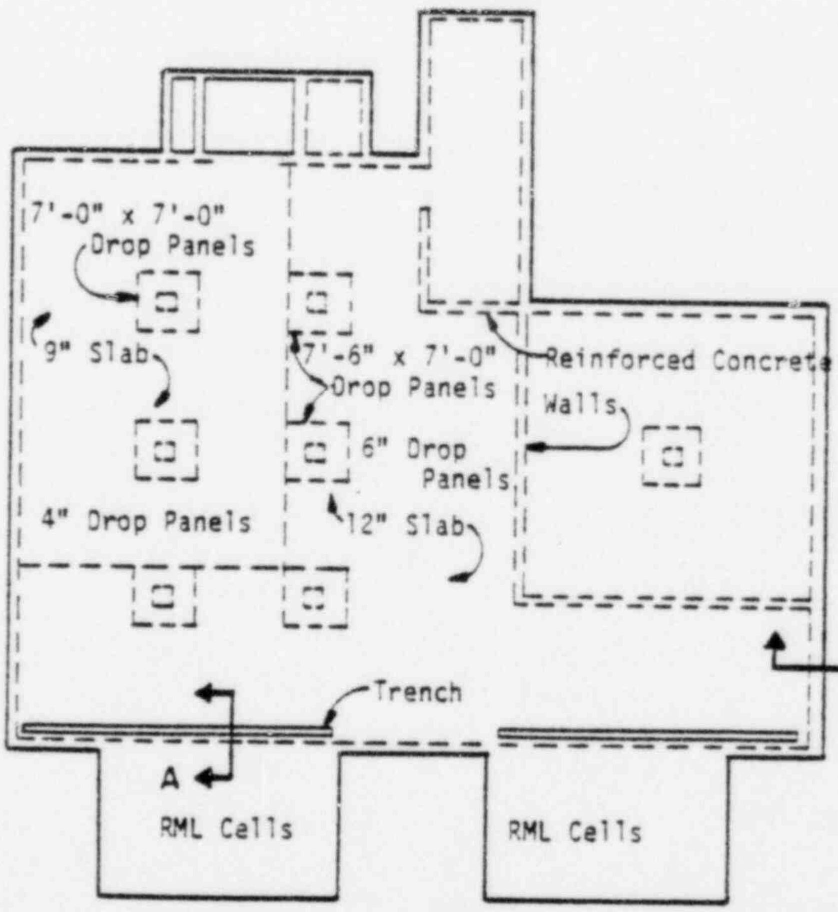

Fig. A-13.
Ground floor slab over basement.

V. BASEMENT AREA AND AFL

The foundation plan, basement plan, and construction details for the basement are shown in Figs. 2 and A-14. The AFL that is located within the basement of Building 102 is shown in Fig. 6 in the text.

The basement roof slab is of flat slab construction with drop panels. The basement columns are square, tied, and bear on rectangular spread footings, and the reinforced concrete basement walls are supported on spread footings. The basement floor slab was placed on grade, and it is not connected to the walls, footings, or columns. Also, the floor slab is grooved, and a portion of the slab reinforcing is interrupted at the grooves to control shrinkage cracks in the floor.

The AFL confining walls were not included in the original construction of Building 102, but were added at a later date. Concrete block partition walls were constructed to form the various laboratory areas.

Construction joints are located at the tops of the footings, columns, and walls. The reinforced concrete exterior walls were considered to act as simple beams supported at the floor and ceiling slab levels and loaded by earth pressure. The basement floor slab transmits applied loads directly to the soil and cannot be displaced horizontally; therefore, no further analysis was necessary for this slab.

The 8-in. concrete block walls enclosing the AFL area are filled-cell construction. These block walls are constrained by the heavy overhead reinforced concrete floor slab and the basement floor slab. Over a period of time, these walls have become bearing walls even though they were constructed after the reinforced concrete construction was completed. The walls are in sound condition without apparent cracks.

VI. CRITICAL EQUIPMENT

Mishima has designated five glove boxes in the basement AFL areas as potential sources of release of various types of plutonium compounds.[24] These enclosures or glove boxes are designated as glove boxes 37, 50, 51, 51A, and 23 (Fig. A-15). Glove boxes 38, 41, 44 are similar in construction to glove box 37. Glove boxes 38, 41, and 44 contain dry mixed oxide powders, but they are similar in construction to glove box 37.

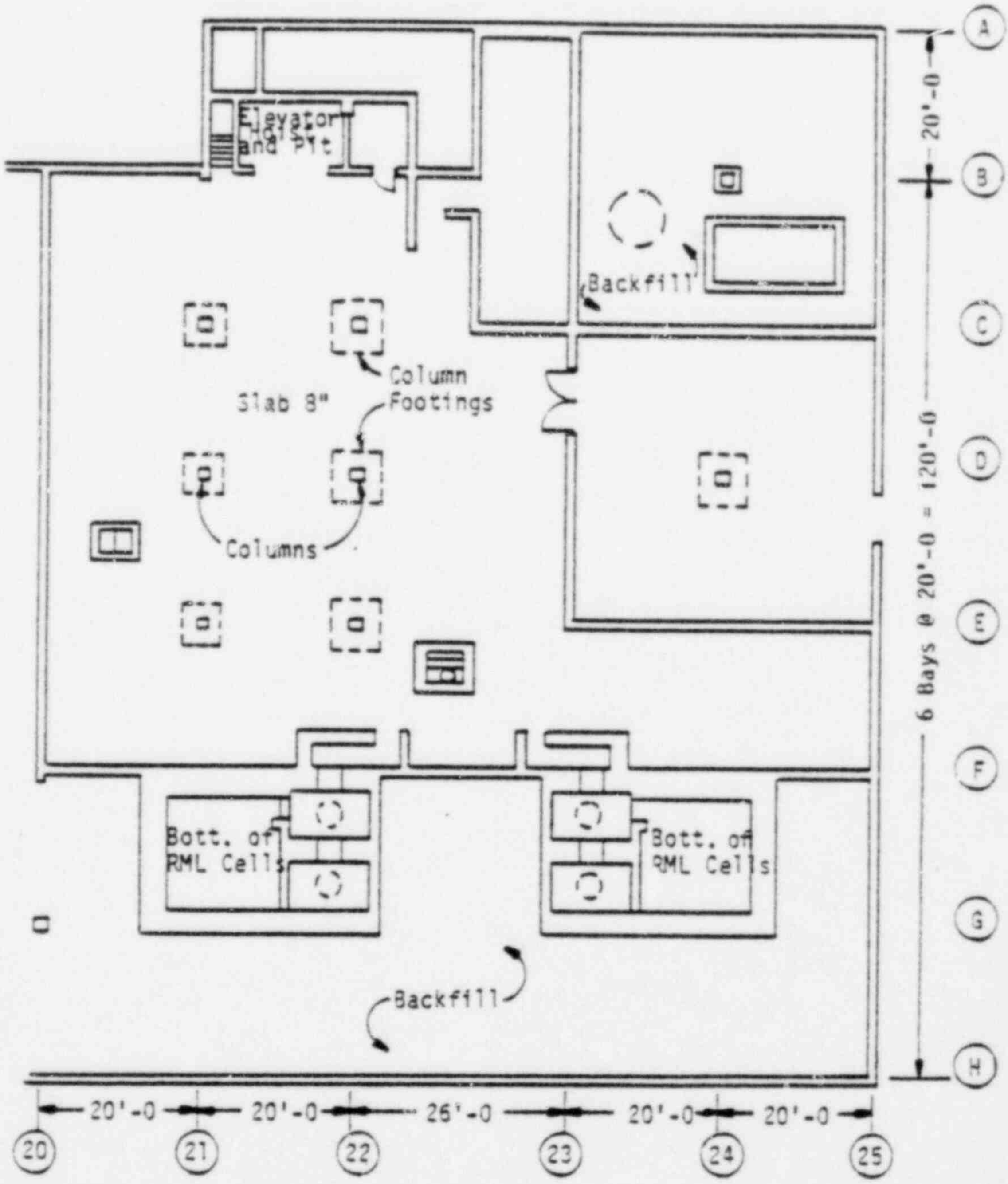

Fig. A-14.
Basement floor plan.

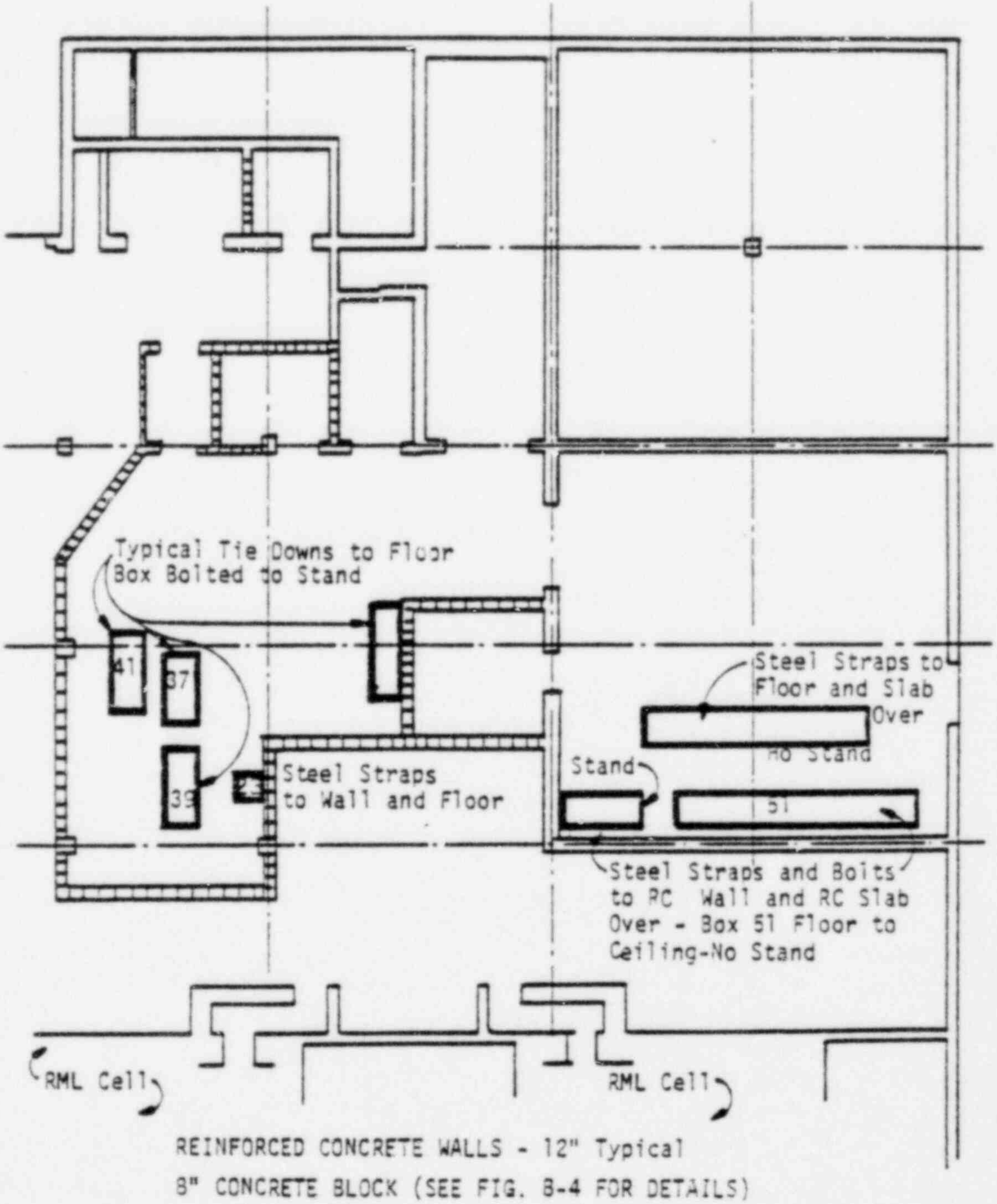

Fig. A-15.
Glove boxes of interest and connections.

The structural details of the glove boxes are shown in Figs. A-16--A-20. A typical glove box is fabricated from 1/8-in. stainless steel plate with welded joints. It rests on a stand that is fabricated from steel pipe and angles. Bolted connections between the stand and the glove boxes have been added to the critical glove boxes with standard stands (37, 39, 41, and 44) (Fig. 16). At the four bottom corners of the glove boxes, 3/8-in. machine bolts have been installed through the stainless steel skin of the glove box and the steel angles forming the top of the stand. When bolts could not be located in the corners of the boxes, connections were made at other locations. These connections consist of four threaded bosses welded to the bottom of the glove box and attached to the stand through clamps. The individual details vary, but the connections have sufficient strength to keep the glove box securely on the stand.

Glov› box 51 is an assembly of floor-to-ceiling boxes connected to each other and to the 12-in. reinforced concrete wall behind the glove box and to the 12-in. reinforced concrete slab over the glove boxes. The connections prevent motion in all directions and are made with steel straps bolted or welded to the glove boxes and connected to the reinforced concrete by expansion bolts.

Glove box 50 is an assembly of floor-to-ceiling boxes connected to the floor and to the ceiling by steel straps and expansion bolt assemblies. The connections provide resistance to motion in all directions.

Glove box 23 is connected by steel straps, welds, and bolts to the concrete block wall behind the glove box and to the floor. As shown in Fig. A-18, a ceiling suspension system consisting of 1/4-in. diam preformed 1 x 19 galvanized aircraft cable and appropriata connections is provided.

Each glove box has an integral exhaust filter that is connected to stainless steel pipe through a flexible connection about 12 in. in length. The exhaust piping is securely braced to the overhead reinforced concrete slab. The exhaust pipes empty into two co lection filters, one in each primary laboratory area. This second stage of filters then connects to ducts that lead to a single large duct and to the final filters that are located in Building 102A. Two levels of filtering are provided in the laboratory area before exhaust products leave the laboratory area. The filter collection boxes in each laboratory area are connected to the overhead reinforced concrete by steel straps and bolts.

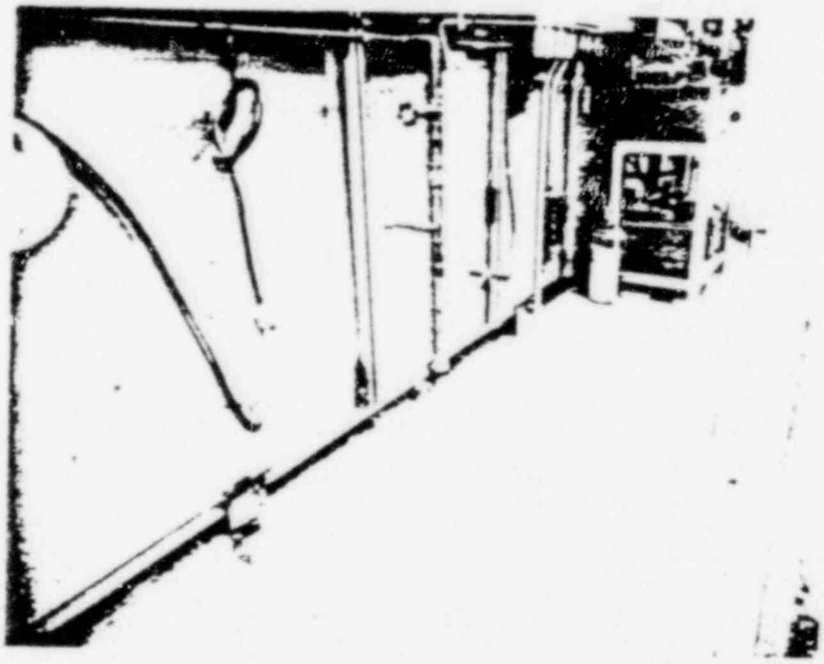

Fig. A-16.
Connection of larger floor to ceiling Glove Box 50 to reinforced concrete floor through welded steel strap and expansion bolts. Similar connection for Glove Boxes 23, 51, and 51A to walls behind glove boxes.

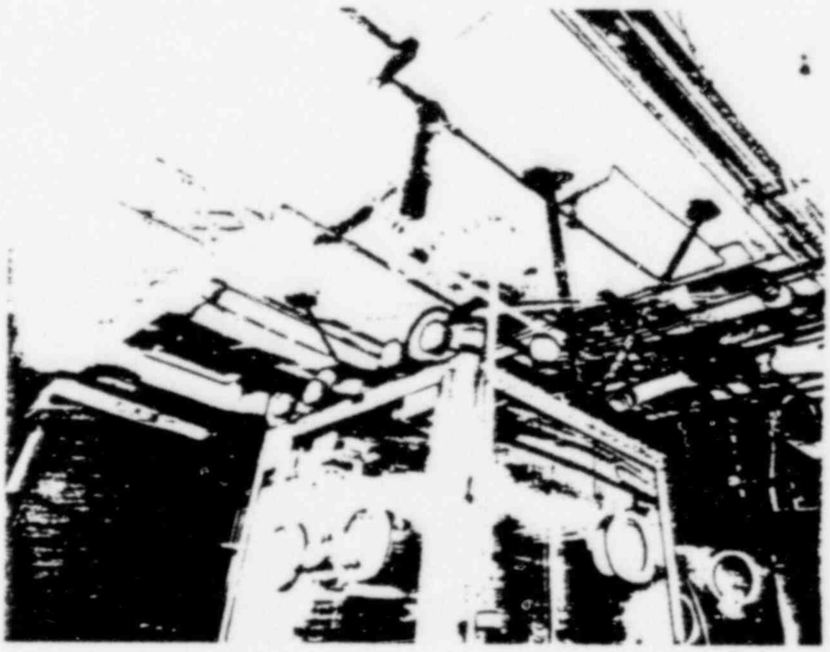

Fig. A-17.
Typical connection of top of Glove Boxes 50, 51, 51A through steel angles welded to boxes and connected to reinforced concrete slab by expansion bolts.

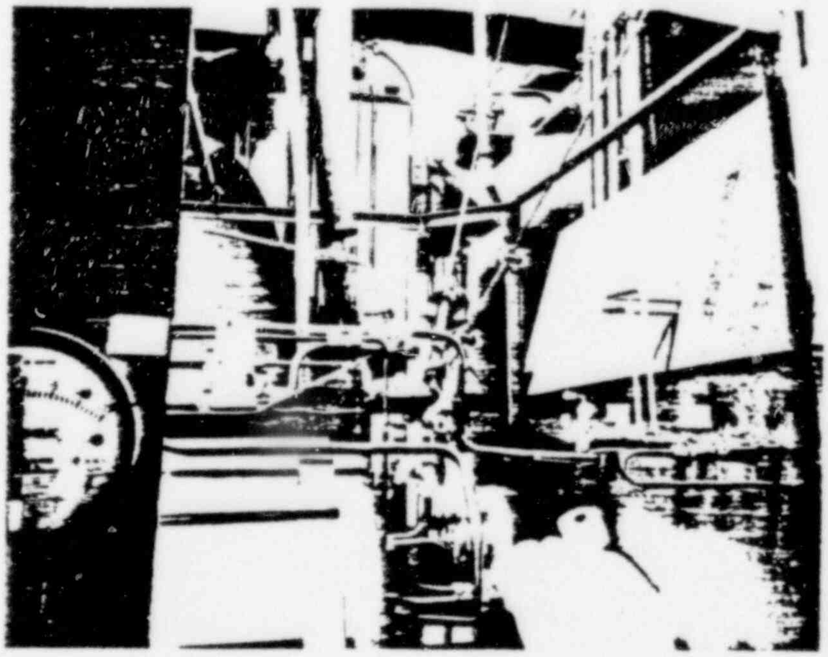

Fig. A-18.
Typical cable support from overhead slab. The cable supports used 1/4-in.-diam. pre-formed 1 by 19 galvanized aircraft cable, heavy-duty thimbles, Crosby rope clips, 3/8-in. turnbuckles and suitably sized eyebolts welded or bolted to the equipment as appropriate to the application. Provided at Glove Box 23 in addition to connections to walls and floor.

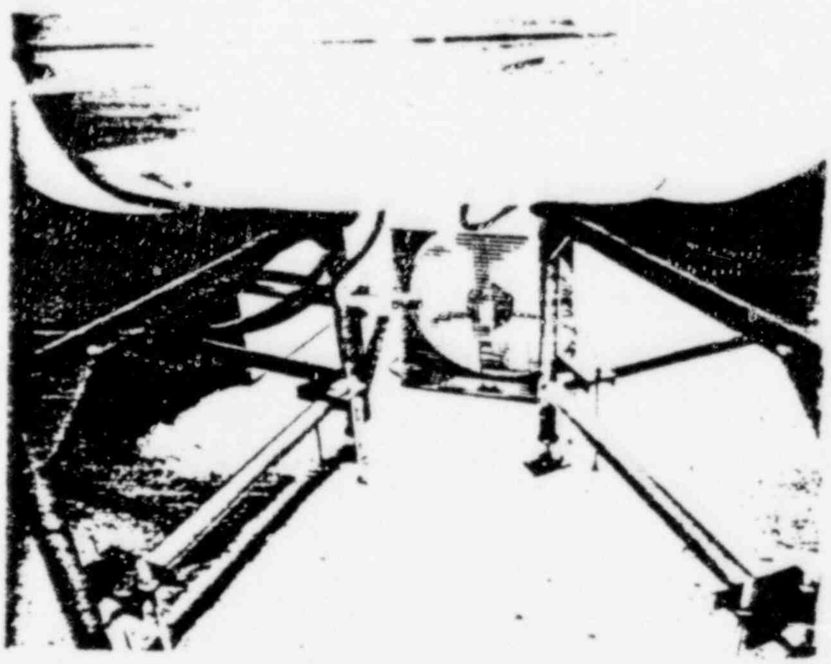

Fig. A-19.
View of typical saddle connection of stands for Glove Boxes 37, 39, 41, and 44 to floor slab.

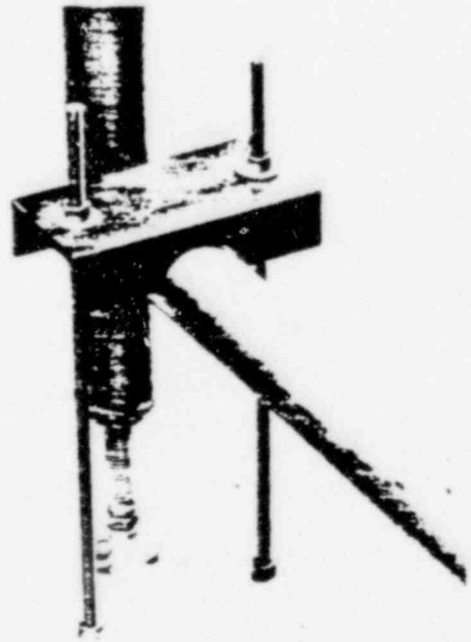

Fig. A-20.
Typical saddle connection and 1/4-in. expansion bolt connection at foot of stand. (Glove Boxes 37, 39, 41, and 44)

The equipment in the AFL is connected to 12-in. reinforced concrete slabs overhead, 12-in. reinforced concrete walls, or to 8-in. concrete block walls and floor.

APPENDIX B
STRENGTH AND DEFORMATION CHARACTERISTICS OF BUILDING 102 STRUCTURAL ELEMENTS

I. INTRODUCTION

The strength and deformation characteristics of the structural elements of Building 102 are presented and discussed. The analytical techniques discussed in Task I Appendices B, C, and D are used in the shear wall response studies.

II. PERFORMANCE CHARACTERISTICS OF SHEAR WALLS

The details of the 8-in. concrete block shear wall construction are given in Task I (Table 3-1 and Figs. 3-10 through 3-13).[12] In all cases, the strength contribution of the block shear walls without a bounding steel frame is limited by the 12-in.-long, 1/2-in. round dowels at 48-in. spacing that connect the steel beams or roof deck to the block wall. The dowels are of mild steel and without hooks. The wall extends from the floor to the junction with the previously erected structural steel. A small gap exists between the top of the wall and the steel. The block-to-dowel bond is through mortar that was pressed into place. The top blocks were split and were placed from each side of the wall such that mortar was pressed in and around the dowels. The ultimate bearing capacity of this mortar is no more than 2 ksi. If the ultimate shear strength of the dowel connection is taken as 3.0 kips, a bearing area of 1.5 $in.^2$ is needed; therefore, bearing development along the top three in. of the dowel is required. The limit for small deflection response (elastic) was taken as 1.5 kips.

The dowel connection will be loose after the first high-level loading cycle; therefore, successive cycles involve very little energy absorption, and the connection capacity degrades rapidly to zero after ultimate strength is reached.

Typical bays are 20 ft in length (center to center of columns), and five dowels are provided per bay; therefore, the mean elastic capacity is 7.5 kips, and the mean ultimate capacity per bay is 15 kips.

Computations made in accordance with ATC-3 (see Task I report) show that an 8-in. block wall that is 19 ft 7 in. long has a shear capacity of 16.5 kips. Block couplet tests (Task I, Appendix D, Table I) show a mean pure shear strength of 57 psi (1.5 times the average stress).[12] Using this strength value and an effective wall thickness of 3.5 in., the shear capacity of a wall in a 20-ft bay is 31 kips. The shear capacity of the connection to the floor slab is in excess of 31 kips; therefore, for a nominal 20-ft wall, the maximum shear force that can be transmitted to the roof system is determined by the dowel connection. The mean shear capacities are 7.5 kips elastic and 15 kips ultimate.

The structural steel roof framing and columns form a steel bounding frame for many of the shear walls. The test results reported in Appendix D of the Task I report were extrapolated to the Building 102 shear walls with a structural steel bounding frame. The test block walls have the same height-to-length ratio as those in Building 102; however, they differ in length and height, doweling to the structural steel, and size of the steel frame. The steel frame of the test wall had sufficient strength to produce failure in the wall panels; however, the steel frame of Building 102 shear walls does not have the strength to fully develop the capacity of the concrete block panels. If the steel bounding frame were sufficiently strong to crack and fail the block panel, the test results show that the shear capacities and associated deflections for a typical bent of Building 102 are as follows.

Condition	Load	Deflection	K
First crack	117 kips	0.49 in.	239 k/in.
Ultimate	176 kips	1.3 in.	

The properties of the 8-in. concrete block shear walls with a bounding structural steel frame are shown in Fig. B-1. The elastic capacity of the beam-to-wall connection is estimated at 7.5 kips (mean). At this load level, the columns contribute little to the composite strength because of their high flexibility. At ultimate, the total dowel capacity is estimated to be 15 kips (mean). With yielding of the dowels, the structural steel columns bend as shown in Fig. B-1. One of the columns shown moves away from the wall; hence, the wall shear strength that can be developed by this end column depends upon the column connection capacity.

Neglecting minor axial effects and using the mean yield strength of 40 ksi, the mean plastic moment capacity of the steel column is 34 kip-ft. The mean shear load that the column can transmit to the wall is 45 kips (Fig. B-1). The column that moves away from the wall can transmit to the wall a mean shear force of about 2.2 kips. The ultimate mean shear force that can be applied to the top of this wall is 62.2 kips. The block panel should not be cracked at this load level.

The steel frame has little influence on the elastic stiffness of the wall. Considering shear deformations only and an effective G of 270 ksi, a nominal 20-ft wall has an elastic stiffness K of 1115 kpi.

Several of the block walls do not connect to the roof. In these cases, the load that can be applied to the walls depends upon the steel that bears on the end of the walls, and the capacity is therefore limited by yielding in the columns. The column that tends to pull away from the wall has a minor contribution to the shear capacity. The wall stiffness is therefore determined by the single participating steel column.

For the walls that are connected to the roof diaphragm and for loads applied perpendicular to the block wall face, the capacity is determined by yielding of the vertical wall reinforcing. Assuming that these walls act as simple beams supported at their tops and bottoms, the walls reach ultimate strength at a load of 51 psf. The ultimate strength is associated with yielding of the vertical reinforcing steel and has an elastic-plastic behavior until the deflections become large.

The wall has a weight of 61 lbs/ft^2 so that ultimate is associated with a constant acceleration of about 0.84 g's. Assuming elastic behavior and

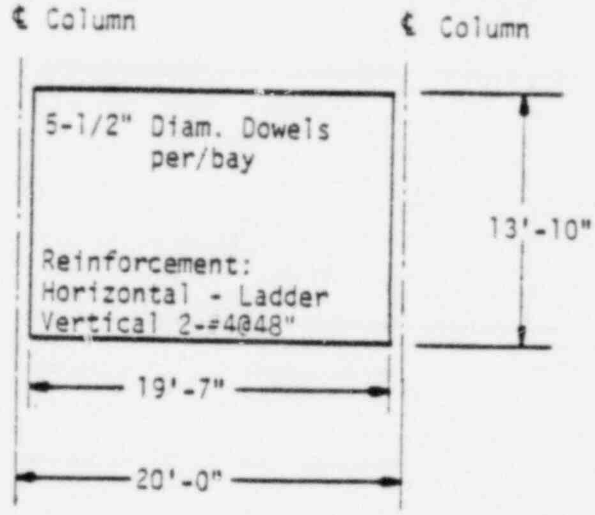

a. Eight-in. concrete block wall

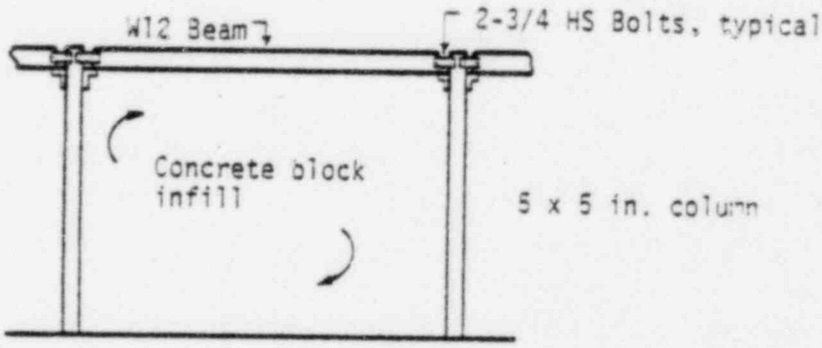

b. Structural steel bounding frame

Fig. B-1.
Block wall properties.

uncracked masonry, the frequency of the first mode is 2.7 cps (period with 0.37 s). The fundamental period of the wall will increase as the wall cracks and the stiffness degrades. The cracked wall has a period of about 1 s. A ductility of at least two can be justified, and the spectral acceleration at a period of 1 s with 10% damping is 1.0 g's. The capacity of the wall connection to the metal roof deck has a larger capacity than this loading. An earthquake acceleration perpendicular to the wall face will produce cracking of the walls at a load of about 0.6--1.0 g's; however, the wall will not collapse.

Block walls with a complete bounding structural steel frame are strengthened by the steel members. The moment of inertia of the steel columns is small, and its influence on the uncracked fundamental period can be neglected. The walls have horizontal ladder-type reinforcing steel and dowels between the steel columns and the walls; therefore, forces can be transmitted from the wall panel to the steel columns. The ultimate capacity corresponding to a constant acceleration of 1.75 g's is 107 psf normal to the wall face. The coefficient of variation remains 0.2 because the properties of the load paths are dependent. The period of vibration is the same as that for a block wall without a steel frame. Using a ductility of 2 with 10% damping, the typical wall will likely remain elastic in response up to 1.0 g's or more.

The basic procedures used in evaluating the exterior precast concrete are discussed in Appendix C, Task I. The light-angle inserts in the top of the panel limit the shear load that can be transmitted to the top of the panel to 5 kips elastic and 10 kips ultimate (mean) for a 20 ft panel.

The light-angle inserts are welded to the structural steel framing and are connected to the wall panel by a 1/2-in. round dowel that is 9 in. long with a 2 in. hook. The connection capacity is determined by either the capacity of the weld between the clip and the dowel or by the dowel. The ultimate bearing capacity on the concrete was taken as 5 kips/in.^{2} A connection load of 2.0 kips fully develops the dowel in plastic bending. Equilibrium dictates that a simultaneous tension of about 2.0 kips exists at the same point. The dowel-to-angle connection is therefore subjected to bending, shear, and tension. The concrete will not yield to allow the dowel to become a tension member; hence, a shear connection capacity of 2.0 kips ultimate and 1.0 kip elastic was used.

The connections have a brittle response (little ductility). The rigidity, assuming that the shear wall acts as a cantilever beam, is estimated at 7800 kips/in. Considering the influence of the bottom clip inserts and the weight of the panel, the overturning shear capacity is 18.4 kips. The shear capacity of the top clips limits the shear load that can be applied to a panel to 10 kips.

Because of the flexible nature of the doweling connecting the panels to the steel column and the pour joint details, the structural steel columns are only effective in resisting overturning after the response becomes inelastic. In the low-bay area, a limited amount of horizontal shear load in the direction of the walls can be applied to the wall panels through the short column studs. The mean capacity is estimated to be about 4 kips per column.

For motion perpendicular to the wall face, the solid precast concrete panels in the low roof area have mean fundamental periods of vibration of about 0.35 s if uncracked and 1.4 s if cracked. The steel columns strengthen, but do not effectively stiffen the walls. Neglecting the small effects of the steel columns, the walls crack at an equivalent static side-on PGA of 0.84 g's and fail at 1.05 g's. The ultimate strength with a single steel column tributary to the wall is 1.84 g's equivalent static loading. The panel-to-roof connection has a static capacity of 0.46 g's elastic and 1.26 g's ultimate, and this connection has little ductility. At 5% damping and a period of 0.35 s, the connection will fail at a load of about 0.9 g's using a ductility of two. The dowels at the panel ends and the column studs are much more flexible than the inserts at the top of the wall, so that failure of the inserts will be followed by development of the wall-end connections. The latter connections are also brittle in nature because they depend on small sections of concrete cast in place between the ends of the wall panels, and the capacity of the connection is about the same as the connection to the roof.

III. BASEMENT WALLS

The exterior basement walls are constructed of reinforced concrete. Except for the lengths of the RML cells, these walls form the entire perimeter of the basement area. They are 12 or 24 in. thick and span 11 ft vertically. The distances between lateral supports varies from about 10--80 ft. The basement walls act as soil retaining walls, shear walls, and vertical supports for the roof slab. There are three different wall sections, two of which differ only in the amount of reinforcing steel. These sections are shown in Fig. B-2 along with their strength capacities. The location of these walls with respect to the basement area is indicated in Fig. B-3. The strengths given in Fig. B-2 are for one-way slabs and for a unit wall width (1 ft).

There is a construction joint at the interface of the walls and the roof slab (Fig. B-4). Separation of the wall from the roof slab would occur along this construction joint. The walls are not structurally joined to the floor slab.

The procedures for estimating the passive soil pressures acting on the basement walls is given in Ref. 22 . Faulting disturbs the soil locally; hence, it is likely that the soil pressures computed by the methods in Ref. 22 are larger than the actual pressures in a fault. The soil pressures were computed assuming that the basement walls could not rotate, only translate.

IV. COLUMNS

Reinforced concrete columns are located within the basement area (Fig. A-15) to support the roof slab. They are rectangular tied columns and two different sizes were used. Their outside dimensions are 20 by 24 and 18 by 20 in. (Fig. B-5). These columns rest on square reinforced concrete footings and their connection to the roof slab includes drop panels. The footing and column-to-roof slab connection is considered as part of the column. The floor slab is not structurally connected to the columns or footings. The column cross sections and their strength capacities are given in Fig. B-5. They are classified as short columns; hence, the strengths were not reduced because of their height.

From Fig. B-5, we see that the column capacity is governed by the punching shear capacity of the column-to-roof slab connection. The axial service loads are less than half of their axial ultimate capacity; hence, they possess a large reserve strength.

The columns have ties spaced at 18 in. This width is too large to ensure ductile behavior. Several of the columns are braced by concrete masonry walls (Fig. B-3). For the columns to be subjected to moments and shear, the roof

Wall Section 1

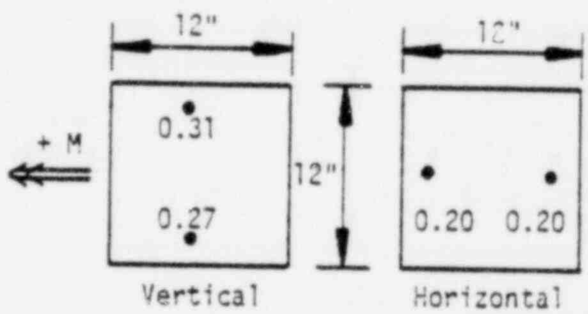

Wall Section 2

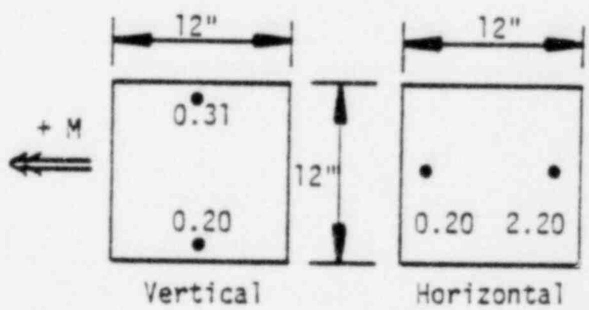

Section	Moments (- $\frac{lb\text{-}ft}{ft}$) $\overline{M}_u^+$	$\overline{M}_u^-$	Mcr	Minimum Shear (lb/ft)	Axial (Vert.) (lbs/ft)	Min Hor. Shear (lb/ft)
1 (Vert.)	12 100	13 270	9 840	12 870	137 800	35 900
1 (Hor.)	8 920	8 920	9 840	12 870		
2 (Vert.)	9 660	12 870	9 840	12 870	137 800	35 900
2 (Hor.)	8 920	8 920	9 840	12 870		

Shear Strength for shear wall (minimum)

$$\overline{V} = 3.3\sqrt{3000}\,(12)\,(12)\,(.8) + \frac{(.4)(47\ 000)(12)(.8)}{12} = 35\ 900\ \text{lb/ft.}$$

Fig. B-2.
Basement wall sections.

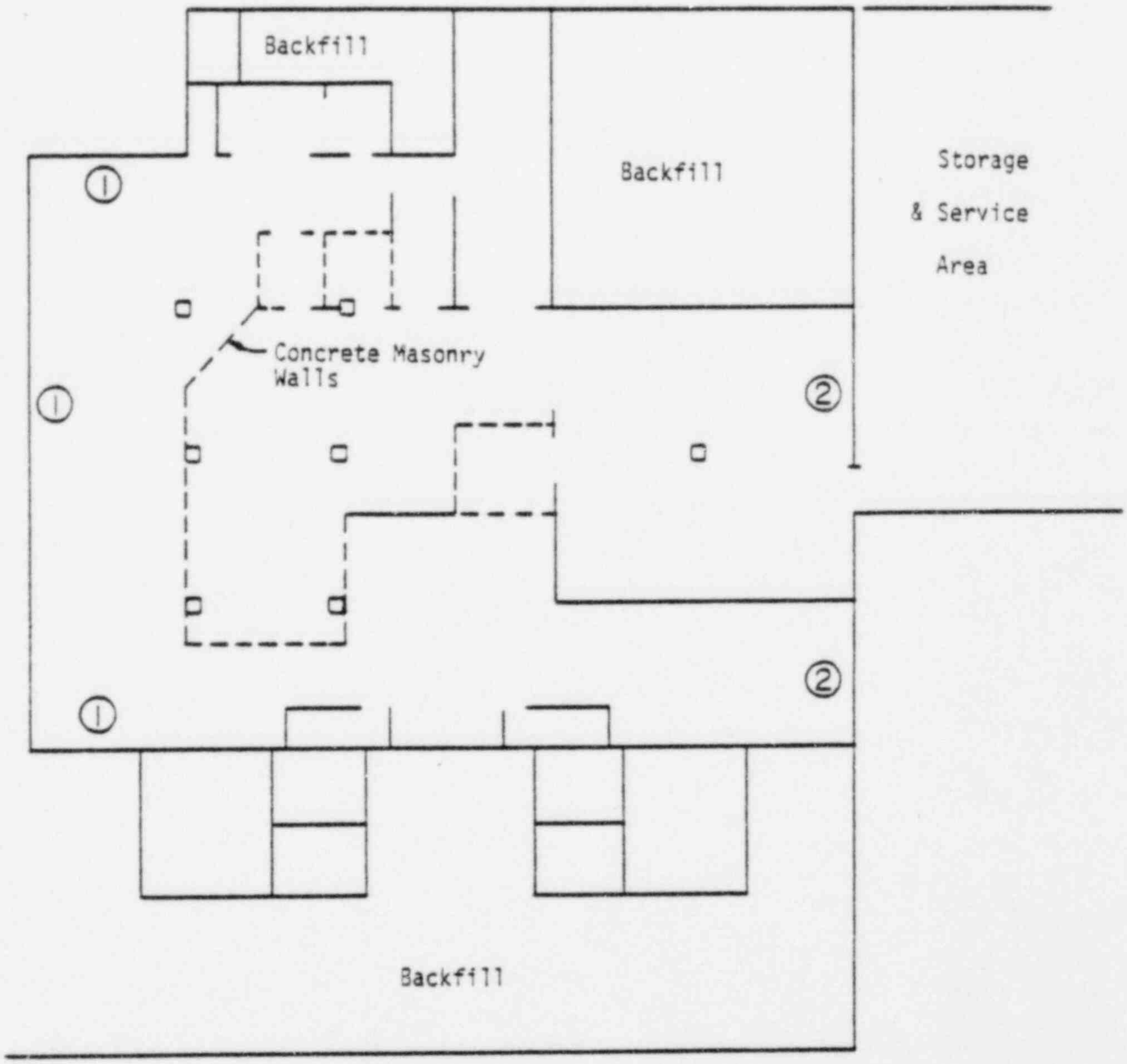

Fig. B-3.
Location of basement wall sections.

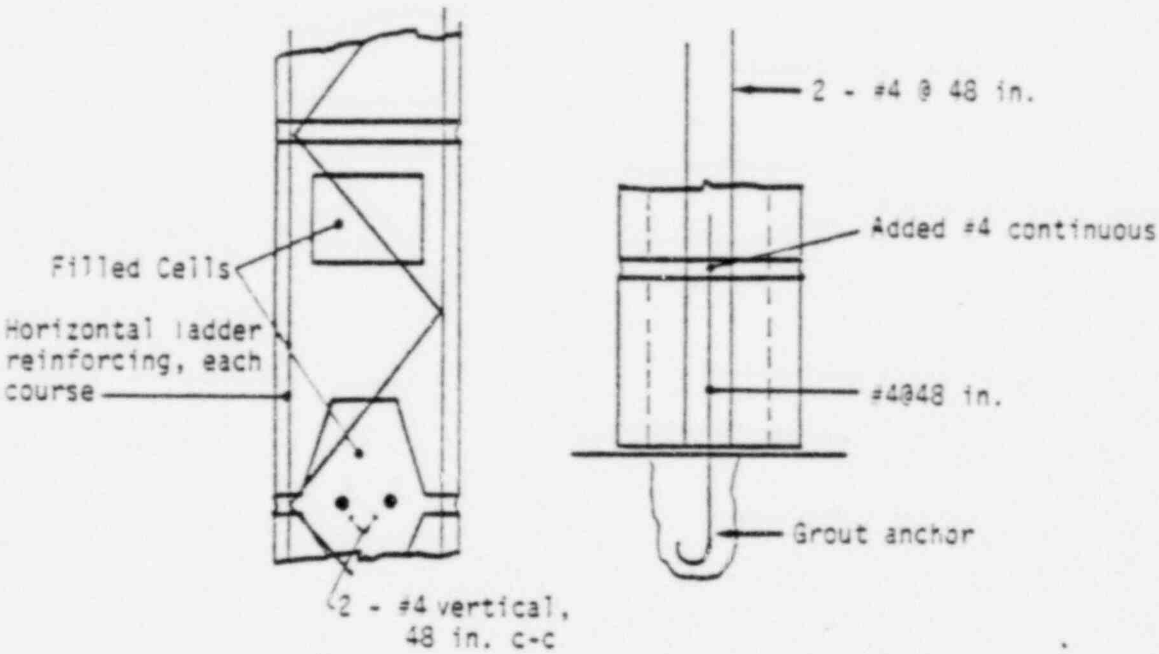

a. Basement block wall construction

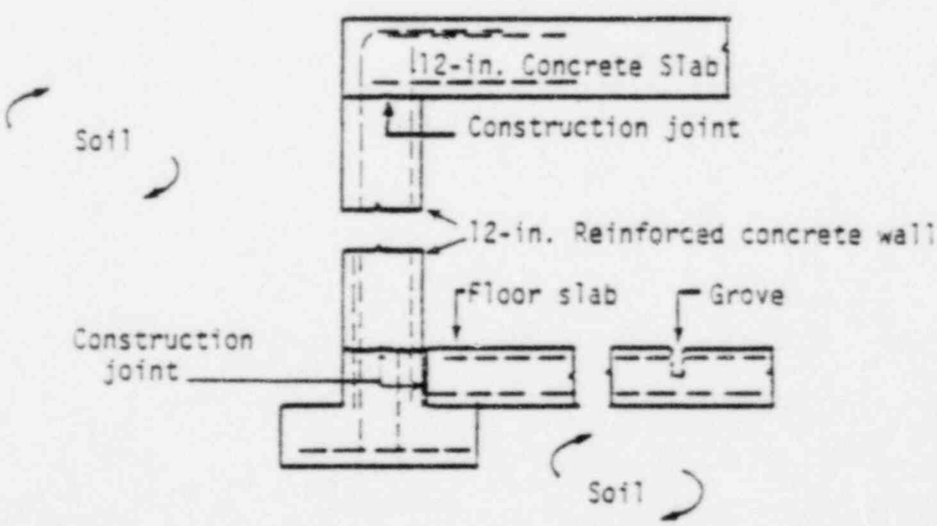

b. Basement construction

Fig. B-4.
Construction details of concrete block walls and basement construction.

COLUMN CAPACITIES

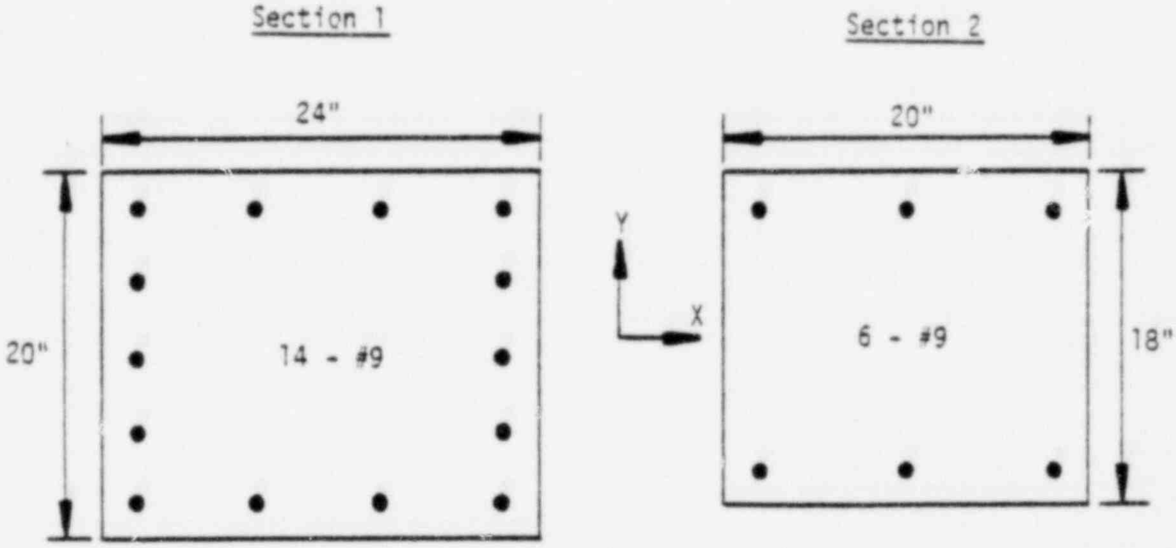

Section	Axial Load (kips)	$\overline{M}_u^y$ (lb-ft)	$\overline{M}_u^x$ (lb-ft)	Punching Shear (kips) Footing	Roof Slab	Service Load (kips)
1	1 400	482 000	425 000	775	535*	140
2	915	167 000	148 000	700	291*	140

*Low

Fig. B-5.
Column capacities.

slab must move relative to the floor slab. Because of the many interior and exterior walls, this relative movement would be insignificant. The principal rose of the columns will be to transmit vertical loads.

V. BASEMENT ROOF SLAB

The roof slab over the basement area has thicknesses of 9 and 12 in. as indicated in Fig. B-6, Sections C and F. The roof slab is supported by the exterior basement walls, the columns, the interior reinforced concrete walls, and the interior concrete masonry walls. Drop panels of 3 or 6 in. are located above the columns. The amount of steel reinforcing varies from strip to strip. Flexural and shear capacities at locations indicated in Fig. B-7 are given in Table B-I. The slab is supported in both directions at 20-ft intervals; hence, its vertical load capacity evaluation must consider two-way slab action. The weakest slab section can support a load of 870 psf[2]. The service load is about 360 psf. The roof slab is continuous except for the construction joints indicated in Fig. B-7. Steel reinforcing was provided to transmit the shear from one section to another. The shear capacity through the construction joints is about the same as the shear capacity of the adjacent slab.

The basement roof slab serves a number of functions. It provides a roof for the basement area, supports parts of the ground floor construction of Building 102, and supports ground floor activities within Building 102. If a fault occurs, it will serve as a tension or compression flange if the basement structure acts as a beam. This slab is the structural element that connects to all the other structural elements to form the load-resisting basement structure.

VI. BASEMENT FLOOR SLAB

The basement floor slab is 8 in. thick and rests directly on soil. Because it is not tied to the basement walls nor the column footings, it contributes little to the load-resisting basement structure. It functions as a floor for supporting activities within the basement area and as a foundation for the concrete masonry walls. If the basement structure were to act as a beam, the floor slab could serve as a compression flange.

BASEMENT ROOF SLAB SECTION

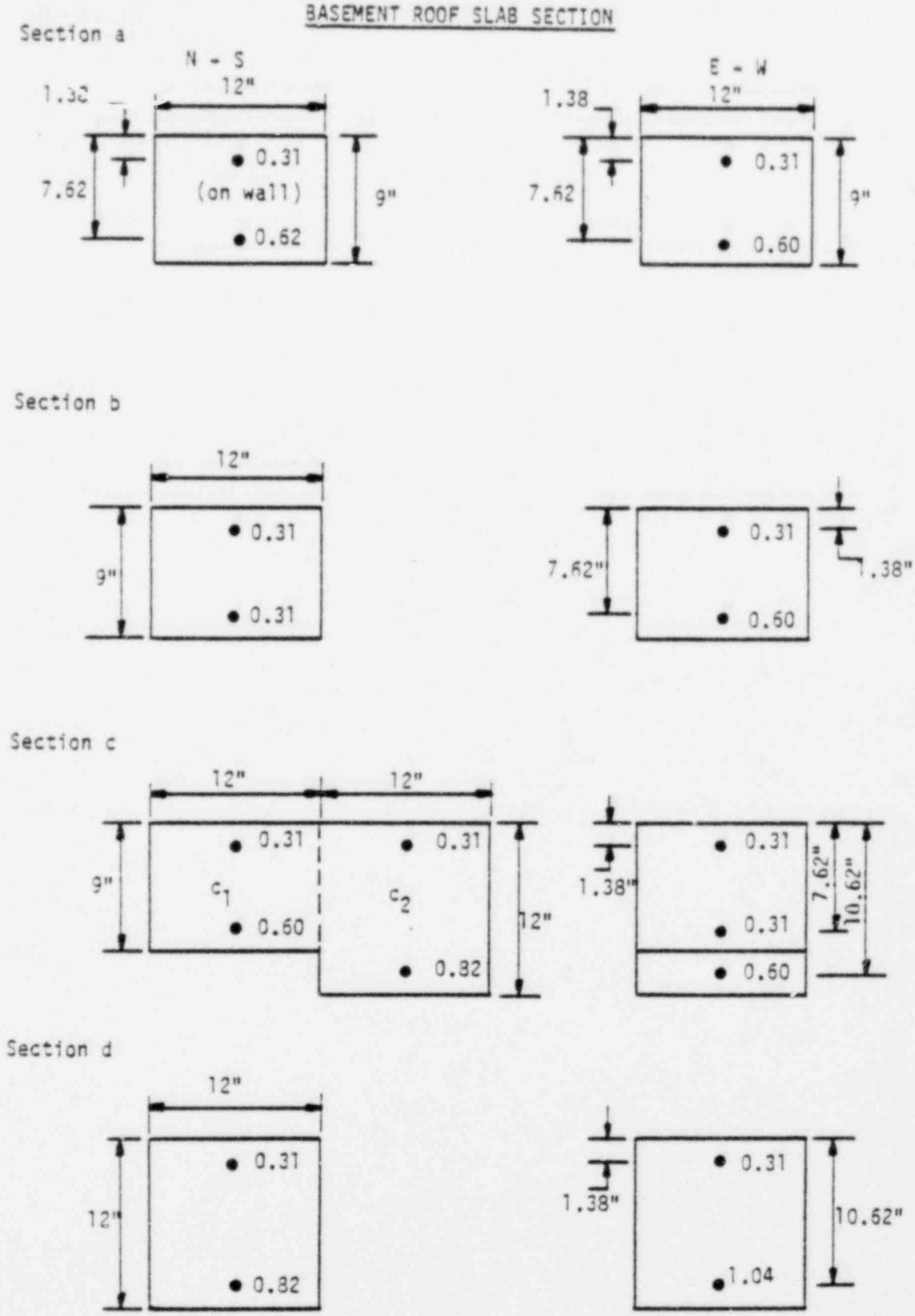

Fig. B-6.
Basement roof slab sections.

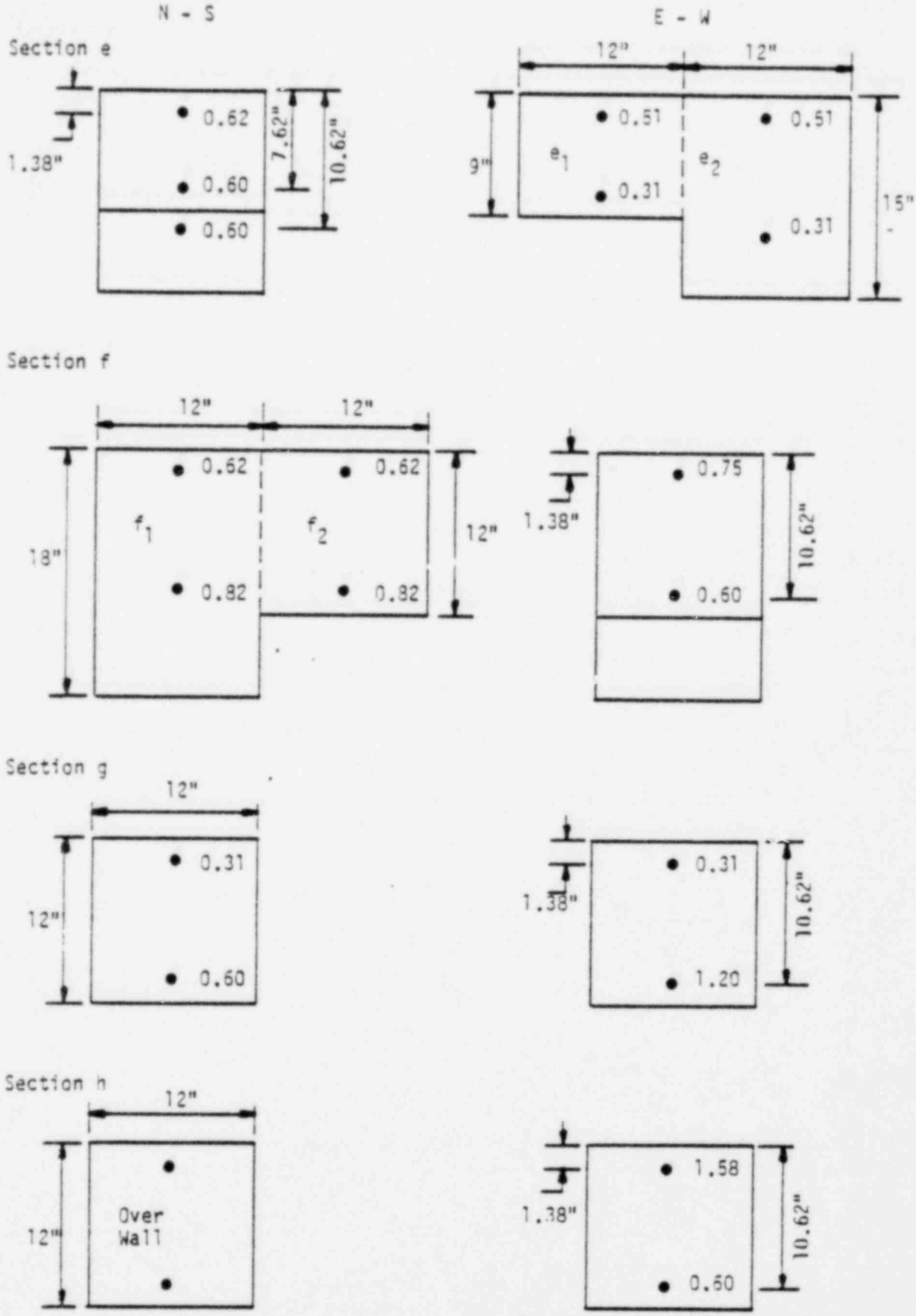
N - S
E - W
Section e
1.38"
0.62
0.60
0.60
7.62"
10.62"
12"
12"
9"
0.51
0.51
e1
e2
0.31
0.31
15"
Section f
12"
12"
18"
0.62
0.62
f1
f2
0.82
0.82
12"
1.38"
0.75
0.60
10.62"
Section g
12"
12"
0.31
0.60
1.38"
0.31
1.20
10.62"
Section h
12"
12"
Over
Wall
1.38"
1.58
0.60
10.62"

Fig. B-6 CONT.

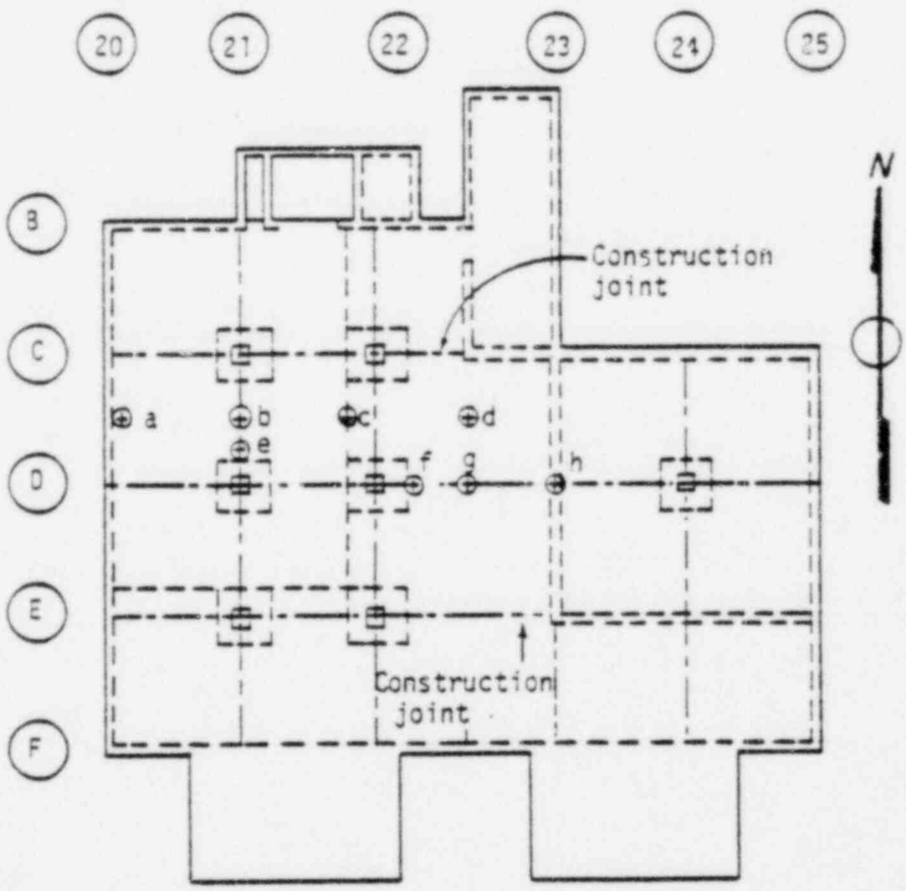

Fig. B-7.
Slab cross section locations.

TABLE B-I

BASEMENT ROOF SLAB MOMENT AND SHEAR CAPACITIES

FOR LOCATIONS SHOWN IN FIG. B-7

Section	N - S Pos M (lb-ft/ft)	N - S Neg M (lb-ft/ft)	E - W Pos M (lb-ft/ft)	E - W Neg M (lb-ft/ft)	Min. Shear (lb/ft)
a	--	--	16 900	9 740	10 000
b	9 620	9 620	16 900	9 740	10 000
c_1	16 900	9 740	9 620	9 620	10 000
c_2	32 100	13 430	24 000	13 390	13 960
d	32 100	13 430	40 100	13 460	13 960
e_1	16 980	17 470	9 720	14 680	10 000
e_2	24 000	38 890	13 360	20 670	13 960
f_1	32 070	57 820	24 000	60 680	13 960
f_2	32 070	24 770	24 000	29 500	13 960
g	24 000	13 390	45 800	13 480	13 960
h	--	--	24 060	59 360	13 960

VII. INTERIOR CONCRETE MASONRY WALLS

Cavity-filled concrete masonry walls 8 in. thick were contructed to serve as a secondary confinement barrier for radioactive products. These walls are doweled to both the roof and floor slabs. Vertical reinforcing consists of 2-#4 spaced at 48 in., and the horizontal reinforcing consists of a 3/16-diam reinforced ladder in each course.

These walls were constructed to separate the basement area containing the glove boxes from the rest of the basement area; hence, they were not designed to carry loads. These walls will serve as shear walls if the roof slab displaces relative to the floor slab and as roof slab supports if the columns shorten. Because the axial loads acting in these walls are unknown, their actual moment capacities cannot be estimated.

REFERENCES

1. A. J. Ayer and W. Burkhardt, "Analysis of the Effects of Abnormal Natural Phenomena on Existing Plutonium Fabrication Plants," US Nuclear Regulatory Commission, Washington, D. C. (1976).

2. D. G. Herd, Open File Map 77-689, "Geologic Map of the Los Positas, Greenville, and Verona Faults, Alameda County, California," USGS (1977).

3. H. W. Menard, "General Electric Test Reactor, Vallecitos Nuclear Center, Vallecitos, California," Letter to H. R. Denton, September 5, 1979. Appendix A-Safety Evaluation Report Input, Geosciences Branch, September 10, 1979.

4. TERA Corporation, "Seismic Risk Analysis for General Electric Nuclear Center, Pleasanton, California" (December 5, 1977).

5. Nathan M. Newmark, "Seismic Evaluation of the Vallecitos Site," Preliminary Report.

6. Dames and Moore, "Report of Preliminary Site Investigation, Foley Ranch," San Francisco, California (October 31, 1955).

7. Shannon and Wilson, Inc., "Investigation of Foundation Conditions, GE Test Reactor," Burlingame, California (June 1973).

8. Shannon & Wilson/Agbabian Associates, "Soil Behavior Under Earthquake Loading Conditions, State-of-the-Art Evaluation of Soil Characteristics for Seismic Response Analyses," TID 26444 (1972).

9. F. E. Richart, J. R. Hall, and R. D. Woods, Vibration of Soils and Foundations (Prentice-Hall, Inc., New Jersey, 1970).

10. Agbabian Associates, "Seismic Soil/Structure Interaction Analysis Guidelines: Vol. II - State-of-the-Art Procedures," SAN/1011-111, ERDA Contract No. EY-76-C-03-1011 (April 1976).

11. Shannon & Wilson/Agbabian Associates, "Procedures for Evaluation of Vibratory Ground-Motion Characteristics of Soil Deposits at Nuclear Plant Sites," USAEC Contract No. AT(04-3)-954 (June 1975).

12. Engineering Decision Analysis Company, Inc., "Structural Condition Documentation and Structural Capacity Evaluation of Building 102 of the General Electric Company Vallecitos Nuclear Center for Earthquake and Flood: Task I - Structural Condition," EDAC 175-03 draft report to Lawrence Livermore Laboratory (NRC Natural Hazards Study) (November 1977).

13. Engineering Decision Analysis Company, Inc., "Structural Condition Documentation and Structural Capacity Evaluation of Building 102 of the General Electric Company Vallecitos Nuclear Center for Earthquake and Flood: Task II - Structural Capacity Evaluation," EDAC 175-060.01, draft report to Lawrence Livermore Laboratory (NRC Natural Hazards Study) (February 1978).

14. Engineering Decision Analysis Company, Inc., "Analysis of Structural Consequences of Fault Displacement Through RML Cells of Building 102 General Electric Nuclear Facility, Vallecitos, California," EDAC 175-061.1, draft report to Lawrence Livermore Laboratory (NRC Natural Hazards Study) (March 1978).

15. N. M. Newmark, "Ine.astic Design of Nuclear Reactor Structures and Its Implications on Design of Critical Equipment," Fourth International Conference on Structural Mechanics In Reactor Technology (SMiRT) (1977), Paper K 4/1.

16. N. M. Newmark, "A Response Spectrum Approach for Inelastic Seismic Design of Nuclear Reactor Facilities," Transactions, Third International Conference on Structural Mechanics in Reactor Technology (SMiRT) (1975), Paper K 5/1, Vol. 4, Part K.

17. N. M. Newmark and W. J. Hall, "Procedures and Criteria for Earthquake Resistant Design," Building Practices for Disaster Mitigation, National Bureau of Standards, Building Science Series 46, Vol. 1, 209-236, (Washington, DC, February 1975).

18. Applied Technology Counc'l, "An Evaluation of a Response Spectrum Approach for Inelastic Seismic Design of Nuclear Reactor Facilities," US Department of Commerce, National Bureau of Standards (1974).

19. N. M. Newmark and E. Rosenblueth Fundamentals of Earthquake Engineering (Prentice Hall, Inc., 1971), Chap. 11.

20. G. W. Clough and J. M. Duncan, "Finite Element Analyses of Retaining Wall Behavior," Journal of the Soil Mechanics and Foundation Division, ASCE, SM12, 1657-1673 (December 1971).

21. P. W. Rowe and K. Peaker, "Passive Earth Pressure Measurements," Geotechnique, 15, No. 1, 57-58 (March 1965).

22. D. R. P. Hettiaratchi and A. R. Reece, "The Calculation of Passive Soil Resistance," Geotechnique, 24, No. 3, 289-310.

23. Z. Wilun and K. Starzewski, Soil Mechanics in Foundation Engineering (Halsted Press-John Wiley and Sons, New York, 1972).

24. J. Mishima, L. C. Schewendiman, and A. J. Ayer, "Identification of Features Within Plutonium Fabrication Facilities Whose Failure May have Significant Effect on the Source Terms," Working Paper, Part of USNRC Study of Analysis of the Effect of Natural Phenomena Upon Existing Plutonium Fabrication Facilties, Battelle, Pacific Northwest Laboratory, Richland, Washington (1977).

25. M. Novak, "Vibrations of Embedded Footings and Structures," Meeting Preprint 2029, ASCE National Structural Engineering Meeting, San Francisco (April 1973).

26. H. B. Seed and R. V. Whitman, "Design of Earth Retaining Structures for Dynamic Loads," ASCE Specialty Conference on Lateral Stress, Cornell University, 1970, 103-147.

27. J. M. Duncan and G. Lefebvre, "Earth Pressures on Structures Due to Fault Movement," Journal of the Soil Mechanics and Foundation Division, ASCE, SM12, 1153-1163 (December 1973).

28. R. Park, "Ultimate Strength of Rectangular Concrete Slabs Under Short-term Uniform Loading with Edges Restrained Against Lateral Movement," paper 6705, Proceedings of the Institution of Civil Engineers, Vol. 28, 1964, 125-150.

29. Holmes & Narver, Inc., "Antiseismic Design of a PWR Nuclear Power Station," HN-192, USAEC Contract No. W-7405-ENG-2 (April 1968).

30. M. R. Niccum, L. S. Cluff, F. Chamorro, and L. A. Wyllie, "Banco Central De Nicaragua: A Case History of a High-Rise Building that Survived Surface Fault Rupture, Sixth World Conference on Earthquake, New Delhi, India (1977).